University of Alberta

Phenanthrene Metabolism and Transport Across the Cell Membranes of
Pseudomonas fluorescens LP6a Strains

by

Angela Y. Smith   Ⓒ

A thesis submitted to the Faculty of Graduate Studies and Research
in partial fulfillment of the requirements for the degree of

Master of Science

in

Chemical Engineering

Department of Chemical and Materials Engineering

Edmonton, Alberta
Fall 2006

Canada

Abstract

Gram-negative bacteria can control the intracellular concentration of antibiotics and hydrophobic compounds by using efflux pumps. *Pseudomonas fluorescens* LP6a possesses an efflux system (EmhABC) that also pumps polycyclic aromatic hydrocarbons (PAHs). LP6a mineralizes phenanthrene; therefore its biodegradation kinetics are affected by active efflux. The partitioning of phenanthrene and its metabolites between the pellet and supernatant was measured using radiolabeled transport assays. Three strains were studied with and without active efflux: wild type LP6a; a transposon mutant unable to mineralize phenanthrene; and a cured strain lacking PAH metabolism. Azide was added to inhibit efflux. For the metabolizing strains, irrespective of azide addition, the label in the supernatant increased over time and decreased in the pellet, indicating that the metabolites are not substrates of the efflux system. Statistical analysis showed that the rate of degradation was faster for the efflux-deficient mutant than for the mutant with efflux activity.

Acknowledgements

I am extremely thankful for the support I received from Dr. Murray Gray and Dr. Julia Foght over the past two years. Not only did they allow me to proceed in my own way, they helped me to get back on track afterwards.

I would also like to thank the Department of Chemical and Materials Engineering and Alberta Advanced Education for their financial support.

I am grateful to Trevor Bugg, who developed the transport assay procedure, and to Dr. Elizabeth Hearn, who provided me with much needed guidance in the construction of WEN and OREN. I would especially like to thank Elizabeth for her patience, support and encouragement.

The time I spent in the laboratory was thoroughly enjoyable due to the friendly microbiologists that welcomed an engineer into their wing. I'd especially like to thank Kathy Semple, for the time she took to help me in the development of the extraction procedure as well as the biometer flask experiment. I would also like to thank the attendees of the bio-group meetings for the helpful discussions of my results, and the useful suggestions on what to do next.

Lastly, I would like to thank my friends (a.k.a. "the movers"), my family and my almost-family, for their encouragement, support and kindness. These special people have made my experience in Edmonton a truly happy one.

Table of Contents

List of Tables

List of Figures

List of Abbreviations

BCA: bicinchoninic acid

BSA: bovine serum albumin

BSTFA: N,O-bis(trimethylsilyl)-trifluoroacetamide

CFU: colony forming units

DBT: dibenzothiophene

DCM: dichloromethane

DMF: N,N-dimethylformamide

dpm: disintegrations per minute

GC-MS: gas chromatography-mass spectrometry

HMN: 2,2,4,4,6,8,8-heptamethylnonane

K_{ow}: octanol-water partition coefficient

NEP: *P. fluorescens* cLP6a, no metabolism, efflux positive

NEN: *P. fluorescens* cLP6a-1, no metabolism, efflux negative

OD_{600}: optical density at 600 nm

OREP: *P. fluorescens* LP6a p21-41, partial metabolism, efflux positive

OREN: *P. fluorescens* cLP6a-1 p21-41, partial metabolism, efflux negative

PB: potassium phosphate buffer

RND: resistance-nodulation-division superfamily

SDS: sodium dodecyl sulphate

t: time

TLC: thin layer chromatography

TSB: tryptic soy broth

TMS: trimethylsilyl

WEP: *P. fluorescens* LP6a, full metabolism, efflux positive

WEN: *P. fluorescens* cLP6a-1 pLP6a, full metabolism, efflux negative

1.0 INTRODUCTION

Polycyclic aromatic hydrocarbons (PAHs) are ubiquitous environmental pollutants that can exhibit carcinogenic and mutagenic effects (Cerniglia 1992). Therefore, much attention is devoted to the removal of these compounds from the environment. Although many remediation techniques can be used to remove these compounds from aqueous and soil systems, bioremediation is commonly employed as it is cost-effective, minimally invasive and successful in the removal of xenobiotic compounds. Bioremediation involves the use of microorganisms to transform pollutants into less harmful compounds (Jördening and Winter 2005). In order to increase the rate and extent of degradation, the specific bacterial species responsible for the removal of PAHs are being studied.

Pseudomonas fluorescens LP6a, a gram-negative bacterium, was isolated from condensate-contaminated soil due to its ability to mineralize PAHs including phenanthrene, anthracene and fluoranthene (Foght and Westlake 1996). The enzymes for the degradation of PAHs are encoded on a plasmid, pLP6a.

An active efflux system designated as EmhABC was identified and characterized in *P. fluorescens* LP6a by Hearn *et al.* (2003). Previous studies have shown that LP6a actively effluxes a wide variety of compounds including antibiotics, toluene and PAHs (Bugg *et al.* 2000; Hearn *et al.* 2003). Because antibiotics and toluene are toxic to LP6a, the efflux of these compounds is not surprising given that multidrug and solvent efflux systems are prevalent in other bacterial strains. However, the efflux of PAHs is unexpected because they are not toxic to the bacterium and they can be used as growth substrates. The kinetics of PAH degradation may be affected by the efflux mechanism because active efflux would likely reduce the intracellular concentration of the substrate, and possibly limit the activity of the cytoplasmic enzymes.

1

Two main hypotheses were postulated at the onset of this research project: phenanthrene metabolites are substrates of the EmhABC efflux system and the rate of biodegradation is higher in strains without efflux capabilities. To test these hypotheses, six different strains of *P. fluorescens* LP6a were used. Cured strains (i.e. those lacking the catabolic plasmid pLP6a) with and without efflux capabilities (non-metabolizing efflux positive (NEP) and non-metabolizing efflux negative (NEN) respectively) were used to confirm that the radiolabeled transport assays were sufficiently sensitive to demonstrate inhibition of active efflux by the addition of sodium azide. As NEP and NEN are unable to metabolize phenanthrene, the results provide insight into phenanthrene partitioning between the cell-free supernatant and pellet fractions.

The wild type efflux positive strain, WEP, is capable of mineralizing phenanthrene and thus produces a suite of metabolites. Due to the low concentrations of phenanthrene used in the transport experiments, minute quantities of numerous metabolites would be produced making the elucidation of metabolites arduous. Consequently, the transposon mutant *P. fluorescens* LP6a p21-41 (open-ring efflux positive (OREP)) constructed by Foght and Westlake (1996) was used in an attempt to accumulate 4-(1-hydroxynaphth-2-yl)-2-oxobut-3-enoic acid, a phenanthrene metabolite, since OREP is unable to produce the aldolase enzyme required to break down this compound.

In order to evaluate the effects of the efflux system on the rate of degradation, efflux-deficient strains were compared to strains that possessed the EmhABC efflux system. Therefore, efflux negative mutants of WEP and OREP were constructed (wild type efflux negative (WEN) and open-ring efflux negative (OREN) respectively).

To determine whether or not metabolites are effluxed by EmhABC, azide was added at various times during the transport assays and the changes in the cell-free supernatant and pellet were analyzed. The slopes of the curves obtained from the transport assays were used to calculate the rate of phenanthrene degradation. Statistical analysis of the rates was performed to determine if the rate was affected by the presence of the efflux system.

2

2.0 LITERATURE REVIEW

2.1 Environmental Contamination and Clean-Up Solutions

As a result of numerous processes, including the burning of fossil fuels, spills of hazardous chemicals and irresponsible disposal of wastes, xenobiotic compounds are continually introduced into the environment. The fate and ultimate effect of these pollutants on the environment and the general population tend to be difficult to predict because these compounds can react with many systems and individual compounds to cause numerous unwanted effects and products. Therefore it is important to limit the release of pollutants to the environment and to develop methods to remove existing pollution to minimize adverse effects on human health and environmental quality.

Researchers continue to extract information from both *in situ* and *ex situ* investigations and thus the fate of these recalcitrant compounds is becoming increasingly better understood. Improved methods for the removal and destruction of environmental pollutants are highly desirable. There is a great drive to better determine how pollutants can be safely removed from the environment without causing an extensive financial burden. As with all processes, one must consider the capital costs of the operation, the operating costs, the inputs and outputs of the process, and the time taken to achieve results.

2.1.1 Xenobiotic Compounds

Many different classes of compounds are released daily into the environment by the petroleum industry, the agricultural industry and the chemical processing industry. These unwanted compounds include aliphatic and aromatic hydrocarbons including benzene, toluene, ethylbenzene, and xylene (BTEX) compounds, polychlorinated biphenyls, phthalate esters, heavy metals and pesticides.

3

Polycyclic aromatic hydrocarbons (PAHs) are ubiquitous environmental contaminants that can be found in soils, sediments, aerosols, waters, animals and plants (Budzinski *et al.* 2000). The release of PAHs causes great concern since they are relatively stable in the environment and they are known to cause ecotoxic, mutagenic and carcinogenic effects (Moody *et al.* 2001). Structures of common PAHs are illustrated in Figure 2.1 below.

Naphthalene   Phenanthrene

Anthracene   Fluoranthene
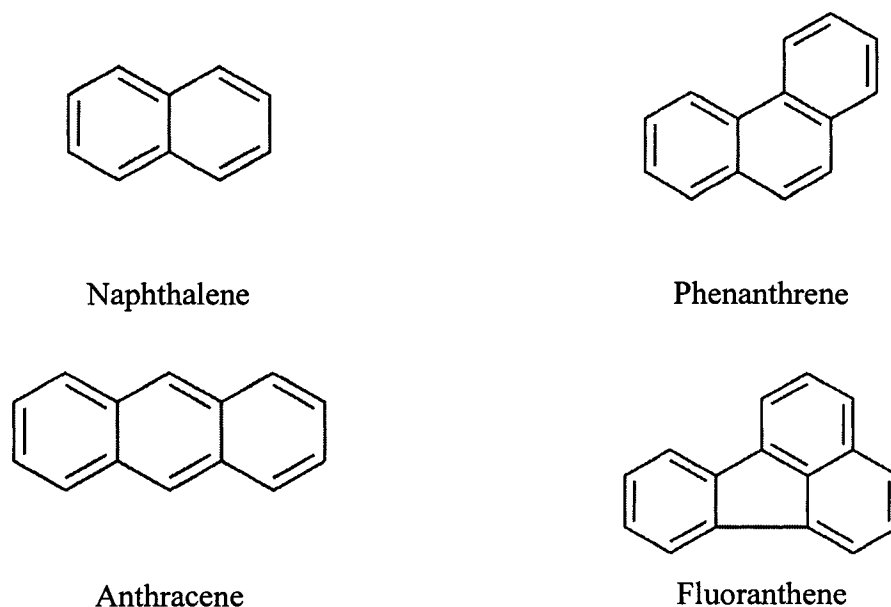
Figure 2.1 Structure of PAHs commonly found in the environment.

PAHs are released into the environment through many different mechanisms including: incomplete combustion of organic materials such as coal, oil, petroleum products and wood; leakage of industrial or sewage effluents; and the accidental release of petroleum products during transport (Cerniglia 1992; Budzinski *et al.* 2000; Moody *et al.* 2001). Substituted phenanthrenic compounds can account for as much as 13% of the aromatic fraction of crude oil (Budzinski *et al.* 2000). Due to the hydrophobic nature of these compounds, PAHs tend to sorb to particles and are thus commonly deposited in sediments and soils, making them far more difficult to target. PAHs are also subject to "volatilization, photooxidation, chemical oxidation, bioaccumulation, leaching and microbial degradation" once they are released to the environment (Cerniglia 1992).

4

2.1.2 Toxicology of PAHs

PAHs cause concern for society because many are suspected carcinogens (Knightes and Peters 2003). There are more than 100 known PAH compounds and the risks associated with each of these compounds are not well understood (Moody *et al.* 2001). Of these 100 compounds, the United States Environmental Protection Agency has listed 16 PAHs as priority pollutants for remediation (Samanta *et al.* 2002). To comply with soil remediation standards, PAHs must be removed from the soil according to individual PAH standards (Moody *et al.* 2004).

PAHs are highly lipid-soluble and thus are easily absorbed and distributed in a wide variety of mammalian tissues and tend to localize in body fat (Samanta *et al.* 2002). Phenanthrene has been shown to be toxic to fish and algae (Moody *et al.* 2001). Although phenanthrene and anthracene do not exhibit genotoxic or carcinogenic effects on humans, their metabolites have been known to cause unwanted effects (Moody *et al.* 2001) and may in fact be more toxic than phenanthrene itself (Zink and Lorber 1995). PAHs are oxidized by mammalian enzymes (the P450 monooxygenase enzymes) to form epoxides that can form covalent adducts with DNA causing mutations that may eventually cause a tumor (Atlas and Philp 2005).

Standardized toxicological tests are used to determine the acute and chronic toxicities of various chemicals (Atlas and Philp 2005). The Microtox ® assay is one such procedure that measures the decrease in respiration and subsequent light output of the luminescent bacterium *Vibrio fischeri* as the toxic response. Many researchers are interested in the effects of metabolite toxicity on PAH-degrading bacteria since the rate of degradation of these xenobiotic compounds will be compromised.

Park and his colleagues (2004) have shown that catechol-related compounds and their condensation products can accumulate to toxic levels in stationary phase cells of the naphthalene-degrading bacterium *Pseudomonas putida* NCIB 9812-4. This finding is highly undesirable as it limits the potential benefit of this microorganism in the environment.

5

2.1.3 Remedial Technologies

The techniques used to remove contaminants from ecosystems are quite diverse. The most simple option is known as passive remediation since little to no interference is required for contaminant removal. Landfilling is one common passive remediation technique that is used but, unfortunately, it takes a considerable amount of time to mineralize the contaminants (Jördening and Winter 2005).

Incineration is another commonly employed remedial option. The major downside to this technique is that the contaminant is not always completely removed, which occasionally results in toxic by-product formation (Jördening and Winter 2005). The costs associated with incineration are quite high and are estimated to be between $400-1200 US/tonne of soil (Atlas and Philp 2005). Other physical treatment processes include excavation and disposal, and encapsulation with geomembranes.

Common chemical remediation treatments include *in situ* chemical oxidation, thermal desorption and solidification/stabilization (Atlas and Philp 2005). All of these techniques are quite costly due to the labour and the expensive reagents that are required. Thus, affordable and effective remediation technologies are highly desirable.

2.1.4 Bioremediation

Biological treatments of environmental contaminants tend to be highly economical relative to the other available options. Bioremediation is defined as the use of microorganisms to detoxify or remove organic contaminants by harnessing their enzymatic activities to transform the contaminants into harmless constituents (Atlas and Philp 2005; Jördening and Winter 2005). The cost of bioremediation is between $20-200 US/tonne of soil (Atlas and Philp 2005) and relatively few capital investments are required. As bioremediation is an emerging field, it currently comprises only 10-15% of all remediation methods used for the treatment of contaminated soils and groundwaters in the United States (Atlas and Philp 2005).

6

Bioremediation techniques can be divided into 2 major categories: *ex situ* and *in situ*. *Ex situ* techniques involve moving the waste and include landfarming, biopiling, and composting. Bioreactors are also commonly used to eliminate contamination from aqueous effluents as well as solid sludge and other similar wastes.

Wastewater treatment facilities commonly use bacteria to remove unwanted compounds from the influent streams. Bacteria are usually recycled as an active sludge mixed with the feed wastewater, or in some cases, immobilized in a bioreactor into which the wastewater is fed. In order for this process to be effective, sufficient residence times in the reactor are required. Time is also required for the selection or adaptation of bacteria in order to achieve favourable degradation rates and extents. Although the implementation of genetically modified bacteria in wastewater treatment facilities would be highly beneficial, these organisms are not used as they require extensive maintenance (Jördening and Winter 2005) and their use is regulated. Bioengineering specific organisms for wastewater treatment is not generally successful due to several factors: the plasmids are unstable; the necessary genes are not expressed in the new environment; the inoculated strains did not survive; and/or the inoculated strains are outcompeted by other strains (Jördening and Winter 2005).

In lieu of genetic modification, the most suitable microorganisms for degrading a certain contaminant are chosen using microbial enrichment procedures (Jördening and Winter 2005). A mixed consortium of bacteria is exposed to a specific contaminant and the cultures that remain viable are selected for further study. Since wastewaters contain numerous carbon sources, the microorganisms are not forced to metabolize the xenobiotic compounds and thus do not need to express genes for degrading xenobiotics (Jördening and Winter 2005).

Common *in situ* techniques include intrinsic remediation (or natural attenuation), biostimulation and bioaugmentation. These technologies allow for clean-up directly at the location where the contamination originated.

7

Bacteria, algae, cyanobacteria, yeasts and lower fungi possess desirable catabolic pathways for total or at least partial degradation and decomposition of recalcitrant compounds in the environment (Van Hamme *et al.* 2003; Jördening and Winter 2005). Biodegradation by indigenous microbial populations is considered an important process affecting the fate of PAHs in the environment (García-Junco *et al.* 2001).

The biological removal of PAH compounds can be achieved through biostimulation or bioaugmentation. Biostimulation involves the alteration of the current conditions to satisfy the needs of the indigenous microbial population. Adding nutrients or inducers to the system, increasing aeration, optimizing the temperature and adjusting the pH, are only a few of the changes that can be made to enhance the activity of the microorganisms. Alternatively, PAH-degrading microorganisms can be added to the system in order to speed up biodegradation. This process is known as bioaugmentation.

The use of microorganisms to clean up waste (bioremediation) is becoming more favourable compared to conventional physical and chemical remedial techniques. In order to enhance the degradative potential of the microbes, the activities of indigenous microorganisms in polluted environments must be explored (Jördening and Winter 2005). The ultimate goal of bioremediation is mineralization, which involves the conversion of the parent compound to carbon dioxide and water. Biodegradation simply refers to any change in the parent compound.

2.1.5 Factors Affecting Biodegradation

The biodegradation of organic pollutants depends largely on the bioavailability and biodegradability of the contaminants, as well as on the environmental conditions (Jördening and Winter 2005). Bioavailability is defined as the "amount of contaminant present that can be readily taken up by living organisms, e.g., microbial cells" (Atlas and Philp 2005). If the substrate is not in contact with or at least close to the degrading organism, little biodegradation will occur. Thus, the solubility of the contaminant in water greatly affects bioavailability.

8

The degree of biological degradation achieved in a remediation process is influenced by many factors including: the reactivity of the contaminant, the concentration of the contaminant in the environment, the physical state of the contaminants and the location of the contaminant (soil or aqueous system) (Jördening and Winter 2005). Solubility of organic compounds is mediated by charge, and forces of attraction including Van der Waals forces, hydrogen bonding and dipole-dipole interactions (Atlas and Philp 2005). The size and shape of the molecule also correlate strongly with the molecule's solubility in water (Bressler and Gray 2003; Atlas and Philp 2005).

Bioremediation is directly impacted by the following factors: energy sources (electron donors), electron acceptors, nutrients, pH, temperature, soil porosity, inhibitory substrates or metabolites and active microbial communities. The bacterial population is highly influenced by the levels of dissolved oxygen in the environment. These factors influence the ability of the bacteria to produce the required enzymes to metabolize PAHs. Therefore, to achieve the maximum rate of degradation, many factors must be considered.

2.1.5.1 Bioavailability

Bioavailability is a general phenomenon that describes the tendency of a pollutant to exist between phases at equilibrium (Atlas and Philp 2005). Bacteria will generally prefer to metabolize substrates present in the aqueous phase but they will also assimilate the substrate if they are in close association with the insoluble phase of the chemical (Efroymson and Alexander 1991). The bioavailability of a contaminant is controlled by a number of physico-chemical processes such as sorption, desorption, diffusion and dissolution. Reduced bioavailability is caused by the slow mass transfer of the contaminant to the degrading microbes (Boopathy 2000).

9

As a result of the importance of bioavailability, there is great interest in the relationship between PAH desorption, dissolution and bioavailability (Knightes and Peters 2003). Due to the hydrophobic nature of PAHs, they tend to readily sorb to surfaces, dissolve in organic phases and/or partition into lipophilic phases as opposed to partitioning into aqueous phases. Thus, PAHs are generally not sufficiently bioavailable for microorganisms present in the aqueous phase of the system whereas charged and highly polar organic and inorganic molecules are readily soluble in water (Atlas and Philp 2005). One of the most important reasons for the lack of biodegradation is limited bioavailability due to the low water solubility and the hydrophobic nature of PAHs (Moody *et al.* 2005). The linear increase of PAH presence in the environment is thought to be largely due to the mass transfer limitation of PAHs from the solid phase to the liquid phase (Atlas and Philp 2005).

The amount of chemical present in the aqueous phase is a function of chemical equilibria but it can also be influenced by various bacterial excretions including biosurfactants that increase the dispersion of the compound dramatically, thus making it highly bioavailable for the degrading species (Efroymson and Alexander 1991). Research is ongoing to determine methods to improve the bioavailability of contaminants. Surfactants have been shown to be a highly promising solution to this problem. Some microorganisms have been shown to gratuitously produce surface-active compounds as well (García-Junco *et al.* 2001). One such organism, *P. aeruginosa,* has been shown to produce rhamnolipids that enhance biodegradation of soild phenanthrene.

Prabhu and Phale (2003) showed that the production of biosurfactant by *Pseudomonas* sp. strain PP2 was constitutive and growth-associated. This was a result of growth-dependent changes in the cell surface hydrophobicity, and emulsification activity experiments. Growth-associated extracellular biosurfactant production and modulation of cell surface hydrophobicity play an important role in hydrocarbon assimilation/uptake. In this study, the levels of mineralization of phenanthrene by strains of *Pseudomonas* increased when cultures were co-inoculated with rhamnolipid-producing *P. aeruginosa* (Prabhu and Phale 2003).

10

2.1.5.2 Oxygen

Many pollutants such as coal tar, creosote, and diesel fuel, are known to be biodegradable, particularly under aerobic conditions (Knightes and Peters 2003). Thus the presence of terminal electron acceptors, such as oxygen, is very important. Aerobic organisms require oxygen whereas anaerobic organisms can utilize a variety of other electron acceptors including nitrate and sulphate. The most rapid and complete biodegradation of many of the most common pollutants occurs under aerobic conditions (Jördening and Winter 2005).

Oxygen is also required to activate oxygenase and dioxygenase enzyme activities. Oxygenases are essential in the initial stages of aerobic PAH degradation and therefore, low oxygen concentrations limit PAH degradation (Kim *et al.* 2005).

2.1.5.3 pH

In a study conducted by Kim *et al.* (2005), it was shown that a one-unit pH drop (from 7.5 to 6.5) considerably increased the rate of phenanthrene degradation by *Mycobacterium vanbaalenii* PYR-1. The acidic pH increased the cell permeability to hydrophobic substrates (Kim *et al.* 2005). The optimum pH levels for enzymatic activity vary greatly among microorganisms; microbial communities exist in environments at pH<1 and at pH>10.

2.1.5.4 Cometabolism

Another interesting phenomenon that affects biodegradation is known as cometabolism. Cometabolism is a process in which an organism growing on a particular substrate is able to gratuitously oxidize another substrate but is not able to assimilate it (Atlas and Philp 2005).

11

Vila *et al.* (2001) found that many bacteria act on a variety of compounds that do not support their growth and produce partially oxidized products. The versatility of these microorganisms is believed to be partly due to the broad substrate specificity of the degradative enzymes. Naphthalene and toluene dioxygenases are among the enzymes that have been shown to act on numerous compounds (Vila *et al.* 2001).

2.1.6 Rate of Biodegradation

One of the major influences on the rate of biodegradation is the size of the molecule that is being attacked. Generally, larger molecules take longer to break down than smaller molecules. The rate of degradation depends even more strongly on the number of sites on a molecule that are available for attack. Carboxylic acids are much more reactive than simple alkanes, regardless of the size of the molecule. Thus, differences in the rate of PAH degradation are related to the features of molecular structure that determine biochemical interactions rather than size-dependent molecular properties (Knightes and Peters 2003).

Knightes and Peters (2003) have shown that the differences in the biodegradation rates of PAHs by a mixed consortium of bacteria are likely to be functions of the relative abundance of each individual chemical species and the availability of specific enzymes. This study also showed compelling evidence that the bacterial enzymes responsible for PAH degradation have broad functionality. As a result of this finding, the biodegradation rate for the mixture of PAHs as a function of enzyme activity was not strongly correlated. Thus, biodegradation rates observed in the field are largely, if not entirely, governed by rate-limiting physical-chemical processes (Knightes and Peters 2003).

12

Every enzymatic reaction system must contain a rate limiting step. The limiting step in the degradation of phenanthrene and other PAHs is their dissolution in water, which controls the extent and rate of degradation (Prabhu and Phale 2003). Several groups have reported improved efficiency and rates of hydrocarbon degradation when the experimental cultures were supplemented with biosynthetic or chemically synthesized surfactants (Prabhu and Phale 2003). Wammer and Peters (2005) have shown that the observed variation in environmental PAH biodegradation rates is due to the processes that control the bioavailability of the compounds.

2.1.7 Bacteria

Many bacterial species are able to degrade phenanthrene as well as other PAHs. Such microbes include *Pseudomonas* sp. (Foght and Westlake 1996); *Nocardioides* sp. (Adachi *et al.* 1999); *Aeromonas*, *Alcaligenes*, *Micrococcus*, *Vibrio* spp. (Kang *et al.* 2003); and *Mycobacterium* sp. PYR-1 and *Sphingomonas* sp. (Moody *et al.* 2001). Crude oil-contaminated sites have been extremely useful in the discovery of species that are able to degrade aromatic hydrocarbons. Soils samples from these sites are used to isolate thriving species. Table 2.1 lists the most common species in groups of gram-positive and gram-negative bacteria shown to degrade aromatic hydrocarbons.

Table 2.1 Common gram-negative and gram-positive bacteria useful in the bioremediation of PAHs (Atlas and Philp 2005).

Gram-Negative Bacteria	Gram-Positive Bacteria
Pseudomonas spp.	*Nocardia* spp.
Acinetobacter spp.	*Mycobacterium* spp.
Alcaligenes sp.	*Corynebacterium* spp.
Flavobacterium/Cytophaga group	*Arthrobacter* spp.
Xanthomonas spp.	*Bacillus* spp.

13

Bacteria are quite advantageous in that they evolve quickly as a result of external stresses due to their small size, large surface-to-volume ratio, rapid rate of growth and division, and extensive genome plasticity (Atlas and Philp 2005). They typically require little attention and thus are extremely advantageous in remediation solutions.

Chemoorganotrophs are the most prevalent degraders of organic pollutants since they are present in the oxic zone of contaminated areas (Atlas and Philp 2005). As a result of the presence of these pollutants, chemoorganotrophs are able to utilize a wide variety of natural and xenobiotic compounds as carbon sources and electron donors in order to generate the energy required for them to survive and multiply.

Mixed microbial communities have shown the most positive results for biodegradation initiatives. This performance is a result of the fact that gene expression of functional enzymes in more than one organism is necessary to degrade the complex mixtures of organic compounds present in contaminated areas (Atlas and Philp 2005).

Pseudomonads, aerobic gram-negative rods that never show fermentative activity, seem to have the highest degradative potential. *P. putida* and *P. fluorescens* are among the species that have shown excellent results thus far. *P. stutzeri* AN10 can utilize naphthalene as a sole carbon and energy source and the genes for this degradation capability are located on the chromosome (Bosch *et al.* 1999). *P. putida* G7 possesses plasmid NAH7 and *P. putida* NCIB9816 possesses the NAH plasmid pWW60. Both of these plasmids encode the necessary information to produce the enzymes required to metabolize naphthalene and in some cases, other PAHs.

In this study, the degradative capabilities of the bacterium *P. fluorescens* LP6a were studied. LP6a was isolated from soil contaminated with petroleum condensate and has been shown to possess broad PAH oxidizing activity (Foght and Westlake 1996). Thus, this bacterium shows great potential in bioremediation applications.

14

Another interesting characteristic of *P. fluorescens* LP6a is that it has the ability to co-metabolize other PAHs and heterocycles when pre-grown with alternate carbon sources (Foght and Westlake 1996). LP6a was able to co-metabolize dibenzothiophene, biphenyl, indole, fluorine, dibenzofuran, 1-methylnaphthalene, acenaphthene and benzothiophene (Foght and Westlake 1996). A different strain of *P. fluorescens* has also been shown to degrade much larger PAHs such as benz[a]anthracene (Moody *et al.* 2005).

2.1.8 Plasmids and Transposable Elements

Although in some bacteria, the ability to degrade aromatic hydrocarbons is chromosomally encoded, many species possess genes that are organized into two operons borne on isofunctional NAH plasmids, comprising a related family of catabolic plasmids (Foght and Westlake 1996). Other gene clusters for dibenzothiophene oxidation (*dox*) and PAH degradation (*pah*), are strikingly similar to the previously described naphthalene degradation (*nah*) genes (Foght and Westlake 1996). These clusters share sequence homology with *nah* genes and are organized into analogous upper and lower pathway operons (Foght and Westlake 1996). Despite genetic similarities among many naphthalene-degrading microorganisms, not all species are capable of degrading the same portfolio of PAHs.

P. fluorescens LP6a has a 63 kilobase (kb) plasmid, pLP6a, which carries genes encoding the enzymes necessary for PAH degradation. This plasmid hybridizes to the classical naphthalene degradative plasmids NAH7 and pWW60, but has different restriction endonuclease patterns (Foght and Westlake 1996). Interestingly, plasmid pLP6a did not hybridize to plasmids that were isolated from several phenanthrene-utilizing strains, which were unable to metabolize naphthalene (Foght and Westlake 1996).

15

Two gene clusters corresponding to the naphthalene degradation upper and lower pathway operons were defined by transposon mutagenesis (Foght and Westlake 1996). The clusters are separated by a cryptic region of 18 kb (Foght and Westlake 1996). Significant differences between pLP6a and the naphthalene-degradative plasmids NAH7 and pWW60 were discovered by Foght and Westlake (1996) upon the hybridization of CsCl-purified pLP6a to the other plasmid fragments.

LP6a was mutagenized by producing spontaneous deletions in pLP6a and by curing the wild type of its plasmid. Roughly thirty of the attempted *Tn5* insertions mapped at sites within the 38 kb degradative region of pLP6a (Foght and Westlake 1996).

2.2 Transport Processes in Bacteria

2.2.1 Membrane Structures and Energetics

Cell wall structures in gram-negative bacteria and gram-positive bacteria are quite different from each other. Gram-negative bacteria possess an outer membrane (in addition to the cytoplasmic or inner membrane) that consists of phospholipids and lipopolysaccharides whereas gram-positive bacteria do not possess an outer membrane (Sikkema *et al.* 1995). This outer layer acts as a barrier, making gram-negative bacteria more tolerant to solvents and other hydrophobic chemicals relative to gram-positive bacteria (Fernandes *et al.* 2003).

The cytoplasmic membrane plays many important roles; it is responsible for energy maintenance, intracellular solute concentration, turgor pressure, and signal transduction (Sikkema *et al.* 1995). The membrane structure is made up of a phospholipid bilayer that harbours enzymes, transport proteins and lipids (Sikkema *et al.* 1995; Stryer 1995).

16

Phospholipids contain fatty acids and a phosphate group and therefore possess hydrophilic and hydrophobic moieties (Stryer 1995). The hydrophilic heads of the phospholipids are in direct contact with the aqueous environment. Hydrophobic materials pass across the outer membrane and accumulate in the inner membrane and the periplasm.

Lipopolysaccharides in the outer membrane present an obstacle for hydrophobic compounds entering the cell (Sikkema *et al.* 1995). The outer cell membrane acts to partially regulate ionic and molecular traffic into and out of the cell (Prescott *et al.* 2002).

Since all enzymes involved in the degradation of PAHs are intracellular, the PAHs must gain access to the cytoplasm in order for degradation of the specific compound to occur. The polarity, size, and functional groups of the molecule determine whether or not the molecule will cross the cell membrane (Bressler and Gray 2003).

2.2.2 Active and Passive Transport Processes

Passive transport is a process by which molecules are transported from a region of high concentration to a region of low concentration through an energy-independent pathway. Small molecules, such as gases and water, can traverse the lipid bilayer in this manner (Stryer 1995). Carrier proteins, known as permeases, facilitate and greatly increase the rate of diffusion across cell membranes (Prescott *et al.* 2002). Porin proteins, which form channels across the outer membrane of gram-negative bacteria, also facilitate the transport of small molecules, such as monosaccharides, into the cell (Prescott *et al.* 2002).

17

The passage of hydrophobic molecules through bacterial outer membranes also occurs by diffusion (Bateman *et al.* 1986). Bateman *et al.* (1986), who studied the uptake of naphthalene by a *Pseudomonas* species, showed that neither ATP nor an electrical potential was required for the uptake of naphthalene (Bateman *et al.* 1986; Sikkema *et al.* 1995). Bugg *et al.* (2000), who studied PAH transport in *P. fluorescens* LP6a, have shown that other PAHs, such as phenanthrene, also traverse cell membranes by passive diffusion.

Active transport processes involve the movement of molecules against a concentration gradient and therefore require the use of metabolic energy (Prescott *et al.* 2002). Protein carrier activity is required to transport molecules, such as nutrients, by active transport processes. ABC transporters, which span the membrane system, bind and hydrolyze ATP to acquire the energy needed to actively transport compounds. Proton gradients generated by electron transport also drive active transport.

2.2.3 Energy Inhibitors

Sodium azide is a compound that is known to stop the transfer of electrons between cytochrome *a* and oxygen because it is a structural analog of oxygen (Prescott *et al.* 2002). As a result, azide inhibits active transport processes by preventing the generation of an energized membrane. Other inhibitors include cyanide and carbon monoxide. Bugg *et al.* (2000) discovered that 30 mM of azide was sufficient to inhibit active transport processes in *P. fluorescens* LP6a strains.

Uncouplers, such as carbonyl cyanide m-chlorophenylhydrazone (CCCP), stop ATP synthesis without affecting electron transport and cause protons to flow freely across the membrane (Prescott *et al.* 2002).

18

2.2.4 Partitioning of Compounds into Biological Membranes

Hydrophobic molecules favour the lipophilic environment of the cell membrane and hence have a tendency to accumulate in this location. Hydrophobicities for each individual chemical species depend qualitatively on the aqueous solubility and the octanol-water partition coefficient, K_{ow}. This coefficient is calculated from the amount of water that will dissolve under saturation conditions in an octanol phase as well as the amount of octanol that will dissolve under saturation conditions in an aqueous phase at equilibrium (Atlas and Philp 2005). K_{ow} is calculated from the ratio of these values as follows:

$$K_{ow} = \frac{C_{oct}}{C_{aq}} \qquad (2.1)$$

where C_{oct} and C_{aq} represent the equilibrium concentrations in the octanol and aqueous phases, respectively.

The logarithm of the partition coefficient is commonly reported as well (Fernandes *et al.* 2003) and it is typically used to quantify the toxicity of chemicals (Atlas and Philp 2005). Compounds with log K_{ow} values above 5 do not cause any adverse effects on microorganisms, whereas compounds with log K_{ow} values between 1 and 5 are toxic to many bacterial and eukaryotic cells (Fernandes *et al.* 2003).

Sikkema *et al.* (1994), who studied the partition coefficients of various hydrocarbons, found that the partitioning of aromatic hydrocarbons, including toluene, naphthalene and phenanthrene in the membrane correlated with the compound's octanol-water partition coefficient. Table 2.2 lists the values of log K_{ow} for compounds of interest in this study.

19

Table 2.2 Structures and physical properties of aromatic compounds.

Compound	MW (g/mol)	Structure	Aqueous Solubility at 25°C(mg/L)	Log K_{ow}
Salicylic acid	138		2240[a]	2.26[b]
Toluene	92		580[b]	2.48[c]
1-Naphthol	144		866[d]	2.84[b]
1-Hydroxy-2-naphthoic acid	188		244[e]	3.30[d]
Naphthalene	128		30.6[f]	3.35[f]
Phenanthrene	178		1.18[f]	4.57[f]
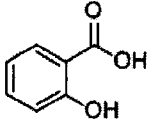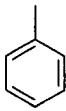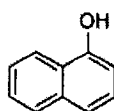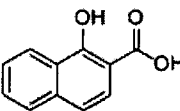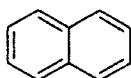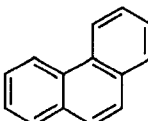
[a] Myrdal *et al.* (1992)
[b] Valko *et al.* (2001)
[c] Neumann *et al.* (2005)
[d] Novoszad *et al.* (2005)
[e] Meylan *et al.* (1996)
[f] Knightes and Peters (2003)

Although octanol-water partition coefficients are commonly determined by experimentation, alternative methods can be used in cases where the compound of interest is not readily available. Valko *et al.* (2001), who studied 86 diverse compounds, developed a method to calculate log K_{ow} values using reversed-phase high performance liquid chromatography (HPLC) retention time and a hydrogen bond acidity term.

Chromatographic Hydrophobicity Indices with acetonitrile (CHI_{ACN}) are also used to determine the hydrophobicity of a compound. The main difference between the CHI_{ACN} scales and the octanol-water partition coefficients is their sensitivity towards the hydrogen bond acidity ($\Sigma\alpha_2^H$) of the compounds (Valko *et al.* 2001). $\Sigma\alpha_2^H$ is calculated from the structure of the compound of interest. The partition coefficients can be calculated using the following equation:

$$\log K_{ow} = 0.054\ CHI_{ACN} + 1.319\Sigma\alpha_2^H - 1.877 \qquad (2.2)$$

Octanol-water partition coefficients have been used extensively by researchers to relate the bioavailability of compounds to their biodegradability (Atlas and Philp 2005). These measurements are useful predictors of the behaviour of many pollutants in the environment (Atlas and Philp 2005). For example, large non-polar molecules with large log K_{ow} values preferentially associate with organic solids in the environment (Atlas and Philp 2005).

2.2.5 Toxicity Effects

The mechanisms for membrane toxicity have yet to be thoroughly understood. The primary site of toxicity is suspected to be the cytoplasmic membrane (Sikkema *et al.* 1994). Membrane-buffer partition coefficients can be used to determine the location of individual chemicals. Aromatic hydrocarbons have been shown to reside in the membrane and the accumulation of these molecules results in swelling of the membrane bilayer (Sikkema *et al.* 1995).

21

Substances that accumulate in the cytoplasmic membrane are known to cause numerous adverse effects on the bacterium. The membrane structure may be altered which can cause numerous other problems. These compounds can prevent the cell from performing essential functions such as controlling pH and electrical potential as well as preventing the normal flow of ions, proteins, lipids and endogenous metabolites across the cell membrane. Membrane protein functions are also inhibited as a result of the undesirable compounds that have partitioned into the membrane. Ultimately, such changes to normal membrane functions can cause cell lysis and death (Fernandes *et al.* 2003).

Many solvents have been shown to cause adverse effects on membrane properties. To minimize these effects, the fatty acids undergo *cis* to *trans* isomerization in the presence of various organic solvents as the *trans*-unsaturated fatty acids are more rigid (Kieboom *et al.* 1998). The phospholipid headgroups and lipopolysaccharides can also be modified causing structural changes to the composition of the membrane.

Toluene destabilizes the inner membrane of gram-negative bacteria by causing the lamellar bilayer state to change to a hexagonal state (Mosqueda and Ramos 2000). As a result of this physical change in the membrane, proteins, lipids, and ions will leak out of the cell (Mosqueda and Ramos 2000). The cell membrane potential is disrupted and ATP synthesis will stop, ultimately leading to cell death (Mosqueda and Ramos 2000).

2.2.6 Efflux Mechanisms

Efflux pumps are prevalent in gram-negative bacteria (Hearn *et al.* 2003) and can contribute to antibiotic resistance and to solvent tolerance. Organic solvents, biocides, antimicrobial compounds and aromatic hydrocarbons are only a few of the compounds that are transported across cell membranes via pumping mechanisms. Antimicrobial compounds not only have the ability to affect membrane structure, they also have the ability to impair biosynthetic pathways that are essential for microbial growth (Fernandes *et al.* 2003). Efflux coupled with degradation can increase the tolerance of a bacterium to a toxic compound.

22

Efflux pumps are becoming better understood as the widespread occurrence of multidrug efflux in certain *Pseudomonas* species and *E. coli* has caused great concern. The dramatic increase in more resistant strains of bacteria may be attributable to any or all of these factors: society's overuse of antibiotics; increased use of household products containing biocide agents; and emission of toxic wastes (Fernandes *et al.* 2003).

Efflux pumps are divided into families including the resistance-nodulation-division superfamily (RND), the small multidrug resistance family (SMR), the major facilitator superfamily (MFS), the multidrug and toxic compound extrusion family (MATE) and the ATP-binding cassette family (ABC) (Poole 2005). Of these families, the ABC family is the only group that is not driven by proton-gradient energy; it is driven by ATP-hydrolysis energy and is commonly found in eukaryotes. Cells may contain more than one type of pump.

The RND pumps are comprised of transport proteins that span the inner and outer membranes of the cell envelope. The pumps contain three essential elements: a transporter protein in the cytoplasmic membrane, a membrane fusion protein and an outer membrane protein (OMP) (Fernandes *et al.* 2003). The OMP is thought to be an outer membrane channel necessary to circumvent the outer membrane barrier and, therefore, enable the pumped molecule to be released into the extracellular environment (Kieboom and de Bont 2001).

Many toxic compounds are pumped out of bacterial cells through multicomponent efflux machineries containing RND and MF transporters (Nikaido 1996). Common structural features among the substrates are difficult to pinpoint since the range of pumped substrates is quite diverse (Nikaido 1996).

The activity of efflux pumps in wild type cells has been shown to be strongly related to the metabolic state of the cells (Málač *et al.* 2005). Málač and his colleagues (2005) have shown that the depletion of cellular ATP levels inhibits the transport activity of the efflux pumps.

P. fluorescens LP6a possesses an active efflux mechanism for toluene, phenanthrene, anthracene and fluoranthene but not for naphthalene (Hearn *et al.* 2006). The efflux pump genes were detected using PCR in a strain that was cured of the plasmid containing the genes for PAH metabolism. The RND efflux system, shown in Figure 2.2, contains the three essential elements – the transporter protein, a membrane fusion protein and an OMP designated EmhB, EmhA and EmhC respectively where Emh stands for the efflux of multicyclic hydrocarbons. The EmhB pump showed homology to the multidrug and solvent efflux pumps in *P. aeruginosa* and *P. putida*: ArpB, TtgB and MexB (Hearn *et al.* 2003).
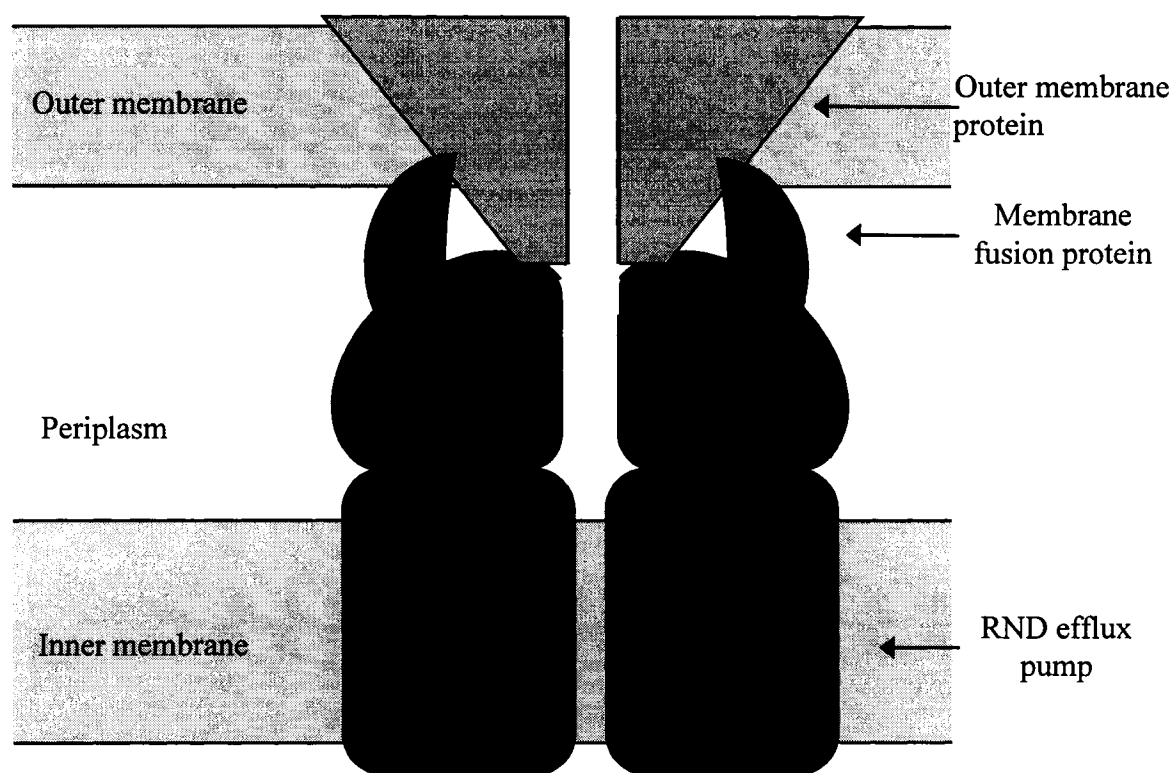
Figure 2.2 Diagram of the EmhABC system (Hearn 2005).

24

In order to better understand the effects of efflux ability, *emh*B was disrupted by inserting an antibiotic resistance cassette into the gene. Although the resistance of *P. fluorescens* cLP6a to tetracycline, erythromycin, trimethoprim or streptomycin did not change, the organism was less resistant to chloramphenicol and nalidixic acid proving that the latter antibiotics are indeed substrates of the pump. The importance of efflux mechanisms to reduce cellular toxicity levels is also emphasized as a result of the genetic manipulation experiment conducted by Hearn *et al.* (2003).

The efflux of PAH metabolites is an area that has been relatively unexplored although evidence of metabolite-specific channels is becoming increasingly stronger (Berezhkovskii *et al.* 2002). In a study conducted by Nair *et al.* (2004), salicylic acid, a common intermediate in the degradation of many PAHs, was shown to be actively effluxed by *Burkholderia cepacia*. Metabolite efflux mechanisms in LP6a strains have yet to be elucidated.

2.3 Metabolic Processes

2.3.1 Phenanthrene Degradation Pathways

Phenanthrene is a growth substrate for many microbial species and therefore it is susceptible to biodegradation (Boopathy 2000). Phenanthrene is often used to model the biodegradation of PAHs because of its low toxicity and its similarity in structure and physical properties to other PAHs (Adachi *et al.* 1999; Korytko *et al.* 2000).

The mineralization of phenanthrene by bacteria is achieved by both an upper and lower pathway. The upper pathway involves the conversion of phenanthrene to 1-hydroxy-2-naphthoic acid and the lower pathway involves the conversion of 1-hydroxy-2-naphthoic acid to CO_2 and H_2O (Figure 2.3). Products of growth-associated degradation include CO_2, H_2O and cell biomass (Jördening and Winter 2005).

25
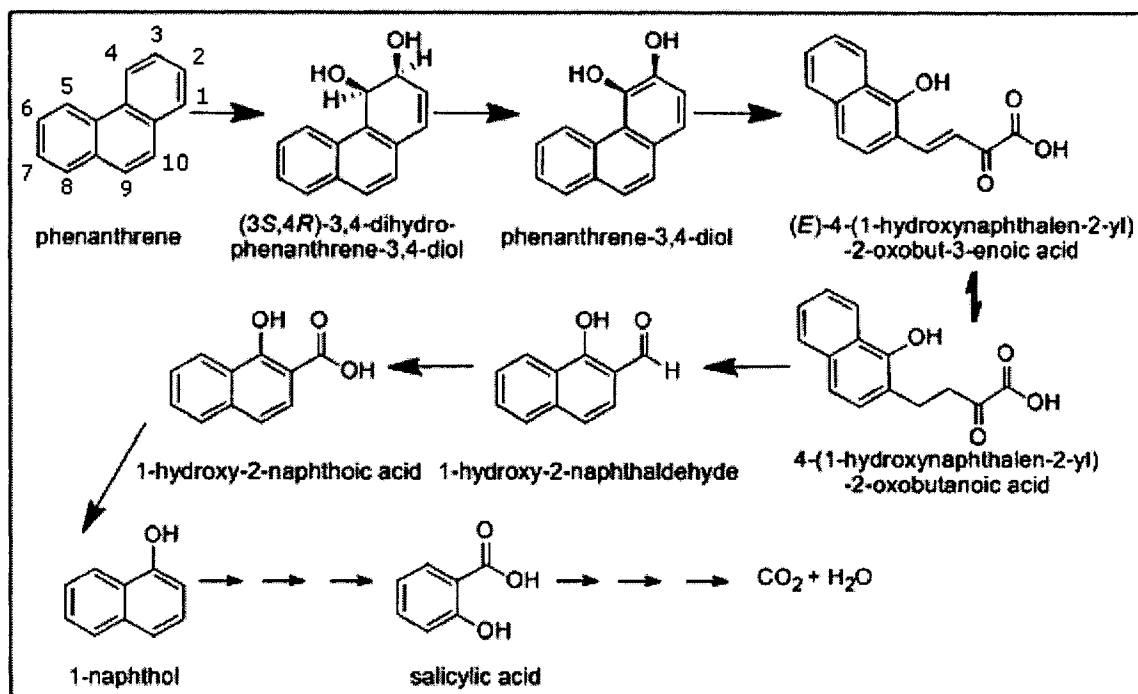
Figure 2.3 Proposed degradation pathway of phenanthrene in *P. fluorescens* LP6a.

Gram-negative bacteria degrade low molecular weight PAHs, such as naphthalene, phenanthrene and anthracene, by a classic dioxygenation at the Bay- or non-K-region of the molecule (Kim *et al.* 2005). *Pseudomonas* species degrade phenanthrene via dioxygenation either at the C-3 and C-4 ring positions, or at the C-1 and C-2 ring positions to form (3S,4R)-cis-3,4-dihydroxy-3,4-dihydrophenanthrene and (1R,2S)-cis-1,2-dihydroxy-1,2-dihydrophenanthrene respectively. The dihydrodiol is then converted to either 1,2- or 3,4-dihydroxyphenanthrene, which is further metabolized to 4-(1-hydroxynaphth-2-yl)-2-oxobut-3-enoic acid by an extradiolic ring fission reaction (Adachi *et al.* 1999; Moody *et al.* 2001). This open-ring compound is converted via 1-hydroxy-2-naphthaldehyde to 1-hydroxy-2-naphthoic acid.

26

The lower pathway varies among different bacteria. In one route, 1-hydroxy-2-naphthoic acid is converted to salicylic acid and catechol whereas in the other route, 1-hydroxy-2-naphthoic acid is converted to o-phthalate and protocatechuate (Moody et $al.$ 2001). Catechol is oxidized by either intradiol $ortho$ cleavage or extradiol $meta$ cleavage (Jördening and Winter 2005). Both ring cleavage reactions are catalyzed by specific dioxygenases. Protocatechuate is metabolized by a homologous set of enzymes (Jördening and Winter 2005).

Samanta et $al.$ (1999) discovered the formation of 1-naphthol, a new intermediate, in the phenanthrene degradative pathways of $Brevibacterium$ sp. HL4 and $Pseudomonas$ sp. DLC-P11. 1-Naphthol, produced from 1,2-dihydroxynaphthalene, is then converted to either salicylic acid or o-phthalic acid depending on the bacterial species (Samanta et $al.$ 1999).

Ultimately, the aerobic metabolism of many organic compounds leads directly or indirectly to the formation of acetyl-CoA as the central intermediate, which enters the tricarboxylic acid (TCA) cycle. The products of hydrocarbon degradation that are fed into the TCA cycle act as substrates of energy metabolism and as building blocks for the synthesis of cell biomass (Jördening and Winter 2005). Aerobic respiration of carbohydrates by bacteria results in roughly one third of the initial energy content being lost as heat (Jördening and Winter 2005). The remaining two thirds of the initial energy are temporarily conserved in ATP (Jördening and Winter 2005).

Biodegradation also has the potential to cause beneficial effects other than the removal of xenobiotics from the environment. Baboshin et $al.$ (2005), have discovered potential biosynthetic pathways as a result of the microbial transformation of phenanthrene and anthracene. These pathways produce hydroxylated PAHs, benzocoumarins, and hydroxy-naphthylalkanoic acids, which serve as chiral synthons in the preparation of chemicals and antioxidants that are of interest to pharmacy and specialty chemical industries (Resnick et $al.$ 1996).

27

The preparation of enantiopure forms of chiral compounds, used in medicinal or agricultural chemistry, is becoming necessary in order to meet specifications given by regulatory agencies (Di Gennaro *et al.* 2006). As many microorganisms produce enzymes that yield desirable enantiopure compounds, synthetic chemists now consider biological alternatives (Di Gennaro *et al.* 2006). Therefore, advanced knowledge of the specific biodegradation pathways and mechanisms will allow for the increased potential of microbes in this area of research.

Aromatic hydrocarbon dioxygenases are the cause of a source of new enantiopure arene cis-diols that cannot be produced by classical chemical synthesis. Therefore this biosynthesis route is a positive lead into "green" synthesis reactions (Gibson and Parales 2000).

2.3.2 Enzymes Involved in Biodegradation

Most of the information on the genetics of PAH metabolism deals with naphthalene catabolic plasmids such as NAH7 from *P. putida* strain G7 (Van Hamme *et al.* 2003). Sanseverino and his colleagues (1993), who studied phenanthrene and anthracene metabolism in three different *Pseudomonas* strains, were the first to report direct evidence showing that NAH catabolic plasmids are involved in degradation of PAHs other than naphthalene (Sanseverino *et al.* 1993).

The enzyme systems involved in PAH oxidation are not specific. Baboshin *et al.* (2005) showed that the naphthalene dioxygenase system of *Pseudomonas* sp. NCIB 9816 oxidizes more than 50 PAHs (Baboshin *et al.* 2005). The broad substrate activity of these enzymes is highly desirable considering the diversity of organic compounds present in contaminated sites.

28

Bacteria commonly group the genes coding for the enzymes in operons as a control strategy. The operons can be located on the main chromosome but are more commonly found on plasmids (Van Hamme *et al.* 2003). Catabolic plasmids are easily transferred via conjugation to other strains of bacteria and therefore have great potential to increase the catabolic activity of microbial communities in the environment.

The enzymes required for the degradation of naphthalene are encoded on two operons. The first *nah* (naphthalene degradation) operon, *nahAaAbAbAdBFCED*, encodes the pathway for the degradation of naphthalene to salicylic acid and the second operon, *nahGTHINLOMKJ*, encodes the transformation of salicyclic acid to catechol via catechol *meta*-cleavage to acetaldehyde and pyruvate (Van Hamme *et al.* 2003). A third operon contains *nahR*, which regulates the first two operons. The enzymes that are encoded on the upper pathway operon are listed in Table 2.3 below.

Table 2.3 Naphthalene degradative enzymes encoded by *nah* operons.

Short-Form	Enzyme
NahA	Naphthalene-1,2-dioxygenase
NahB	1,2-dihydroxy-1,2-dihydronaphthalene dehydrogenase
NahC	1,2-dihydroxynaphthalene dioxygenase
NahD	2-hydroxychromene-2-carboxylate isomerase
NahE	*cis-o*-hydroxybenzylidenepyruvate hydratase-aldolase
NahF	salicylaldehyde dehydrogenase
NahG	salicylate hydroxylase
NahH	catechol-2,3-oxygenase

29

Other bacterial species, such as *Nocardia, Rhodococcus*, and *Mycobacterium* spp., possess isofunctional gene sequences similar to *nah* but also encode genetic information required to degrade PAHs with higher molecular weights than phenanthrene (Van Hamme *et al.* 2003). Gene clusters including *nah, ndo* (naphthalene dioxygenation), *pah* (PAH degradation), and *dox* (dibenzothiophene oxidation) are highly homologous (~90%) and the gene arrangement amongst these sequences is conserved (Foght and Westlake 1996; Van Hamme *et al.* 2003). Many novel gene sequences and gene orders responsible for PAH degradation have also been discovered in various bacterial strains. Lateral gene transfer and genetic recombination may have contributed to the development of these novel metabolic pathways (Van Hamme *et al.* 2003).

Additionally, many clusters of catabolic genes are located on transposons. Due to the fact that transposons move about chromosomes thereby rearranging DNA sequences, new degradation pathways can created (Prescott *et al.* 2002).

The first enzyme involved in the degradation of phenanthrene is phenanthrene dioxygenase. Dioxygenases catalyze the incorporation of oxygen into the molecule (Atlas and Philp 2005). The resulting *cis*-dihydrodiol is subsequently converted to a diol by a dehydrogenase enzyme that cleaves the hydrogen atoms from the C-3 and C-4 positions. The same monooxygenases, dioxygenases and *ortho*-cleavage enzymes are likely involved in initial K-region attack as well as the subsequent ring fission of the dihydroxylated intermediates of phenanthrene (Moody *et al.* 2001).

The open-ring metabolite, 4-(1-hydroxynaphth-2-yl)-2-oxobut-3-enoic acid, is attacked by an aldolase, a hydratase-aldolase and an aldehyde dehydrogenase to yield 1-hydroxy-2-naphthoic acid (Krivobok *et al.* 2003). This compound is then converted to 1,2-dihydroxynaphthalene by a decarboxylase enzyme. This diol then enters the naphthalene degradation pathway and is converted by the enzymes encoded on the NAH7 plasmid as shown in Table 2.3 or it is attacked by the same enzymes that attacked the open-ring compound.

30

ATPases, transport proteins, transferases, various oxidoreductases, and signal-transducing enzymes are known to be located in the cytoplasmic membrane whereas other enzymes are located in the internal or external peripheral regions of the membrane (Sikkema *et al.* 1995). Enzyme activity can be measured spectrophotometrically after the cells are lysed and the cell debris is removed (Parales *et al.* 2000; Park *et al.* 2004; Baboshin *et al.* 2005). Because enzyme assays are performed after the cells have been lysed, the enzymes involved in PAH degradation are assumed to be localized in the cytoplasm (Parales *et al.* 2000).

2.3.3 Induction

When PAH-metabolizing strains are preincubated with either the parent compound or downstream intermediates, PAH dioxygenase activity may be stimulated and the initial rates of phenanthrene removal can increase (Chen and Aitken 1999). Salicylic acid is a known inducer of both the upper and lower operons carried on the NAH7 plasmid (Samanta *et al.* 2002).

Enzyme induction depends on the concentration of the inducing molecules. Typically, micromolar quantities of the inducer are added to the bacterial culture during the final stages of growth (Foght and Westlake 1996; Jördening and Winter 2005). The inducible nature of the enzymes as well as their broad substrate specificity, enhance the ability of bacteria to degrade xenobiotic compounds in the environment (Chen and Aitken 1999).

2.3.4 Microbial Kinetics

Substrates bind to active sites on enzymes to create an enzyme-substrate complex (Prescott *et al.* 2002). The product is released from then enzyme leaving the enzyme free to bind and convert more substrates. Enzymes are responsible for increasing the rate of reaction. As mentioned in Section 2.3.2, many bacterial species are capable of producing enzymes that are involved in phenanthrene degradation.

31

Because the intracellular concentration of PAHs is relatively low, the ability of the enzyme and substrate to form a complex is more difficult (Prescott *et al.* 2002). Thus, the rate of reaction increases as the substrate concentration increases until the active sites become saturated with substrates and the reaction velocity has reached its maximum value (V_{max}) (see Figure 2.4 below). The relationship between the rate of the reaction (velocity) and the substrate concentration is governed by the Michaelis-Menten equation:

$$ v = \frac{V_{max} \times S}{K_m + S} \tag{2.3} $$

where S is the substrate concentration and K_m is the Michaelis-Menten constant. K_m is equal to the substrate concentration that is required to achieve half of the maximum velocity. This constant is used as a measure of the affinity of an enzyme for its substrate (Prescott *et al.* 2002).
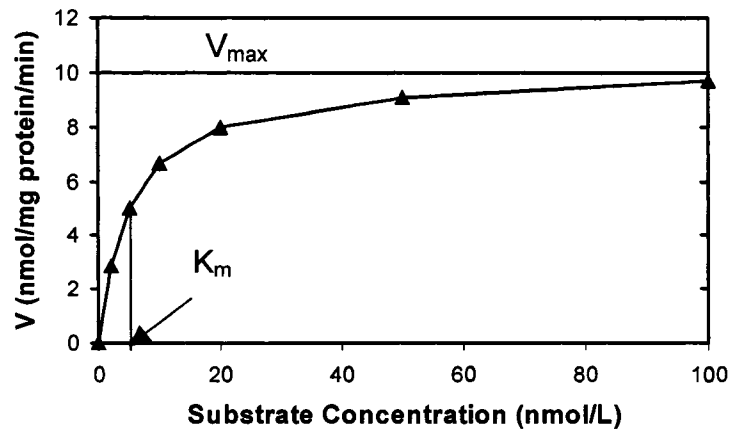
Figure 2.4 Example of Michaelis-Menten kinetics.

More than one molecule may be able to bind to the active site of the enzyme, compromising the conversion of the desired substrate. Such molecules are similar in structure to the substrate and are known as competitive inhibitors (Prescott *et al.* 2002). Enzyme activity is affected by many other external factors including pH and temperature. In order to achieve the highest possible conversion rate of the substrate, the optimal conditions for the specific enzyme involved must be determined.

To improve the rate of PAH degradation, it is necessary to determine the rate-limiting step of the reaction process. Possibilities include the transport of the PAHs across the cell membrane, the diffusion of the substrate in the cytoplasm, the chemical transformation of the PAH and the binding of the substrate to the enzyme (Wammer and Peters 2005).

In order for phenanthrene to be degraded by *P. fluorescens* LP6a strains, the substrate must first cross the outer membrane, the periplasm and the bacterial cell membrane to combine with the dioxygenase enzymes that will commence the degradation process (Wammer and Peters 2005). Bugg *et al.* (2000) proved that phenanthrene enters into the cell by passive diffusion and not by active uptake of the PAH.

Wammer and Peters (2005) stated that "active transport mechanisms are involved only in PAH efflux and do not have significant effects on degradation rate". This statement is based on the lack of correlation between the degradation rate of the PAHs and the octanol-water partition coefficients as well as the lack of correlation between the reaction rate and the diffusivity of the PAHs (Wammer and Peters 2005). Therefore, it is unlikely that the rate-limiting step is the passage across the cell membranes or the diffusion of PAHs through the cytoplasm. Wammer and Peters (2005) were also unable to show that the chemical transformation and the binding of the substrate to the active site of the enzyme were rate-limiting. The rate-limiting step was not determined in this study; rather, a hypothesis was stated that the rate is dependent on the active enzymes and not on transport.

33

In addition to determining the rate-limiting step, it is also highly desirable to discover ways to increase the rate of degradation. Bugg *et al.* (2000) showed that *P. fluorescens* LP6a actively effluxes phenanthrene, a growth substrate for this particular strain. This action is surprising since it would lower the phenanthrene concentration in the cell pellet and therefore, according to the Michaelis-Menten equation, the rate of phenanthrene degradation providing that the rate is not at V_{max}.

Therefore, the information discussed in Section 2.0 is of great importance to this study on phenanthrene metabolism and transport across the cell membranes of *P. fluorescens* LP6a strains.

34

3.0 MATERIALS AND METHODS

3.1 Chemicals

Phenanthrene (98% pure) and o-terphenyl were purchased from Aldrich Chemical Company (St. Louis, MO, USA). Naphthalene and 1-hydroxy-2-naphthoic acid were obtained from Sigma Chemical Company (St. Louis, MO, USA). Salicylic acid was purchased from Analar (British Drug Houses Ltd, Poole, England) and dibenzothiophene (DBT) was purchased from Fluka Chemika (Sigma-Aldrich, Steinheim, Switzerland).

[9-^{14}C]Phenanthrene (96.5% radiochemical purity; 19.3 mCi mmol^{-1}; Amersham, Arlington Heights, IL, USA) and [7-^{14}C] salicylic acid (98% radiochemical purity; 55.70 mCi mmol^{-1}; New England Nuclear, Boston, MA, USA) were used to track the location of the parent compound and its metabolites in the radiolabeled transport assays.

3.2 Other Compounds

Sodium azide and the Chromerge ® cleaner were obtained from Fisher Scientific (Fairlawn, NJ, USA). Aqueous liquid scintillation fluor was obtained from Amersham Ltd. and N,O-bis(trimethylsilyl)-trifluoroacetamide (BSTFA) was purchased from Pierce Chemical Company (Rockford, IL, USA).

N,N-dimethylformamide (DMF) was purchased from Anachemica (Montréal, QC, Canada) and 2,2,4,4,6,8,8-heptamethylnonane (HMN) was purchased from Aldrich Chemical Co. Ethyl acetate and dichloromethane (DCM) (high performance liquid chromatography grade) were from Fisher Scientific. Diethyl ether was from EM Science (Gibbstown, NJ, USA). Hexane (non-UV) was purchased from Caledon Laboratories Ltd. (Georgetown, ON, Canada) and glacial acetic acid was purchased from J.T. Baker (Phillipsburg, NJ, USA).

Bacto Agar, Noble Agar, R2A, tryptic soy broth (TSB) and plate count agar (PCA) were all Difco brand from Becton, Dickinson and Company (Sparks, MD, USA). Kanamycin was obtained from Sigma Chemical Company.

3.3 Bacterial Strains, Plasmids and Growth and Harvesting Conditions

Pseudomonas fluorescens LP6a was chosen for this study because it can utilize polycyclic aromatic hydrocarbons (PAHs) such as phenanthrene as a source of carbon and energy. This bacterium possesses an efflux pump belonging to the resistance-nodulation-division superfamily known as the EmhABC efflux system (Hearn *et al.* 2003). Not only does this bacterium pump compounds that are toxic to it such as antibiotics and organic solvents, it also pumps PAHs, which are not toxic to the bacterium and are in fact used by the microorganism as growth substrates (Bugg *et al.* 2000).

The six bacterial strains that were used in this study are described below in Table 3.1. Four of the six strains have been previously described in studies conducted by Foght (2004), Foght and Westlake (1996), and Hearn *et al.* (2003). Since the goal of this research was to determine the effect of the EmhABC efflux system on the rate of biodegradation of phenanthrene, it was necessary to contrast strains with and without efflux capabilities.

36

Table 3.1 Characterization of each of the six strains of *P. fluorescens* LP6a used in this study.

Strain	Short-Form	Plasmid	Degradation Product	EmhABC
LP6a (wild type)[a]	WEP	pLP6a	CO_2+H_2O	✓
cLP6a-1 pLP6a[b]	WEN	pLP6a		✗
LP6a p21-41[c]	OREP	p21-41		✓
cLP6a-1 p21-41[b]	OREN	p21-41		✗
cLP6a[a]	NEP	-		✓
cLP6a-1[d]	NEN	-		✗
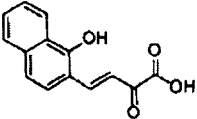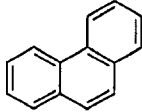
[a] Foght and Westlake (1996)
[b] This study
[c] Foght (2004)
[d] Hearn *et al.* (2003)

The metabolic capability of the strain is described by W, OR or N, where W indicates that the strain possesses the *w*ild type metabolic capabilities, OR indicates that the strain can degrade phenanthrene to the *o*pen-*r*ing compound, and N indicates that the strain has *n*o metabolic capabilities. EP and EN stand for *e*fflux *p*ositive and *e*fflux *n*egative respectively.

WEP is able to mineralize phenanthrene and thus numerous metabolites were expected. Since the exact number of metabolites this biodegradation reaction would produce was unknown, a transposon mutant (OREP) that was blocked partway down the metabolic pathway was studied. This strain was expected to accumulate the open-ring structure for which it is named, trans-4-(1-hydroxynaphth-2-yl)-2-oxobut-3-enoic acid (Foght and Westlake 1996). Additionally, a cured strain (NEP) was studied because it lacks the PAH degradation plasmid and thus the ability to metabolize PAHs.

An efflux-deficient cured strain, NEN, constructed by Hearn et al. (2003) by the insertion of an antibiotic resistance cassette into the emhB gene, was also used in this study. The efflux-deficient strains WEN and OREN were constructed in this study.

The catabolic plasmid pLP6a, known to be 63 kilobases (kb) in length, provides the polycyclic aromatic hydrocarbon (PAH) degradation genes found in the wild type strain of P. fluorescens LP6a (Foght and Westlake 1996). The plasmid p21-41 was created by Foght (2004) by the random insertion of a Tn5 transposon into nahE on pLP6a. The segment of DNA that was added possessed a gene for kanamycin resistance. Therefore, to prevent the loss of the transposon, kanamycin was added to the growth medium.

Cryopreserved glycerol stocks of the P. fluorescens LP6a strains were prepared with overnight seed cultures of each strain grown in tryptic soy broth (TSB) at 30°C on a tube roller. The cultures were centrifuged at 4°C for 10 min at 6 000 x g on a Sorvall RC-5B refrigerated superspeed centrifuge (Dupont Instruments; Newtown, CT, USA). The cells were resuspended in 1 mL of TSB and 1 mL of 50% glycerol was added to the tube. A 1 mL aliquot of this suspension was transferred to a plastic screw-top vial and the tube was incubated at room temperature for 30 min. The vials were stored at −80°C.

38

Loopfulls of the glycerol stocks were streaked onto Plate Count Agar (PCA) or Luria Bertani (LB) agar supplemented with kanamycin. The plates were incubated for 24 to 48 h at 30°C. Fresh plates were prepared from the frozen glycerol stocks prior to each experiment. Five millilitres seed cultures were grown overnight in test tubes that were placed on a tube roller at 28°C. Liquid cultures of *P. fluorescens* strains were grown from a 0.5% (vol/vol) inoculum of seed culture in 100 mL of TSB. The liquid cultures were incubated for 24 h at 28°C with shaking (200 rpm). Kanamycin (25 μg mL^{-1}) was filter-sterilized and added after medium sterilization as required for the efflux-deficient mutants (WEN, OREN and NEN) and the transposon mutant (OREP).

The liquid cultures were harvested by transferring 20 mL of the suspension to a sterile centrifuge tube and centrifuging at 10 000 x g for 10 min on a Sorvall RC-5B refrigerated superspeed centrifuge. The supernatant was removed using Eppendorf pipettes and the pellet was resuspended in 10 mL of 0.1 M potassium phosphate buffer (PB). The cells were then centrifuged and resuspended in 10 mL of 0.1 M PB. The cell suspensions were diluted (50 μL of cell suspension in 950 μL of PB) and the optical densities at 600 nm (OD$_{600}$) were measured with a Philips PU 8740 UV-vis spectrophotometer. The concentrated suspensions were used to obtain a 20-mL suspension with an OD$_{600}$ of 1.

3.4 DNA Techniques

The plasmid preparation procedure developed by Kieser (1984) was slightly modified and used to isolate pLP6a from WEP and p21-41 from OREP. In the modified Kieser plasmid preparation, 1.5 mL of an overnight culture of WEP was pipetted into a microcentrifuge tube and centrifuged for 2 min at 13 500 rpm. The pellet was resuspended by vortex in 0.5 mL of a sterile solution containing 0.3 M sucrose, 25 mM Tris, 25 mM Na$_2$EDTA (pH 8) and then the tube was incubated for 5 min at room temperature. A total of 250 μL of a lysis solution containing 0.3 M NaOH and 2% sodium dodecyl sulphate (SDS; pH 12.5) was added at this time. The tube was gently inverted immediately after the addition of the lysis solution and the suspension turned clear instantaneously. The tube was then incubated for 20 min at 55°C and cooled to

39

room temperature. A 250-μL aliquot of an acidic solution containing phenol and chloroform (5 g crystalline phenol, 5 mL CHCl$_3$, 5 mg 8-hydroxy-quinoline and 1 mL of dH$_2$O) was added to the tube and was mixed by inverting and gentle vortexing. Since the solution was slightly lumpy, an additional 100 μL of lysis solution was added in order to achieve a homogenous mixture in the tube. The tube was then centrifuged at 13 500 rpm for 3 min in order to separate the phases. Roughly 600 μL of the top layer was transferred to a new microcentrifuge tube using a pipette tip that was shortened to reduce the shear force and to avoid disturbing the interphase material. At this point, 250 μL of chloroform was added to the tube. The solution was mixed gently before being centrifuged for 3 min. A 500-μL portion of the upper layer was carefully transferred to a clean tube and 55 μL of 3 M sodium acetate at pH 5.8 was added to the tube. This mixture was diluted 1:3 with cold 95% ethanol. The solution was mixed by gentle inversion. The plasmid DNA precipitated after placing the tube in a –70°C freezer for 30 min. The DNA was subsequently harvested by centrifugation at 13 500 rpm for 15 min at 4°C. The DNA was washed with 70% ethanol, dried and then gently redissolved in 25 μL dH$_2$O.

Initially, several unsuccessful attempts were made at isolating the plasmid pLP6a from WEP using a QIAprep Spin Miniprep kit (Qiagen; Mississauga, ON, Canada). The QIAprep Spin Miniprep kit that was used is only suitable for plasmids smaller than 50 kb.

Restriction digestion reactions of the plasmids were performed according to the supplier's directions (Roche Applied Science; Laval, QC, Canada). The DNA fragments were separated by electrophoresis on agarose gels and the DNA bands were visualized by staining the gels with ethidium bromide.

Electrocompetent NEN cells were prepared by growing cultures in 100 mL of TSB at 28°C with shaking at 200 rpm. The cultures were grown to an OD$_{600}$ of 0.4-0.6, harvested at 4°C by centrifugation at 5 000 x g for 10 min, washed twice in cold 10% (vol/vol) glycerol, and finally concentrated 50-fold in 10% (vol/vol) glycerol. Electrocompetent cells were stored at -80°C.

40

Plasmid DNA was introduced into electrocompetent NEN cells by electroporation with a Gene Pulser at a resistance of 200 Ω, an electric charge of 25 μF, and a voltage of 2.5 kV across a 0.2-cm cuvette (Bio-Rad Laboratories; Mississauga, ON, Canada).

To ensure that plasmids were correctly inserted into NEN, colonies of WEN and OREN were grown on mineral medium (Foght and Westlake 1996) plates that were supplemented with naphthalene in the vapour phase and with salicylic acid added directly to the agar respectively. Solid naphthalene crystals were placed on the lids of the Petri dishes and either 50 μL or 100 μL of a 75 mM sodium salicylate solution was spread onto the MM plate and was allowed to diffuse through the agar for roughly 4 h. If colonies formed within a reasonable period of time (<1 week), the colonies were grown in liquid culture and subjected to further testing.

To show that WEN and OREN possessed the desired plamids, the cells were grown in liquid culture and the DNA was isolated using the modified Kieser plasmid preparation (Kieser 1984). The DNA was then subjected to a restriction digestion reaction and the cut DNA was separated by electrophoresis on agarose gels.

The dibenzothiophene (DBT) spray plate method (Kiyohara *et al.* 1982) was also used to test if colonies of the constructed strains were capable of metabolizing DBT. If metabolism occurs, the colonies should turn bright orange. A small amount of DBT was dissolved in dichloromethane (DCM) and sprayed onto R2A plates that were streaked with cells from the glycerol stocks and grown for 24 h. Additionally, a few crystals of solid DBT were added to aqueous cell suspensions of WEN and OREN respectively, and the cultures were monitored for the production of the orange-coloured, open-ring metabolite.

The final test that was performed to confirm the correct construction of WEN and NEN was to identify phenanthrene metabolites by extracting the WEN and OREN cell suspensions that were exposed to 6.36 μM phenanthrene for a period of 20.5 min. This test is described more thoroughly in Section 3.10.

3.5 Microbial Characterization

3.5.1 Optical Density at 600 nm (OD_{600})

Optical density was used to determine the amount of biomass required for each experiment. A 50-μL sample of the liquid culture in TSB was diluted in 950 μL of TSB and the OD_{600} was measured on a Philips PU 8740 UV-vis spectrophotometer to test for normal growth.

Once the culture was harvested, washed and resuspended in 0.1 M PB, 50 μL of this suspension was diluted in 950 μL of 0.1 M PB and the OD_{600} was measured. This value was used to determine the volume of cells required to make up the final 20-mL suspensions at an OD_{600} of 1 that were used in all experiments.

3.5.2 Colony Forming Units (CFU)

Plate counts were also used to ensure that the OD_{600} values were comparable for all strains. Plate counts were performed by preparing a cell suspension with an OD_{600} of 1 and generating serial dilutions to a dilution factor of 10^{-7}. A total of 0.1 mL of each of the 10^{-5}, 10^{-6} and 10^{-7} dilutions was spread onto PCA plates. Three independent measurements from separate culture flasks were made for each strain. The plates were incubated at 30°C for 24 h. The dilution that produced between 30 and 300 CFU was used to determine the CFU concentration (CFU/mL) for that particular culture.

3.5.3 Bicinchoninic Acid (BCA) Protein Assay

The BCA protein microassay (Smith *et al.* 1985) was used to quantify the amount of protein in a given sample. This colourimetric assay is similar to the Lowry protein assay but it is less sensitive to NaOH and does not need to be precisely timed. BCA is an effective detection reagent for the cuprous cation (Cu^+). The protein in the sample reduces the copper in an alkaline medium. Two molecules of BCA react with copper I, forming an intense purple colour that exhibits strong absorbance at 562 nm.

42

A BCA protein assay kit was obtained from Pierce Chemical Company (Rockford, IL, USA). A stock solution of bovine serum albumin (BSA) was provided in small ampules at a concentration of 2 mg/mL. Standards were prepared in 0.1 N NaOH the range of 0 to 1 000 μg protein/mL and 10 μL of each standard was pipetted in triplicate into designated wells of a 96-well plate. The working reagent was prepared by mixing 1 part Reagent B to 50 parts Reagent A and 200 μL of the working reagent was added to each well. The plate was then incubated at 60°C for 30 min and the A_{562} was measured on a plate reader.

One hundred microlitres of a cell suspension with an OD_{600} of 1 was diluted with 900 μL of 0.1 M PB in a microcentrifuge tube. The tube was then centrifuged for 10 min. The supernatant was removed, the cells were resuspended in 1 mL of 0.1 M PB and the tube was centrifuged for 5 min. The supernatant was then discarded and the pellets were stored in the freezer until all samples were ready for the BCA assay.

The cells were thawed and resuspended by vortex in 100 μL of 0.1 N NaOH. The tube was then incubated at 60°C for 30 min to lyse the cells. The tube was vortexed and 10 μL samples were pipetted in triplicate into wells of a 96-well plate. Two hundred microlitres of working reagent was added to each well and the plate was incubated at 60°C for 30 min before the absorbance at 562 nm (A_{562}) was measured on the plate reader.

3.6 Glassware Treatment

To reduce the amount of PAH adsorption to glassware, Bugg et al. (2000) developed the following procedure to treat the glassware: the glassware was soaked in Chromerge ® overnight, rinsed thoroughly with water and finally rinsed with double-distilled water. The glassware was dried and autoclaved before it was used. All glassware used in this study was acid-washed using this procedure.

43

3.7 Phenanthrene Transport Assays

The partitioning of radiolabeled phenanthrene between the supernatant and pellet phases for each strain was quantified using the rapid centrifugation method described by Bugg *et al.* (2000). All transport assays were performed at room temperature.

Liquid cultures of the various strains were grown overnight to an OD_{600} of roughly 4 in 100 mL TSB, with kanamycin added as required, as described in Section 3.3. The cells were harvested by centrifugation at 10 000 x g and 4°C in a Sorvall RC-5B refrigerated superspeed centrifuge. The supernatant was discarded and the cells were washed twice in 0.1 M PB (pH 7.2) and resuspended to a final OD_{600} of 1 in 0.1 M PB. Twenty millilitres of this suspension were added to 250-mL Erlenmeyer flasks for each transport assay that was conducted.

Thirty microlitres of a mixture of radiolabeled phenanthrene and unlabeled phenanthrene (see Appendix B for detailed calculations) were added to the 20 mL cell suspension resulting in a final phenanthrene concentration of 6.36 μM, which corresponds to 90% of phenanthrene's aqueous solubility limit (Hearn 2005). A total of 100 000 disintegrations per minute (dpm) were added to each flask at the start of the assay (t=0, where t=time).

The accumulation of the label in the cells was measured by taking 1-mL samples of the cell suspension at given time intervals. The samples were added to 1.5-mL microcentrifuge tubes and the cells were harvested by microcentrifugation at 16 000 x g for 20 s. A 0.5-mL aliquot of the supernatant was added to 10 mL of aqueous scintillation fluor. The remaining supernatant was carefully discarded into a waste container and 1.0 mL of fresh 0.1 M PB (pH 7.2) was added to the tube. The pellet was resuspended by gently vortexing. A 0.5-mL aliquot of the pellet fraction was added to 10 mL of aqueous scintillation fluor. Both samples were counted using a Beckman LS3801 liquid scintillation counter.

44

Samples were taken at 0.5, 4.5, 8.5, 12.5, 16.5 and 20.5 min after substrate addition. To ensure all active transport processes were inhibited, sodium azide crystals were added to obtain a final concentration of 30 mM 9.5 min after substrate addition. This time was chosen to allow for the substrate to partition between the pellet and supernatant phases and thus to reach steady state. Sodium azide was also added 1 min before t=0 to help to determine whether or not phenanthrene metabolites are substrates of the EmhABC efflux system. In one series, no azide was added at all to gain an understanding of the natural partitioning and degradation trends. All strains were tested in triplicate from separate culture flasks.

Killed-cell controls of WEP were also assayed in triplicate with sodium azide addition at t=9.5 min. The cells were killed either by autoclaving the 20-mL cell suspensions for 20 min and allowing the cultures to cool to room temperature before t=0, or by adding 1 mL of concentrated HCl to the cell suspension before the start of the assay. Fifty-microlitre aliquots of each suspension were plated on appropriate media and incubated to test for cell viability.

The transport assay was also attempted using [7-^{14}C]salicylic acid as the substrate in order to test the efflux of a metabolic intermediate (see Appendix C). Additionally, transport assays involving the use of induced cultures of WEP were performed in an attempt to obtain higher rates of degradation (see Appendix D).

3.8 Phenanthrene Desorption Kinetics

In order to determine if the rate of phenanthrene partitioning from the sides of the flask to the supernatant was rate-limiting, a simple experiment was performed. Twenty millilitres of 0.1 M PB were added to an acid-washed 250-mL Erlenmeyer flask. A 30-μL aliquot of the radiolabeled phenanthrene solution was added to yield a final concentration of 6.36 μM and 100 000 dpm. A 0.5-mL aliquot of the solution in the flask was taken after 0.5 min and added to 10 mL of aqueous scintillation fluor. The remaining solution was discarded and 20 mL of fresh PB was placed in the flask. After 30 s of manual shaking, another 0.5-mL sample was taken and added to a vial containing aqueous scintillation fluor. This rinsing procedure was continued 3 more times. All the samples were then counted by a liquid scintillation counter. This assay was performed in triplicate.

3.9 Phenanthrene Biodegradation Assay

To extract degradation rate information from the transport assay curves, the residual phenanthrene concentration from the test system after 20.5 min was assumed to be negligible. To prove this assumption, phenanthrene was added to 20 mL of a cell suspension with an OD_{600} of 1 in 3 mM phosphate buffer in an acid-washed, autoclaved flask. Twenty microlitres of a stock phenanthrene solution (in 95% ethanol) was added to the 20 mL cell suspension to yield a final concentration of 6.36 μM. Periodically, the flask was manually shaken over a 20.5-min period. At the end of this time period, 1 mL of concentrated HCl was added to the flask to drop the pH below 1 and to kill the cells. The flask was continuously shaken for 30 s followed by periodic, manual shaking for 15-30 min. Since the total phenanthrene concentration was of interest, the supernatant and the pellet fractions were not separated in this assay. Thirty microlitres of the extraction standard, o-terphenyl, was added to each flask in an ethanolic solution. The flasks were stored at $-20°C$ until they were extracted.

46

The assay was also performed using killed-cell controls in which the cell suspension was acidified with concentrated HCl 30 min prior to substrate addition. The killed-cell controls were required to show that the removal of phenanthrene from the suspension was indeed due to the presence of active microorganisms.

The acidified cell suspensions were thawed to room temperature and they were extracted thrice with 8 mL of DCM. The pooled solvent extract was collected in a glass Corex ® tube and concentrated to a volume of less than 3 mL. Due to the limited quantity of phenanthrene that was added to the flask (22.67 µg), it was not desirable to dry the extract over sodium sulphate. As an alternative to this method, the extract was placed in the freezer overnight so that any water present in the extract would form ice and the solvent could be transferred to a clean, acid-washed Corex ® tube. Unfortunately, due to the thick mucous layer and white chunky material that formed on top of the extract when cells were present, the extract had to be filtered through sodium sulphate to remove the solid material. The extract was transferred to a 1.5-mL gas chromatography (GC) vial. The extract was concentrated to dryness under a stream of nitrogen gas. A second aliquot of the extract in the Corex ® tube was transferred to the vial and concentrated to dryness. This procedure was repeated as many times as was necessary to dry all the extract. Once all of the extract had been concentrated, the Corex ® tube was rinsed 3 times with DCM and the rinse was dried in the same GC vial. A known amount of DBT was added to the vial and the vial was made up to 500 µL with DCM.

o-Terphenyl was used to roughly determine the extraction efficiency of phenanthrene whereas DBT was used to estimate the amount of phenanthrene that was actually extracted. The samples were derivatized with BSTFA in order to determine which metabolites had been produced after 20.5 min. This procedure was repeated for all metabolizing strains. Cell-free extracts were also analyzed by gas chromatography-mass spectrometry (GC-MS) as well as killed-cell controls. Scaling-up was not an option since it was necessary to use the exact conditions that were used in the transport assays in order to correlate these data to the data obtained from the assays.

47

Standard curves for phenanthrene, *o*-terphenyl and DBT were prepared by plotting the peak areas obtained from the gas chromatograms as a function of concentration. Phenanthrene concentrations ranged from 0.002 µg/µL to 1.0 µg/µL.

3.10 Phenanthrene Metabolite Extraction

The extraction procedure was first developed using DBT as the substrate since coloured metabolites are produced, making it easier to determine if the metabolites partition into the organic phase (see Appendix E).

In the preliminary experiments with phenanthrene, the substrate was added in either 2,2,4,4,6,8,8-heptamethylnonane (HMN) or N,N-dimethylformamide (DMF). The use of HMN as a carrier caused numerous hydrocarbon peaks in the gas chromatograms thus making the identification of metabolites difficult. Although DMF did not cause extra peaks in the gas chromatograms, it affected the concentration of the parent compound and its metabolites in the pellet fraction since fine particles of phenanthrene could be trapped in the pellet as a result of the centrifugation process, thus causing overestimation. In subsequent experiments, phenanthrene was added either in DMF when looking for metabolites or in ethanol when looking for phenanthrene.

Liquid cultures of WEN and OREN were induced by adding 0.5 mM of an ethanolic salicylic acid solution during the final 3 h of growth. The cells were harvested and diluted to produce a 100-mL cell suspension with an OD_{600} of 1. A 1-M solution of phenanthrene in DMF was prepared and 50 µL of this solution was added the cell suspension in order to yield a final concentration of 0.5 mM of phenanthrene. After 2 h of incubation with the substrate, the cells were harvested by centrifugation. The supernatant was transferred to an Erlenmeyer flask and the pellet was lysed in 30 mL of lysis solution (0.3 M NaOH and 2% SDS) at 60°C for 30 min. The pellet fraction was then acidified to pH 1 using concentrated HCl.

48

The supernatant fraction was acidified and extracted thrice with 25 mL of DCM followed by 3 x 25 mL of ethyl acetate. The pellet fraction was extracted thrice with 5 mL of DCM followed by 3 x 5 mL of ethyl acetate. The supernatant and pellet extracts were pooled and dried over anhydrous sodium sulphate, concentrated to 1-3 mL on a rotary evaporator, filtered through glass wool and finally concentrated to dryness with nitrogen in glass GC vials. o-Terphenyl, the internal standard, was added to the vial and the solution was made up to 500 μL with DCM. The extract was derivatized with BSTFA before analyzing the samples on the GC-MS.

This exact procedure was followed using WEP, WEN, OREP, OREN and NEP strains with the exception that a mixture of labeled and unlabeled phenanthrene was added at t=0. The reaction time was either 10 min or 20.5 min. In order to separate the pellet from the supernatant, 1.5 mL of the suspension was centrifuged according to the rapid centrifugation method previously described by Bugg et al. (2000). The supernatant was removed to an acid-washed flask containing 1 mL of concentrated HCl, and a second aliquot of the cell suspension was then added to the tube. The centrifuging procedure was repeated until all 20 mL of the suspension had been separated. The flasks were stored at – 20°C until the extraction step.

The supernatant fractions were extracted at room temperature, following the addition of the internal standard, o-terphenyl, to give a final concentration of 10 mg/mL. The supernatant fraction was extracted with 3 x 8 mL of DCM.

The pellet fractions were also stored in the freezer until they were extracted. The cell pellets were resuspended in 1.5 mL of 0.3 N NaOH and incubated at 60°C for 30 min. The pellets were subsequently centrifuged for 40 min to remove cell debris. The supernatant was removed to a Corex ® tube containing 0.5 mL of concentrated HCl and 7 mL of 0.1 M PB. Another 1.5 mL of NaOH was added to the tube and the pellet was once again resuspended. The tube was centrifuged for 5 min and the liquid phase was transferred to the Corex ® tube containing the HCl and PB. o-Terphenyl was added to the

49

tube before the solution was extracted with 3 x 4 mL of DCM. The tubes were left open in the fumehood to evaporate the solvent. To speed up the drying time, the tubes were gently heated in a warm water bath. The tubes were then transferred to the freezer until they were analyzed by TLC/autoradiography.

3.11 Analytical Techniques

3.11.1 Scintillation Counting

Samples of the pellet and supernatant fractions obtained from the transport assays were counted in 10 mL of aqueous scintillation fluor using a Beckman LS3801 liquid scintillation counter with automatic quench correction. The number of disintegrations per minute (dpm) was measured for each sample. The dpm values were then used to determine the fraction of recovered label, relative to the ^{14}C that was added at t=0. The concentration could easily be calculated from the fractional amounts (see Appendix B for details). The samples were dark-adapted for a period of at least 30 min before they were counted to reduce the interference by chemiluminescence.

3.11.2 Gas Chromatography-Mass Spectrometry (GC-MS)

All extracts were analyzed by GC-MS using an Agilent Technologies 5973 gas chromatograph-mass spectrometer. An HP-5 MS capillary column (0.25 mm x 30 m x 0.25 μm) was used in all cases (J&W Scientific; Folsom, CA, USA). The column was operated with the following GC temperature program: 90°C for 1 min followed by an increase of 10°C per min up to 280°C and then held for 5 min. This program was used for all samples and standards.

50

3.11.3 Thin Layer Chromatography (TLC) and Autoradiography

Silica gel GF TLC plates (Analtech; Newark, DE, USA) were used for all thin layer chromatographic separations. The solvent system used was a 70:30:2 mixture of hexane:diethyl ether:glacial acetic acid. A small volume of the solvent mixture was poured into the chamber to obtain a depth of roughly 1 cm. To serve as a wick, a piece of filter paper was cut to an appropriate size and placed in the chamber. The chamber was allowed to equilibrate for at least 1 h.

A 0.5-μL sample was spotted about 1.5 cm from the bottom of the silica plate using an Eppendorf micropipette. The spot was allowed to dry before a second 0.5-μL sample was applied to the same spot if the solution was dilute. Once all the spots were dry, the silica plate was placed in the chamber and developed until the solvent reached 1 cm from the top of the plate. The solvent front was noted and then the plate was dried completely before performing the autoradiography.

In the dark room, with the red light on, an X-OMAT^{TM} AR film (Eastman Kodak Company; Rochester, NY, USA) was placed on top of the TLC plate in an autoradiography cassette with an Gronex ® Lightning enhancer. The cassette was covered with a dark plastic bag and stored at −20°C for at least 24 h. The film was developed in an RGII Fuji X-ray film processor and then the autoradiogram was then overlaid on the TLC plate to identify the spot locations. The corresponding areas were carefully scraped into a vial containing 10 mL of aqueous scintillation fluor. The vial was shaken and then left to adapt in the dark at least 1 h before the sample was counted on the liquid scintillation counter.

51

3.12 Testing for Mineralization

To determine whether or not WEP and WEN mineralized radiolabeled phenanthrene within 20.5 min, biometer flask experiments were conducted. OREP and OREN strains were tested as well to ensure they did not produce radiolabeled carbon dioxide.

Twenty millilitres of a cell suspension with an OD_{600} of 1 was added to each pre-sterilized and acid-washed 250-mL modified biometer flask (Bartha and Pramer 1965). A 2.5-mL aliquot of 1 N KOH was added to the side arm of the biometer flasks to trap the $^{14}CO_2$ produced by the bacterial strain. The main opening of the biometer flask was sealed with a neoprene stopper and the side arm was sealed with a neoprene stopper equipped with a port connected to a needle and fine-gauge tubing. A syringe was attached to the port in the side arm stopper to allow for sampling of the KOH solution. A 0.5-mL sample was taken from the side arm before the radioactivity was added to the flask as a blank control.

Thirty microlitres of the mixed labeled and unlabeled phenanthrene solution was added to the biometer flask at t=0, giving a phenanthrene concentration of 6.36 μM and 100 000 dpm. The flask was sealed immediately after the addition of the substrate to entrap any $^{14}CO_2$ that was produced. The flask was manually shaken for 20.5 min at which point 1 mL of concentrated HCl was added through the neoprene stopper into the flask to stop the reaction and to acidify the solution. The flask was shaken manually for 30 s. To allow time for equilibration of the carbon dioxide in the KOH solution, the flask was shaken at 100 rpm overnight. After 24 h, a 0.5-mL sample of the KOH solution was taken and added to a vial containing 10 mL of aqueous scintillation fluor, 1.5 mL of water and 0.1 mL of glacial acetic acid. The purpose of adding the acid was to reduce the chemiluminescence caused by the KOH (Cross *et al.* 2006). The samples were counted using a Beckman LS 3801 liquid scintillation counter.

3.13 Statistical Analysis

Statistical analysis of the transport data was performed to determine whether the rate of phenanthrene biodegradation was statistically significantly different between the strains with and without efflux activity.

The data used to calculate the degradation rates were obtained from the transport assays. The supernatant fractions were used to calculate the rates of accumulation of metabolites and the pellet fractions were used to calculate the rates of degradation of phenanthrene. In order to obtain the best estimate of the linear portion of each curve, certain points were eliminated from the rate calculations.

The data from the transport assay curves were converted to concentrations and divided by the amount of biomass present in order to obtain a rate with units of nmol phenanthrene/mg protein/min.

Simple linear regression was performed on each data set to obtain the rates. Since the transport assays were repeated in triplicate, both the average and individual data were examined. Although this technique allows for rate calculations, it does not allow groups of data to be compared to each other. Therefore, multiple linear regression was performed to determine if significant differences between the strains could be detected. A statistical model was developed and is described in Appendix F.

A Matlab ® program was written and used to calculate the statistics required for the least squares regression analysis. Analysis of covariance (ANCOVA) techniques were used to compare the slopes of the linear sections of the transport curves between groups of data because these slopes represent the rates of degradation or the rates of metabolite accumulation. The statistics were used to determine whether or not the difference in rate for the paired strains was significant.

In least squares regression analysis, the goal is to minimize the sum of squares of residuals. The error associated with the prediction must be computed and can be

53

accomplished by estimating the variance σ^2, which is equal to the variance in ε. The ANOVA table (Table 3.2) is a common way to report important information obtained from fitting the data to the regression line.

Table 3.2 The ANOVA table (Johnson and Bhattacharyya 1996).

Variation	DOF	Sum of Squares	Mean Square	Fo
Regression	k	$SSR = \sum(\hat{y}_i - \bar{y}_i)^2$	$MSR = \dfrac{SSR}{k} = \dfrac{\hat{\beta}X^TY}{k}$	$F_o = \dfrac{MSR}{MS\,\mathrm{Re}\,s}$
Residual	n-p where p=k+1	$SS\,\mathrm{Re}\,s = \sum(y_i - \hat{y}_i)^2$	$MS\,\mathrm{Re}\,s = \dfrac{SS\,\mathrm{Re}\,s}{n-p} = s^2$ $and\ s^2 = \dfrac{Y^TY - \hat{\beta}^T X^T Y}{n-p}$	
Total	n-1	$SST = \sum(y_i - \bar{y}_i)^2$		

The statistic F_o from the ANOVA table and the p-value were the two most important factors in deciding whether or not the difference was statistically significant. Hypothesis tests on the slopes were performed using the F_o statistic. If $F_o > F_{\alpha=0.05}$, the difference between the two strains is significant at the 95% confidence level. The p-value is equal to the probability of getting an observation as large as the current observation by random chance (Johnson and Bhattacharyya 1996). If the p-value is less than 0.05, the observation (the difference in this case) is significant.

54

4.0 RESULTS AND DISCUSSION

4.1 Characterization of Microbial Strains

4.1.1 Mutants of Wild Type LP6a

In order to determine if phenanthrene metabolites were effluxed and if the EmhABC efflux system significantly affects the rate of degradation of phenanthrene by *P. fluorescens* LP6a strains, it was necessary to compare strains that were efflux-deficient to strains that possessed the EmhABC efflux system. Therefore, efflux negative mutants of the wild type efflux positive strain (WEP) and the open-ring efflux positive strain (OREP) were constructed.

Plasmid DNA from both WEP and OREP was extracted and purified using the modified Kieser plasmid preparation procedure (Kieser 1984). Plasmids pLP6a and p21-41 were introduced into electrocompetent non-metabolizing efflux negative (NEN) cells via electroporation, creating the wild type efflux negative strain (WEN) and the open-ring efflux negative strain (OREN) respectively.

To confirm that the WEN and OREN strains possessed the expected plasmids, the plasmid DNA was extracted from WEN and OREN, and subsequently separated by gel electrophoresis. The bands seen in Figure 4.1 were comparable to bands obtained by Foght and Westlake (1996) for *Eco*R1 restriction enzyme digests of pLP6a, as well as to plasmid DNA from WEP and OREP. Therefore, this test confirmed that WEN and OREN were properly constructed.

55
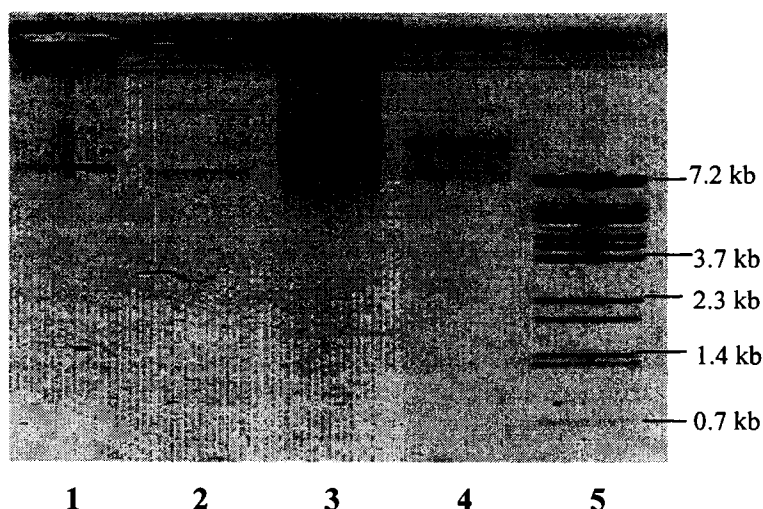
Figure 4.1 Photograph of agarose gel showing the *Eco*R1 restriction enzyme digests of the pLP6a plasmid preparations isolated from WEP and WEN and the p21-41 plasmid preparations isolated from OREP and OREN. Lane 1, WEP; lane 2, WEN; lane 3, OREP; lane 4, OREN; lane 5, lambda *Bst*EII digest.

To verify the metabolic capability of these strains, WEN and OREN were exposed to DBT in two different experiments. In the first method, a few crystals of solid DBT were added to aqueous cell suspensions of WEN and OREN respectively. After only a few minutes, both the WEN and OREN suspensions turned a bright orange colour, indicating the presence of metabolites in solution. DBT was also sprayed onto R2A plates of WEN and OREN colonies. The colonies and agar also turned a bright orange colour after overnight incubation at 30°C, confirming that metabolism was occurring.

4.1.2 Metabolite Identification

To confirm that WEN and OREN produced the expected metabolites, cell cultures of both strains were tested. A 0.5 mM solution of phenanthrene in DMF was added to both WEN and OREN cultures to accumulate metabolites. Due to the fact that phenanthrene was supplied in excess of the aqueous solubility limit, the cells were harvested after 2 h of incubation at 30°C to permit biodegradation of the excess phenanthrene.

56

The supernatant and pellet fractions of the WEN and OREN cell suspensions were extracted separately. The cell pellets were lysed by the addition of a NaOH solution containing sodium dodecyl sulphate (SDS) with heating at 60°C. As a result of the lysis procedure, the pellet fraction became slightly viscous due to the release of intracellular material. The separation of the organic and aqueous layers took much longer in the pellet fraction than in the supernatant fraction. Each fraction was extracted three times; once with DCM at neutral pH, once with ethyl acetate at a pH of 2 and once with ethyl acetate at a pH < 1. This methodology is consistent with extraction procedures for phenanthrene and DBT metabolites in the literature (Foght and Westlake 1996; Samanta *et al.* 1999; Pinyakong *et al.* 2000; Bressler and Fedorak 2001; Prabhu and Phale 2003; Baboshin *et al.* 2005; Kim *et al.* 2005), and was verified after preliminary experiments using DBT as the substrate due to the production of coloured metabolites (see Appendix E for more information on extraction method development). A faint yellow colour was observed in the acidic (pH<1) extractions of the cell suspensions, which was possibly due to the presence of a coloured metabolite in solution. The extracts for each phase were pooled, derivatized and analyzed by GC-MS.

As expected, the trimethylsilyl (TMS)-derivatized extracts of the supernatant fractions for WEN and OREN both contained a significant amount of the saturated open-ring metabolite, 4-(1-hydroxynaphth-2-yl)-2-oxobutanoic acid (retention time of 16.39 min, see Table 4.1 for major ions). The saturated open-ring metabolite was not detected in the pellet fractions. The structure and major fragments found in the mass spectrum of the TMS derivative of 4-(1-hydroxynaphth-2-yl)-2-oxobutanoic acid are shown below in Figure 4.2.

Many additional peaks, including some of significant size, were observed in the gas chromatograms of the derivatized extracts. The identity of these peaks was not determined since the presence of the open-ring compounds confirmed that WEN and OREN were able to metabolize phenanthrene.

57

To determine if WEP produced the same metabolites as WEN and if OREP produced the same metabolites as OREN, aqueous cell suspensions of each strain were incubated with an ethanolic phenanthrene solution to give a total phenanthrene concentration of 6.36 μM. At the end of the reaction time (20.5 min), the cells were killed and the cultures were subsequently extracted with DCM at a pH less than 1 to ensure that the polar metabolites had partitioned into the organic phase. Aliquots of the killed cultures were plated and no colonies formed, confirming that the cells were no longer viable.

TMS derivatives of the metabolites were identified by comparing the mass fragmentation patterns from the mass spectra to literature values (see Table 4.1). The TMS extracts for WEP contained 4-(1-hydroxynaphth-2-yl)-2-oxobutanoic acid and 1-hydroxy-2-naphthoic acid (retention time of 14.55 min, see Table 4.1 for major ions of the TMS derivatives). The underivatized extract of WEP contained 1-naphthol (retention time 10.09, see Table 4.1 for major ions) indicating that the lower naphthalene degradation pathway was active, as expected. The mass spectrum for TMS 1-hydroxy-2-naphthoic acid matches the spectrum obtained by Zink and Lorber (1995) and the mass spectrum for 1-naphthol matches the spectrum in the NIST Chemistry WebBook (2005). The R_f values that were calculated are also given in this table and will be discussed in Section 4.1.2.

58

Table 4.1 Characterization of phenanthrene metabolites identified in this study.

Structure	Compound	Characteristic Peaks in Mass Spectrum (m/z)	Retention Time (min)	R_f, TLC
	TMS 4-(1-hydroxynaphth-2-yl)-2-oxobutanoic acid	388, 271, 229, 147, 73[a]	16.29 & 16.39	0.09[a]
	TMS 1-hydroxy-2-naphthoic acid	332, 317, 243, 185, 147, 73[b]	14.55	0.36[b]
	1-naphthol	144, 116, 115, 57[c]	10.09	nd
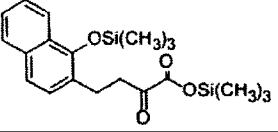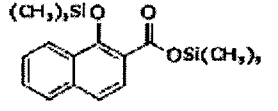
[a] This study
[b] Zink and Lorber (1995)
[c] NIST (2005)
nd: not detected

59
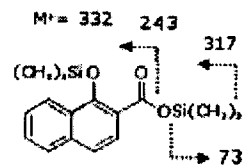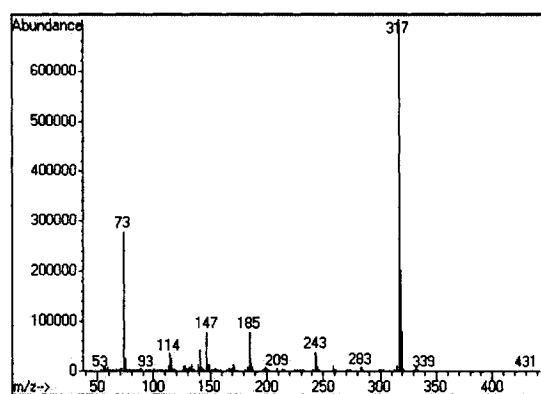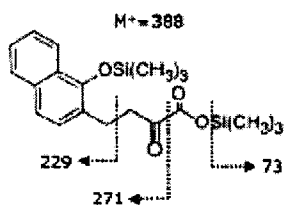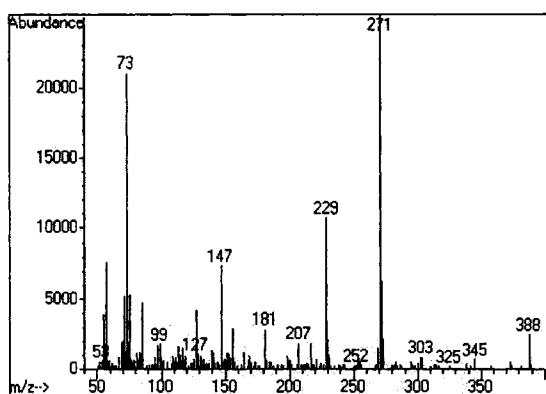
a)
TMS 4-(1-hydroxynaphth-2-yl)-2-oxobutanoic acid

b)
TMS 1-hydroxy-2-naphthoic acid
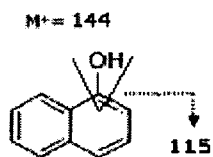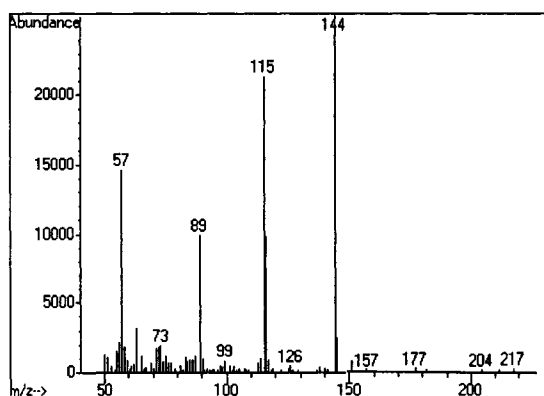
c)
1-naphthol

Figure 4.2 Mass spectra for the reported phenanthrene metabolites.

Only the saturated open-ring compound and a trace amount of 1-hydroxy-2-naphthoic acid were detected in the WEN culture. This finding was unexpected due to the fact that WEN possesses pLP6a and therefore should produce significant fractions of lower pathway metabolites. The lack of these metabolites was consistent with inhibition of the lower pathway. The reason why WEN was different than WEP may be due to the genetic manipulation techniques that were used. Hearn et al. (2006), who constructed a plasmid that carried a histidine-tagged emhB gene and transformed it into NEN, showed that the EmhB$_{His}$ pump was slightly less efficient than the wild type. Therefore the transformation of pLP6a into NEN might also result in decreased efficiency of the phenanthrene degradation when compared to the wild type.

OREN and OREP both produced appreciable amounts of the saturated open-ring compound. Foght and Westlake (1996) showed accumulation of trans-4-[2-(3-hydroxy)-thianaphthenyl]-2-oxobut-3-enoic acid, which is analogous to the open-ring compound, in OREP due to the inability of the strain to produce the aldolase enzyme required to further degrade this compound. The relative amounts of metabolites in each culture extract are summarized in Table 4.2 below. The table also contains information on the mineralization of phenanthrene, which will be discussed in Section 4.1.3 and the TLC/autoradiography results that are discussed in this section.

61

Table 4.2 Detection of metabolites in cultures of WEP, WEN, OREP and OREN.
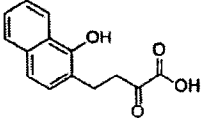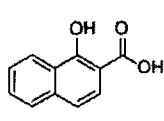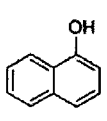
	Phenanthrene Metabolites[12]			
	(naphthalene with OH and propanoic-oxo acid structure)	(1-hydroxy-2-naphthoic acid structure)	(1-naphthol structure)	$^{14}CO_2$[a]
WEP	✓ $R_f = 0.09$	✓ $R_f = 0.33$	✓	42±7%
WEN	✓ $R_f = 0.09$	tr	bdl	0
OREP	✓ $R_f = 0.12$	bdl	bdl	0
OREN	✓ $R_f = 0.09$	bdl	bdl	0

[1]Metabolites present in extract based on GC-MS results:
(✓) over 1% of initial phenanthrene
(tr) trace, less than 1% of initial phenanthrene
(bdl) below detection limit
detection limit: <1 µg
[2] R_f values based on TLC/Autoradiography
[a] Percentage of the initial ^{14}C added to the flask as phenanthrene

Additionally, [9-^{14}C]phenanthrene was supplied to WEP, WEN, OREP and OREN cultures and the cell supernatant and pellet fractions were extracted using the method previously described after 10 min (t=10) and after 20.5 min (t=20.5) of incubation. The extracts were separated by TLC and the silica plates were then subjected to autoradiography. Authentic standards of 1-hydroxy-2-naphthoic acid (R_f=0.36), salicylic acid (R_f=0.42) and phenanthrene (R_f=0.67) were developed in order to help identify the compounds found on the TLC plates.

62

Only the supernatant fractions produced spots detected by autoradiography and UV light with the exception of the WEP (t=20.5) pellet, which produced a spot with an R_f value of 0.42 that was only detected by UV light. Even though this R_f value is identical to the R_f of the salicylic acid standard, the exact identity of the spot cannot be confirmed. The WEP supernatant extracts at both t=10 and t=20.5 contained two compounds that were detected by autoradiography with R_f values of 0.09 and 0.33. These compounds were tentatively identified as the open-ring compound 4-(1-hydroxynaphth-2-yl)-2-oxobutanoic acid, and 1-hydroxy-2-naphthoic acid respectively. The spots tentatively identified as 1-hydroxy-2-naphthoic acid were scraped into vials containing aqueous scintillation fluor and were counted on the liquid scintillation counter. The spots represented 5% (t=10) and 6% (t=20.5) of the initial label added as ^{14}C phenanthrene.

Both of the WEN extracts contained compounds with R_f values of 0.02 and 0.09 that were detectable by autoradiography. The spots with R_f =0.09, assumed to be the open-ring compound, were counted and accounted for 14% (t=10) and 6% (t=20.5) of the initial label added. The decrease in the percentage of the label with time could be due to the degradation of the open-ring compound. The compound with an R_f value of 0.02 may be an upper pathway metabolite. These results also confirmed that WEN did not produce the same phenanthrene metabolites as WEP.

Due to an experimental error, only the OREP (t=20.5) extract data could be used. This extract contained compounds with R_f values of 0.02 and 0.12 that were detected by autoradiography. The spot at 0.12 was likely the open-ring compound and it accounted for 11% of the initial label added at t=0. In OREN, only one compound, with an R_f of 0.09, was detected by autoradiography. The OREN (t=10) sample accounted for 17% of the initial label and the OREN (t=20.5) sample accounted for 11% of the initial ^{14}C added. Therefore, these results support the hypothesis that OREN and OREP accumulated the open-ring metabolite.

63

Spots with R$_f$ values of 0.67, 0.68, 0.62 and 0.69 were identified in WEP,WEN, OREP and OREN supernatant extracts by UV light only. Despite the fact that these R$_f$ values are very similar to the R$_f$ value obtained for phenanthrene (0.67), the absence of spots on the autoradiogram indicated that these compounds are likely the internal standard, o-terphenyl. The R$_f$ values for the major metabolites are given in Table 4.1.

Bateman et al. (1986), who attempted to determine the amount of naphthalene associated with the pellet fraction of P. putida cells by chromatography and subsequent autoradiography of the intracellular contents, showed that it was not technically possible to do so due to the fact that naphthalene readily sublimes. As phenanthrene is significantly less volatile than naphthalene (vapour pressure of phenanthrene= 0.113 Pa and vapour pressure of naphthalene= 36.8 Pa; Knightes and Peters (2003)), this method was suitable for this study.

4.1.3 Mineralization of Phenanthrene

Biometer flask experiments were performed to determine if radiolabeled carbon dioxide was produced by the strains during the 20.5-min incubation time. After killing the cells, the biometer flasks were shaken overnight to allow for the carbon dioxide to diffuse into the side arm and dissolve into the KOH solution. WEP, the only culture that produced carbon dioxide during this short time period, converted 42±7% of the initial phenanthrene added to CO_2 within 20.5 min. The lack of mineralization by WEN was unexpected given that it possesses the plasmid encoding the enzymes required to mineralize phenanthrene, but the lack of CO_2 production was consistent with the absence of lower pathway metabolites in the GC-MS analysis (see Table 4.2). To confirm that WEN was not able to mineralize phenanthrene, the experiment was repeated 11 times. Less than 1% of the initial label was recovered as [14]CO_2 in all cases. These data suggested that the activity of a key enzyme was inhibited in WEN, the transcription of the gene encoding the enzyme was repressed, or an inhibitory compound accumulated to a toxic level due to the fact that WEN is efflux-deficient.

64

4.1.4 Optical Density at 600 nm (OD_{600})

The OD_{600} was used as a measure of the amount of biomass added to each culture flask. The optical density of a diluted cell suspension was measured and this value was used to prepare a cell suspension with an OD_{600} of 1 in 0.1 M potassium phosphate buffer (PB). The differences amongst the six strains are not large, as illustrated in Figure 4.3; therefore, this technique was used to ensure that the amount of biomass in each experiment was the same so that the rates of phenanthrene degradation for each strain could be compared.

The average OD_{600} obtained from the dilution of 50 μL of concentrated cell cultures in 950 μL of PB was 0.39. As 20-mL cell suspensions were prepared at an OD_{600} of 1, 2.6 mL of the concentrated culture was added to 17.4 mL of 0.1 M PB on average.
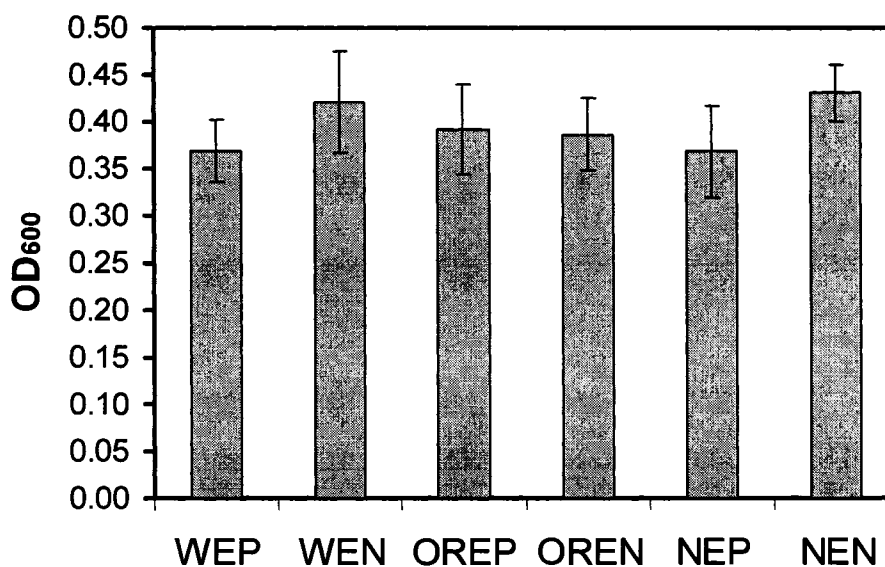
Figure 4.3 Optical density at 600 nm for each of the six strains of LP6a. The error bars represent one standard deviation of the mean value where the number of observations, n, is equal to 19, 22, 17, 22, 6 and 10 for WEP, WEN, OREP, OREN, NEP and NEN respectively.

65

4.1.5 Colony-Forming Units (CFU)

To confirm that the OD_{600} absorbance values were similar amongst the 6 strains, the number of colonies that formed from 100-µL aliquots of various dilutions from a dilution series was determined. Three independent measurements were obtained for the WEP, WEN, OREN, NEP and NEN strains. Only two independent measurements were made for OREP due to an experimental error.

The number of colonies counted for each strain is shown in Figure 4.4. Although NEP and NEN are significantly different from the metabolizing strains, it was not a point of concern due to the fact that they are unable to metabolize phenanthrene and therefore were not compared to any other strain. The average value obtained for the four metabolizing strains was 1.79×10^9 CFU/mL. This value is quite similar to the concentration obtained by Bugg (2000) for WEP of 1.93×10^9 CFU/mL.
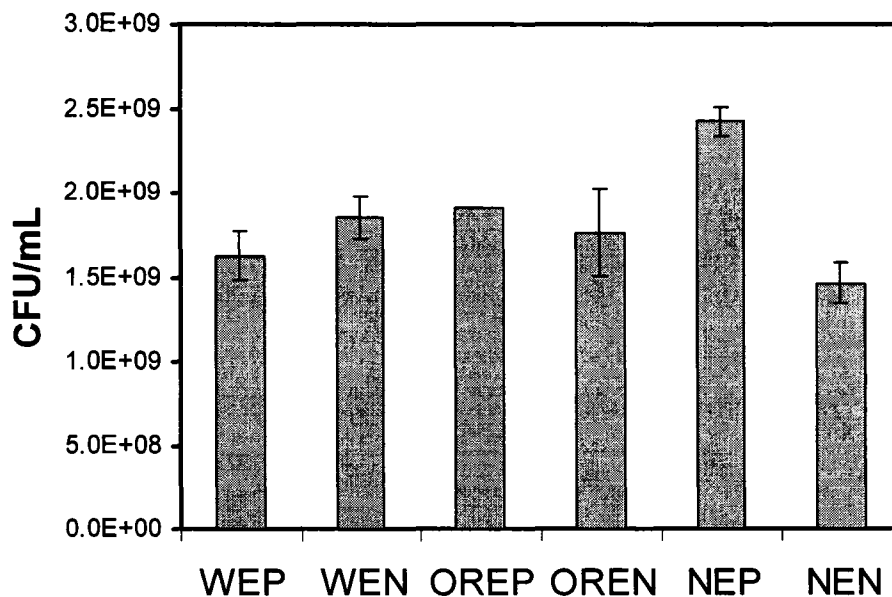
Figure 4.4 Colony forming units/mL calculated from the 10^{-6} dilutions for the six strains of LP6a. The error bars represent one standard deviation of the mean value of three independent experiments except for OREP. Only two independent measurements were made for OREP and therefore the standard deviation is not shown.

66

4.1.6 Bicinchoninic Acid (BCA) Protein Assay

The amount of protein in a suspension of cells at an OD_{600} of 1 was measured using the BCA protein assay. The standard curve in Figure 4.5 was prepared in order to determine the amount of protein added as BSA in the standards from the absorbances at 562 nm (A_{562}).

The relationship between the absorbance (A_{562}) and protein concentration in µg/mL (C_p) was calculated from the standard curve to be

$$A_{562} = (1.17 \times 10^{-3}) C_p + (2.24 \times 10^{-2})$$

(4.1)

The relationship showed excellent agreement with the data ($R^2 = 0.997$). Three independent culture flasks were tested for each strain with the exception of OREP due to an experimental error.

Figure 4.6 shows the average protein concentration for the six strains of LP6a. Simple ANOVA statistics were calculated to determine if the mean values for each strain are significantly different from each other. An F value of 0.8051 and a p-value of 0.5712 were obtained, proving that the differences amongst the six strains were not significant. Therefore the average protein concentration from the six strains (156.9 µg/mL) was used to convert the radiolabel concentrations on a basis of mg of protein.

As previously shown by Bugg (2000) and Hearn (2005), various mutants of LP6a do not show significant differences in growth and yield of biomass; therefore the results in this study are not surprising. However, in order to compare the metabolic activity of different strains, it was necessary to quantify the number of cells used in each experiment and to confirm that the strains constructed in this study were similar to the previously described strains.

67
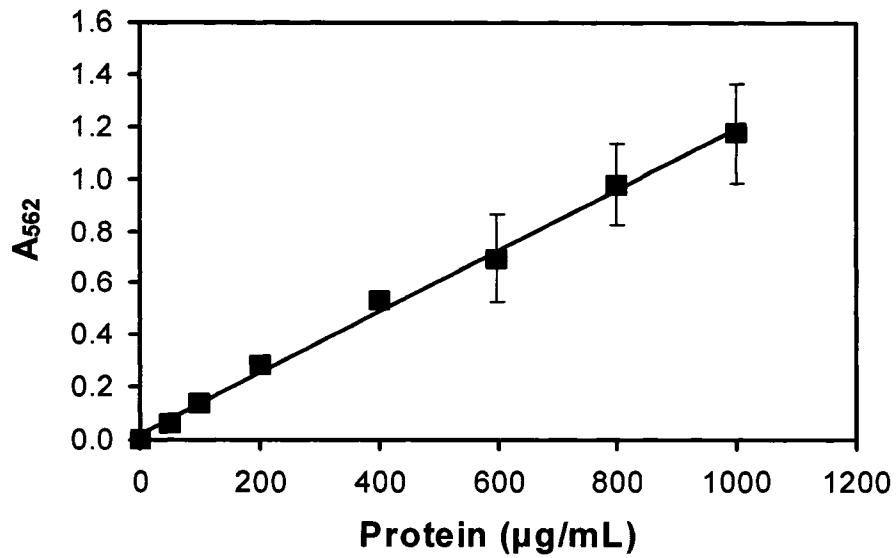
Figure 4.5 Calibration curve obtained from the absorbance of BSA as a function of the protein concentration using the BCA protein assay. The data points are an average of three measurements of the same sample and the error bars represent one standard deviation.
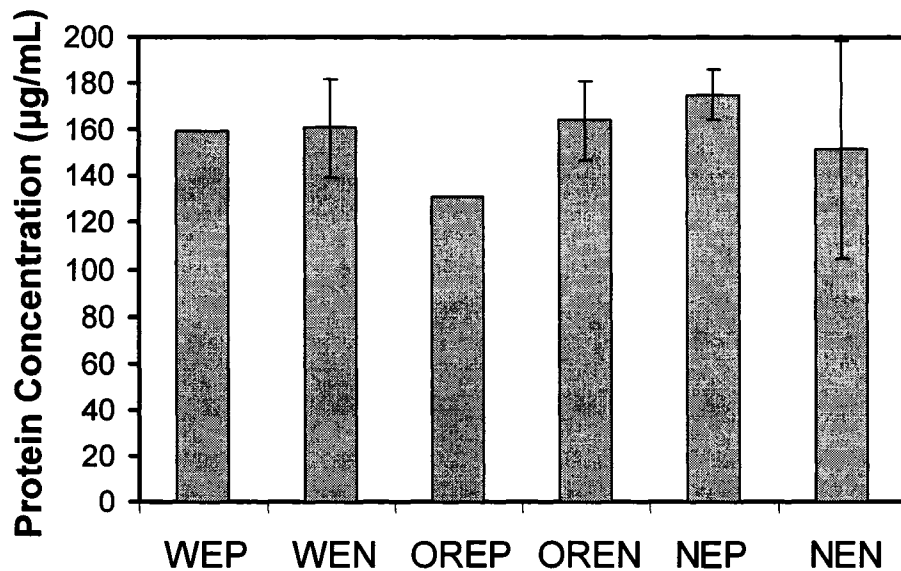
Figure 4.6 Protein concentrations for each of the six strains of LP6a as determined from the BCA protein assay. The error bars represent three measurements of three independent samples for all strains showing error bars. Only two independent cultures were measured for the OREP strain and therefore the standard deviation is not shown. An error was made in the analysis of one WEP culture and therefore the standard deviation was not calculated.

68

4.2 Transport of Phenanthrene and Metabolites

4.2.1 Radiolabeled Transport Assays

To quantify the partitioning of phenanthrene compounds between the cell pellet and the supernatant fractions, radiolabeled transport assays were first performed using NEP and NEN because they are unable to metabolize phenanthrene. Figure 4.7 illustrates the change in the fraction of ^{14}C added as phenanthrene as a function of time for the pellet and supernatant fractions of NEP. Samples were taken until steady state was reached and then sodium azide was added at t=9.5 min. Because azide inhibits all active transport processes, the phenanthrene concentration in the pellet increases due to the lack of efflux and as a consequence, the supernatant concentration drops. This observation proves that this technique is sufficiently sensitive to monitor changes in the partitioning of the labeled phenanthrene between the supernatant and the cell pellet fractions.

The transport curves for NEN shown in Figure 4.8 confirm that azide has no effect on the partitioning of the radiolabel when the pumping mechanism is blocked. The results confirm that phenanthrene enters the pellet fraction via passive transport as shown by Bugg *et al.* (2000). The total phenanthrene concentration in the NEN suspension remained constant over the 20.5-min assay. Although efflux systems other than EmhABC might transport phenanthrene, their contribution must be insignificant. Approximately 50% of the label is accounted for by the data in Figure 4.7 and Figure 4.8 at all times, suggesting that the balance of the phenanthrene was sorbed onto the sides of the glassware (see Section 4.2.2). The concentration of phenanthrene in the NEN pellet should be equal to the concentration in the NEP pellet after azide has been added, as shown in Figures 4.7 and 4.8. The steady state partitioning of ^{14}C in the pellet fractions of NEP and NEN was different due to the presence of the efflux system. The initial fractional amount of ^{14}C in the pellet fraction of NEP was only 0.20 ± 0.03 compared to the fractional amount in NEN of 0.30 ± 0.02.

69
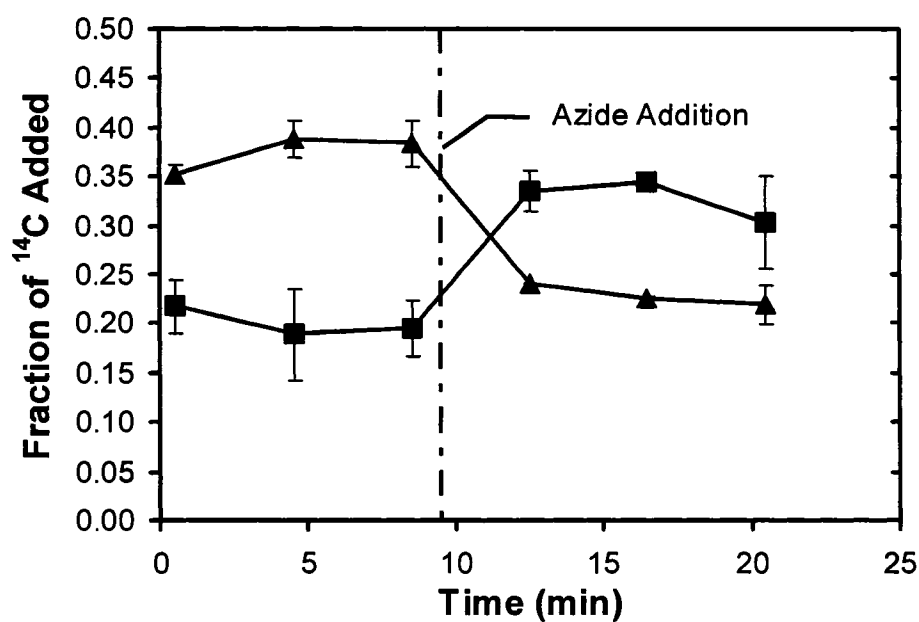
Figure 4.7 Distribution of the radiolabel, added as [9-^{14}C]phenanthrene, between the supernatant (▲) and cell pellet (■) of NEP over time. The data points are an average of three independent experiments and the error bars represent one standard deviation.
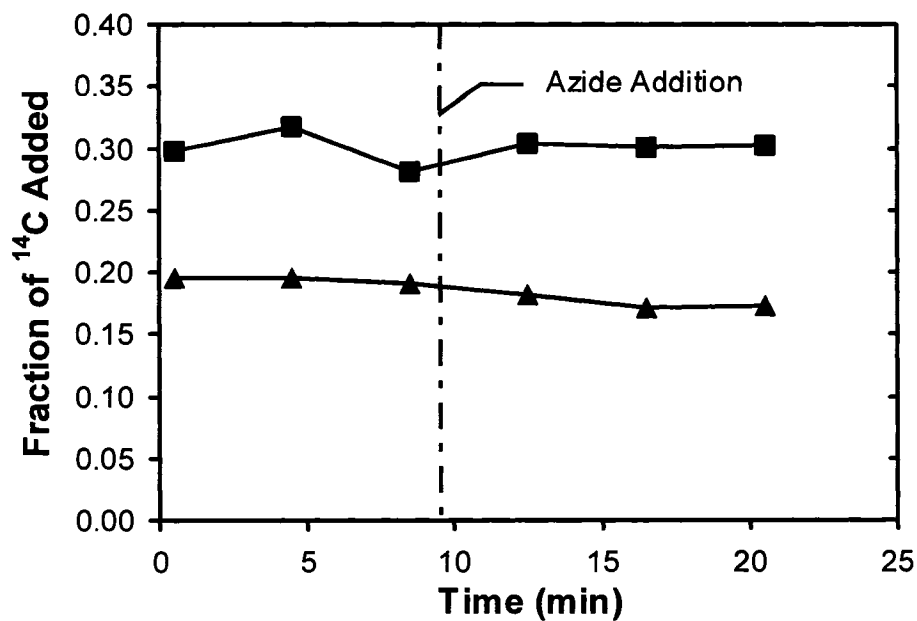
Figure 4.8 Distribution of the radiolabel, added as [9-^{14}C]phenanthrene, between the supernatant (▲) and cell pellet (■) of NEN over time.

70

For both cured strains, average fractions before and after azide addition were taken since the samples at t=0.5, t=4.5 and t=8.5 min were equivalent and the samples at t=12.5, t=16.5 and t=20.5 min were also equivalent according to hypothesis testing performed on the means. The average values as well as the F statistics and p-values are given in Section 4.4.1. Similarly, averages were taken for the killed-cell controls.

4.2.2 Release of Sorbed Phenanthrene

The above data suggested that a significant amount of the phenanthrene was adsorbed on the walls of the flask, consistent with observations by Bugg (2000). If the phenanthrene desorbed slowly, its apparent rate of metabolism would be reduced. On the other hand, rapid desorption would ensure that the disappearance of phenanthrene was affected only by metabolism and efflux from the cells. A simple experiment was performed to confirm that the rate of desorption of phenanthrene into the supernatant from the sides of the flask was much faster than the rate of metabolism. In this experiment, 20 mL of PB was added to an acid-washed Erlenmeyer flask and 100 000 dpm of ^{14}C phenanthrene was added to the flask. A sample was taken after shaking for 30 s and the remaining supernatant was discarded. The flask was then rinsed three times with 20 mL of PB and samples were taken. All the samples were counted by liquid scintillation counting and the fractions of the ^{14}C added were plotted as a function of the number of rinses (see Figure 4.9). After the second rinse, 96% of the phenanthrene was removed and after the third and fourth rinses, 99% and 100% of the initial phenanthrene concentration had been removed respectively. Because phenanthrene was not strongly sorbed to the sides of the glassware, the rate of phenanthrene removal and consequently the rate of metabolite formation were not limited by the mass transfer of phenanthrene to the supernatant.

71
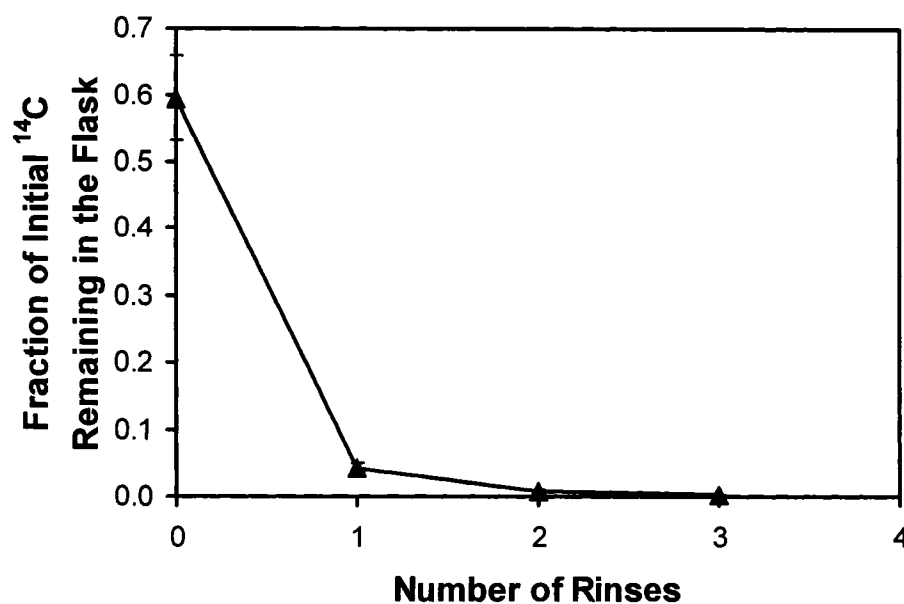
Figure 4.9 Desorption of radiolabel, added as [9-^{14}C]phenanthrene, from the glassware by gentle rinsing with 0.1 M potassium phosphate buffer after 30 s. The data points are an average of three independent experiments and the error bars, where visible, represent one standard deviation.

4.2.3 Killed-Cell Controls

To verify that the fractionation between the supernatant and pellet was due to the effects of the EmhABC system, transport assays with killed cells were performed. The cells were killed either by the addition of 1 mL of concentrated HCl 30 min prior to the start of the assay (Figure 4.10) or by heat sterilization (Figure 4.11). The two methods were used to verify that the addition of acid was as effective at killing the cells as the heat sterilization method. The concentrations in each phase did not depend on time. The data for the killed-cell controls are also similar to the results obtained for the NEN culture (Figure 4.8). The azide addition did not cause any significant change in the partitioning and the recoverable amount of phenanthrene did not change over the course of the assay. Autoclaving could cause the cells to lyse therefore increasing the amount of recoverable phenanthrene in comparison to the acid-killed cells (see Figure 4.10 and Figure 4.11).

72
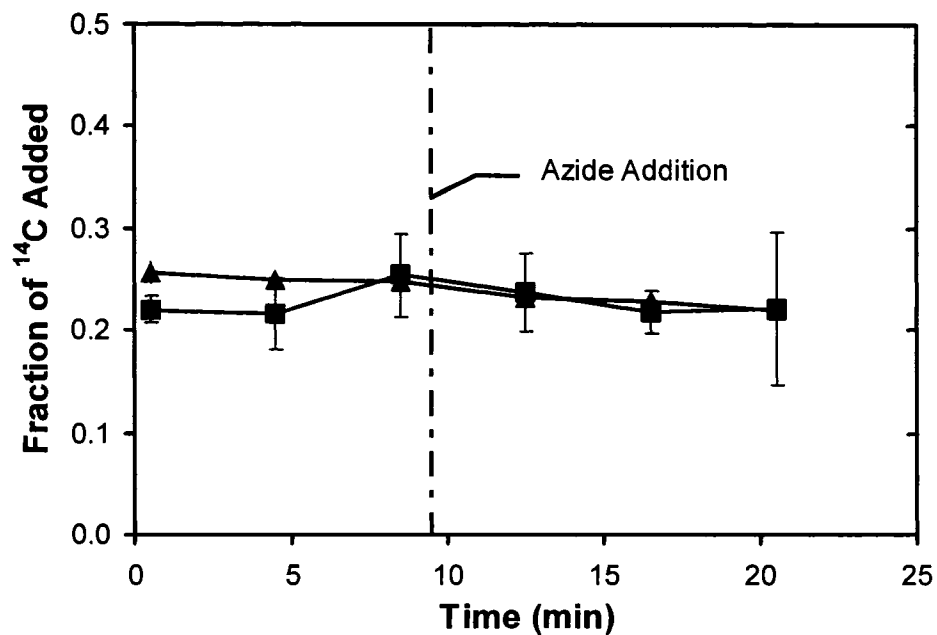
Figure 4.10 Distribution of the radiolabel, added as [9-^{14}C]phenanthrene, between the supernatant (▲) and cell pellet (■) of acid-killed WEP over time. The data points are an average of three independent experiments and the error bars represent one standard deviation.
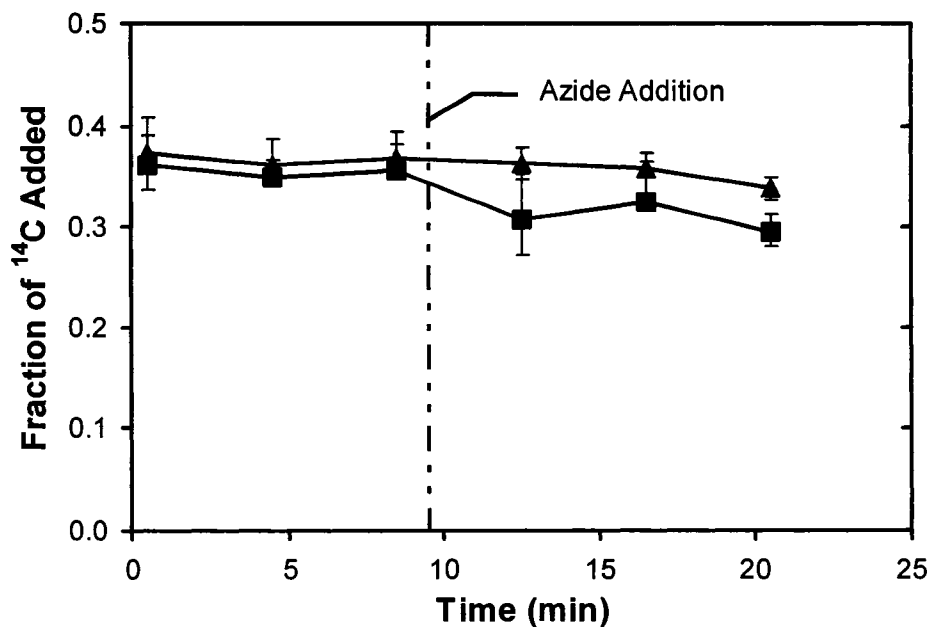
Figure 4.11 Distribution of the radiolabel, added as [9-^{14}C]phenanthrene, between the supernatant (▲) and cell pellet (■) of heat-killed WEP over time. The data points are an average of three independent experiments and the error bars represent one standard deviation.

73

4.2.4 Verification of Phenanthrene Degradation

In order to verify that the mutant strains of *P. fluorescens* LP6a were active for phenanthrene degradation during the time period of the transport assay, the concentration of residual phenanthrene was determined. Acid-killed cell controls as well as viable cultures of WEP, WEN, OREP and OREN were all identically prepared. After a 20.5-min incubation period with 6.36 μM of phenanthrene, the viable cells were killed by the addition of 1 mL of concentrated HCl. The cell suspensions were extracted and the extracts were analyzed by GC-MS. The retention time for phenanthrene was determined to be 12.55 min. Phenanthrene peaks were not detected in the gas chromatograms obtained for the extracts from viable cells whereas peaks accounting for at least 12 wt% of the initial amount of phenanthrene added were detected in all of the killed cell controls with the exception of the WEN extract (see Table 4.3). This anomaly was likely due to an error made during the extraction procedure.

Table 4.3 Phenanthrene remaining after a 20.5-min incubation in viable and killed-cell cultures.

Strain	Phenanthrene Present?	
	Killed	Viable
WEP	✓	bdl
WEN	bdl	bdl
OREP	✓	bdl
OREN	✓	bdl

(bdl) below detection limit
detection limit: <1 μg

These results confirmed that the mutant strains were capable of degrading the available phenanthrene during the 20.5 min duration of the transport assay. Bugg (2000) also showed that the majority of the phenanthrene in solution after 25 min was metabolized by the wild type strain of LP6a.

4.2.5 Metabolism of Phenanthrene With and Without Efflux

The transport of phenanthrene and its metabolites was studied using the radioisotope tracer method developed by Bugg *et al.* (2000) described in Section 3.7. Radiolabeled transport assays were performed for WEP, WEN, OREP and OREN under each of the following conditions: first, azide was added 1 min before the start of the transport assay, second, azide was added at t=9.5 min or third, no azide was added at all. The fraction of ^{14}C added (or phenanthrene concentration) was monitored as a function of time in both the pellet and supernatant fractions. The slopes of the curves obtained from the transport assays were then used to determine rates of change of the label in the supernatant, due mainly to metabolites, and in the cell pellet, due mainly to the remaining phenanthrene. Because hydrophobic compounds partition more readily into the pellet fraction than hydrophilic compounds, the fraction of the ^{14}C label in the pellet was likely dominated by unconverted phenanthrene.

The shape of the curves in the case where azide was added at t=9.5 min to a WEP cell suspension (Figure 4.12) is quite different from the curves obtained from the non-metabolizing stains, NEP and NEN (Figures 4.7 and 4.8). The concentrations in the WEP pellet and supernatant showed very limited response to the addition of azide; there was no inflection in the curve to indicate a redistribution of the label between the supernatant and the pellet as in the case of NEP (Figure 4.7). Even after active transport processes were inhibited by the addition of azide, the concentration in the supernatant continued to increase and the pellet concentration continued to drop, consistent with previous observations by Bugg *et al.* (2000). At the end of the assay, 83±6% of the label was accounted for. Because only 50% was accounted for in the cured strains, the increase in recovery of the label with time must be attributed to the production of more hydrophilic metabolites accumulating in the supernatant.

75
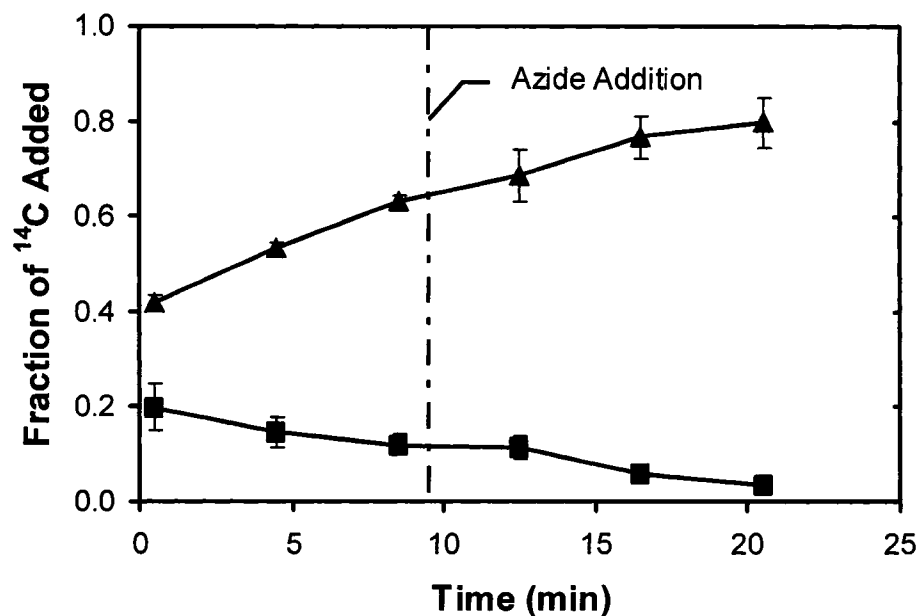
Figure 4.12 Distribution of the radiolabel, added as [9-^{14}C]phenanthrene, between the supernatant (▲) and cell pellet (■) of WEP over time. The data points are an average of three independent experiments and the error bars represent one standard deviation.

Additionally, non-linear kinetics were observed near the end of the assay indicating that phenanthrene levels had been depleted. These data suggested that metabolites exited the pellet fraction and entered the supernatant through an alternative mechanism to the EmhABC system because the addition of azide had no impact on the rate of accumulation of metabolites in the supernatant.

WEN, on the other hand, showed a slight response to azide addition (Figure 4.13). The inflection in the pellet and supernatant curves at the time of azide addition was observably larger, suggesting that more phenanthrene left the supernatant and entered the cells than in the case of WEP. However, after only a very short period of time, the concentration of phenanthrene in the supernatant resumed its increase. At the end of the assay, 83±6% of the label was accounted for in WEN also confirming the accumulation of metabolites in the supernatant. Therefore, phenanthrene metabolites were not effluxed by EmhABC since WEN does not possess EmhB.

76
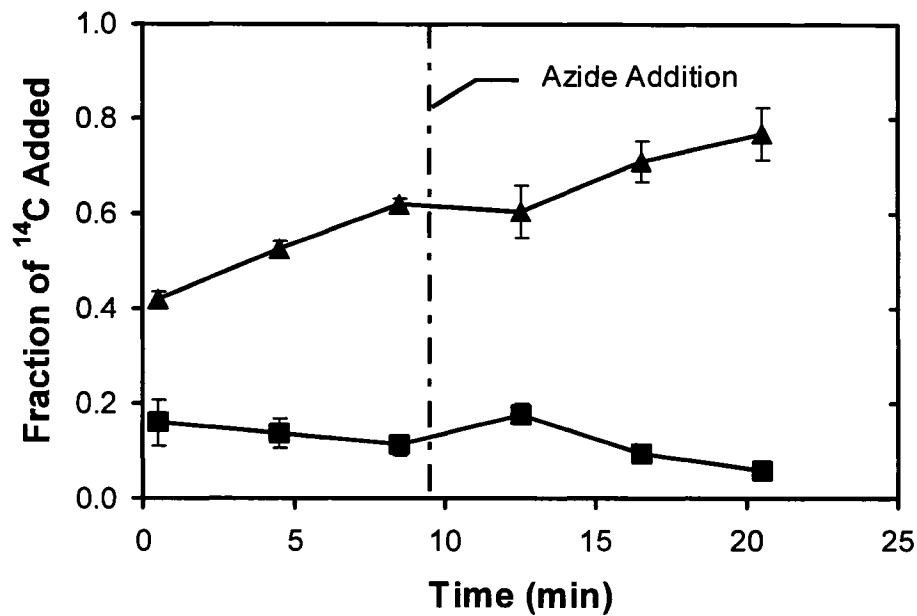
Figure 4.13 Distribution of the radiolabel, added as [9-^{14}C]phenanthrene, between the supernatant (▲) and cell pellet (■) of WEN over time. The data points are an average of three independent experiments and the error bars represent one standard deviation.

In order to further study the efflux of metabolites by the EmhABC system, azide was added 1 min prior to the start of the assay. In this assay, active transport mechanisms could not interfere with the rate of degradation since azide acts as a proton conductor and all active transport processes were inhibited almost immediately after azide addition (see Figure 4.7). The results from this case were then compared to the cases in which azide was added at t=9.5 min and when no azide at all was added.

77

As shown in Figure 4.14, the curves for the accumulation of radiolabel in the supernatant in WEP (t=9.5), WEP (t=0) and WEP (none) are not significantly different from one another. Thus, inhibition of active transport did not make a significant difference in the rate of radiolabel accumulation. After analyzing the results for all cases in each strain, similar conclusions were drawn. The transport curves show that metabolites are entering into the supernatant in WEP (Figure 4.15), WEN (Figure 4.16), OREP (Figure 4.17) and OREN (Figure 4.18), regardless of whether azide was added or not; therefore, phenanthrene metabolites were likely not substrates of the EmhABC efflux system.

Another interesting finding was that when azide was added 1 min prior to the start of the assay, $92\pm6\%$, $87\pm6\%$, $88\pm4\%$ and $100\pm6\%$ of the ^{14}C added was accounted for at the end of the assay in WEP, WEN OREP and OREN cultures respectively. In the case where no metabolism was occurring and also in the case for the killed-cell controls, only approximately 50% of the added phenanthrene was accounted for at all times. Thus, a 100% recovery of the label was consistent with the assumption that the more polar metabolites accumulate in the supernatant over the course of the assay. These hydrophilic metabolites would not sorb onto the glassware; therefore, an increase in the supernatant concentration was observed when compared to NEP, NEN and the killed controls.

78
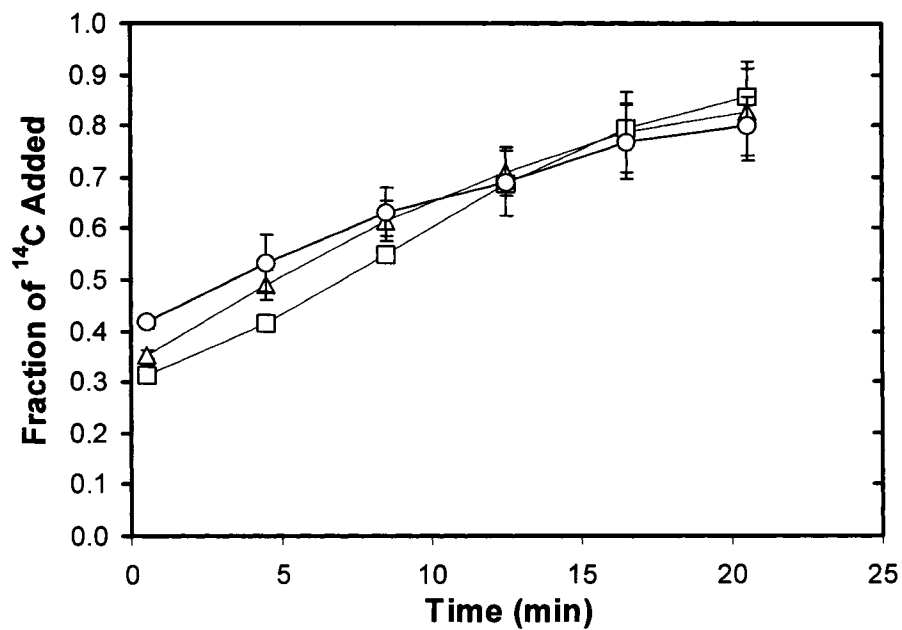
Figure 4.14 Distribution of the radiolabel, added as [9-^{14}C]phenanthrene, in the supernatant for the following three cases: azide added at t=9.5 min (○), azide added 1 min before t=0 (□) and no azide addition (△). The data points are an average of three independent experiments and the error bars, where visible, represent one standard deviation.
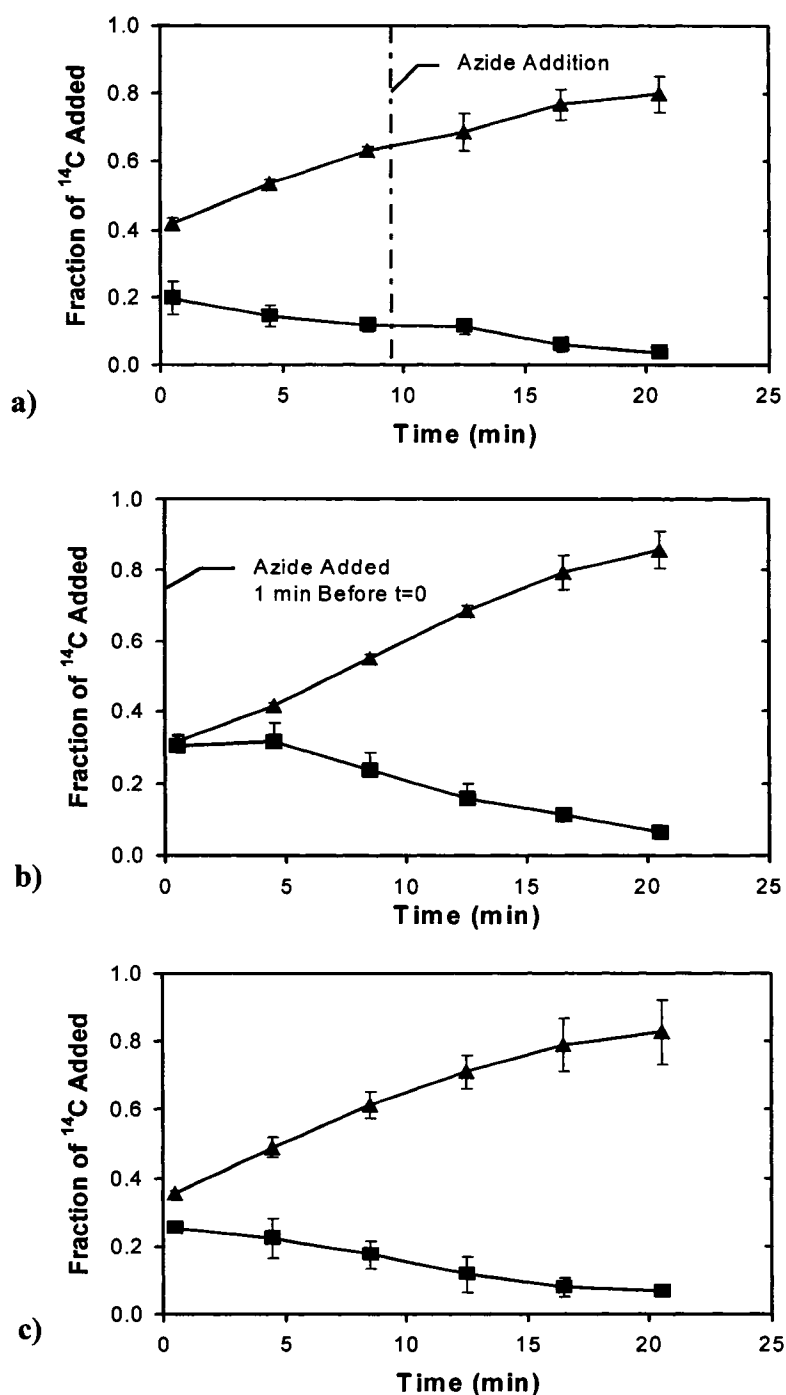
Figure 4.15 Distribution of the radiolabel, added as [9-^{14}C]phenanthrene, between the supernatant (▲) and cell pellet (■) of WEP over time with a) azide added at t=9.5 min, b) azide added 1 min before the label was added, c) no azide addition. The data points are an average of three independent experiments and the error bars represent one standard deviation.

80
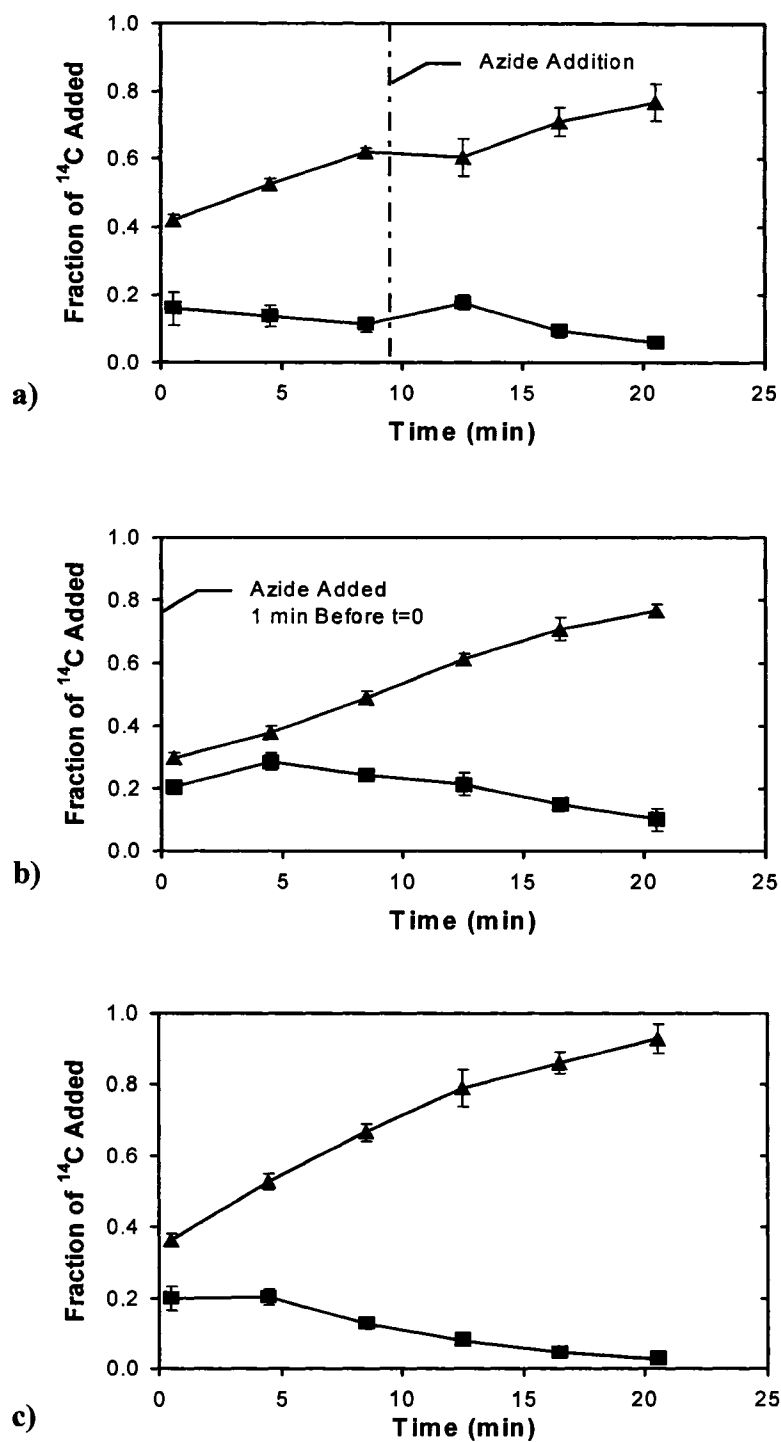
Figure 4.16 Distribution of the radiolabel, added as [9-^{14}C]phenanthrene, between the supernatant (▲) and cell pellet (■) of WEN over time with a) azide added at t=9.5 min, b) azide added 1 min before the label was added, c) no azide addition. The data points are an average of three independent experiments and the error bars represent one standard deviation.

81
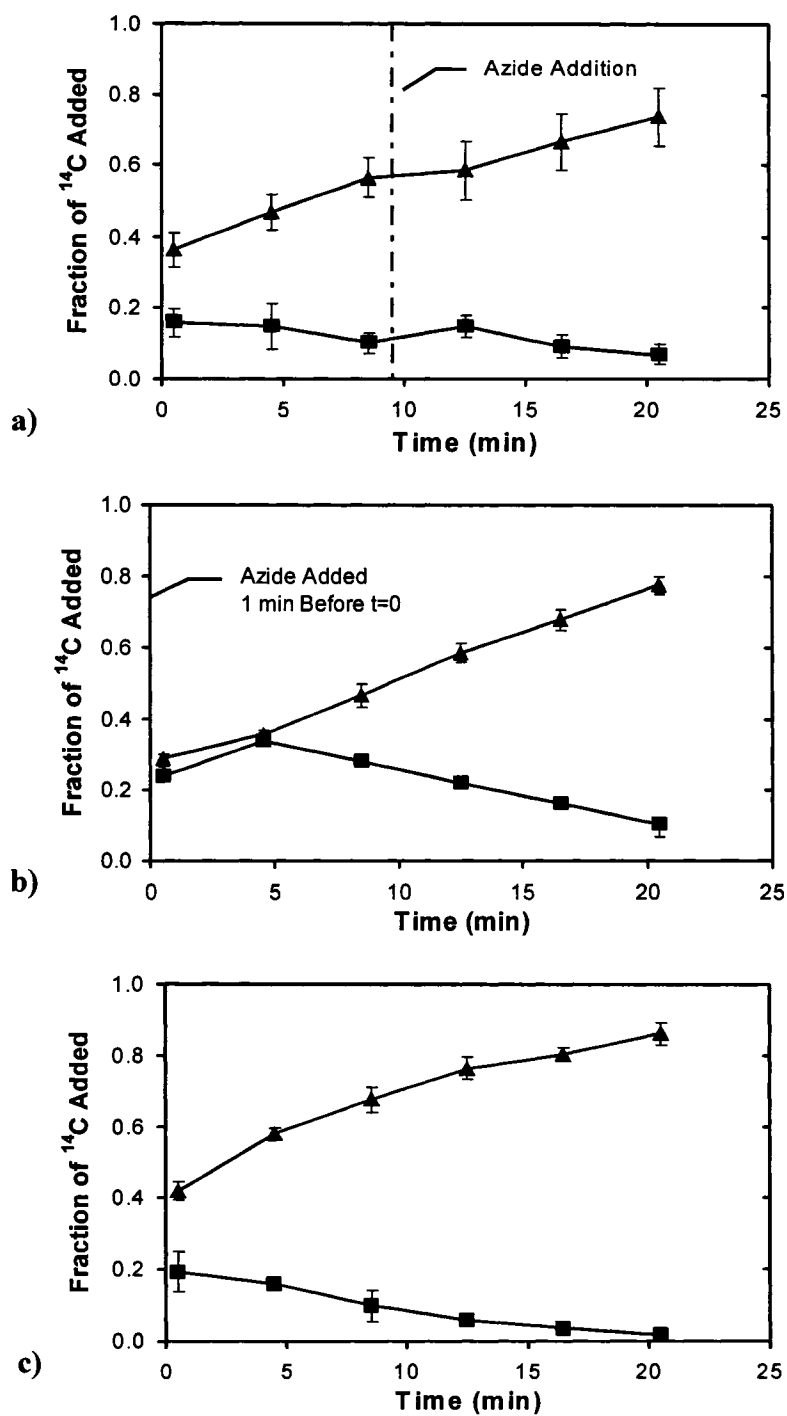
Figure 4.17 Distribution of the radiolabel, added as [9-^{14}C]phenanthrene, between the supernatant (▲) and cell pellet (■) of OREP over time with a) azide added at t=9.5 min, b) azide added 1 min before the label was added, c) no azide addition. The data points are an average of three independent experiments and the error bars represent one standard deviation.

82
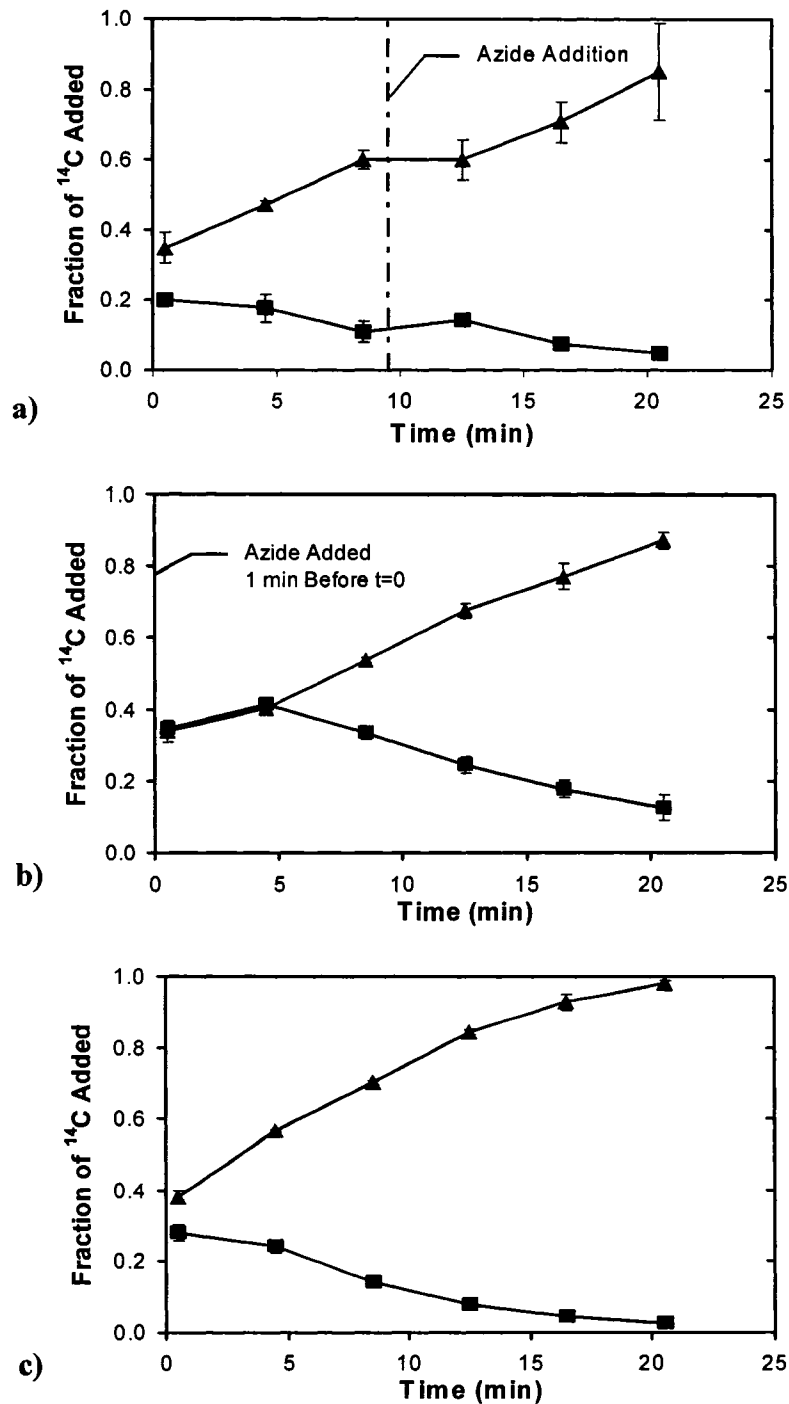
Figure 4.18 Distribution of the radiolabel, added as [9-^{14}C]phenanthrene, between the supernatant (▲) and cell pellet (■) of OREN over time with a) azide added at t=9.5 min, b) azide added 1 min before the label was added, c) no azide addition. The data points are an average of three independent experiments and the error bars represent one standard deviation.

83

At the end of the 20.5-min assay, the majority of the phenanthrene should have been metabolized into more hydrophobic metabolites and therefore the remaining, very low, pellet concentration was presumably predominated by hydrophilic compounds. A change in partitioning of metabolites in the lipid membranes of the cells due to inhibition of efflux at t=20.5 min would not be detectable by the transport assay. However, the initial rate of release of the metabolites would be much more sensitive to the effects of efflux.

Previous research on the active efflux of toluene by a *P. putida* strain unable to degrade toluene showed that the partitioning of this hydrophilic compound in the cells was not instantaneous and that the concentration in the cells increased exponentially over the 10-min sampling period (Isken and de Bont 1996). In contrast, phenanthrene partitioning in NEP reached steady state partitioning between the cells and the supernatant prior to the first sample at 30 s (see Figure 4.7). The flux of hydrophobic compounds by diffusion across cell membranes is proportional to the partition coefficients of the specific solutes (Gray and Bugg 2001). Toluene, which has a low log K_{ow} value of 2.48 (Neumann *et al.* 2005) in comparison to phenanthrene at 4.57 (Knightes and Peters 2003), will permeate the membrane at only 2% of the rate of phenanthrene (Gray and Bugg 2001).

Phenanthrene metabolites such as 1-naphthol and salicylic acid have log K_{ow} values similar to toluene (see Table 2.2) and would, therefore, permeate quite slowly across the cell membranes by diffusion alone. Rapid metabolism coupled with slow diffusion of metabolites across the membrane would give intracellular accumulation of the metabolites. Efflux of the metabolites would prevent such accumulation. If the metabolites were actively effluxed, the addition of azide at t=0 would reduce the rate of release of label into the supernatant and reduce the rate of decrease in the pellet concentration of labeled compounds. Since the supernatant concentration continued to increase as a function of time regardless of the azide addition, the transport assay was sensitive enough to detect that phenanthrene metabolites in general were not substrates of the EmhABC system.

84

4.3 Impact of Efflux on Phenanthrene Degradation

The curves obtained from the transport assays were used to determine the rates of change in the pellet and supernatant fractions. The results from the phenanthrene disappearance experiment in Section 4.2.4 proved that the behaviour of the label at the end of the transport assays was largely, if not totally, due to radiolabeled phenanthrene metabolites, rather than phenanthrene itself. Therefore, the change in concentration as a function of time can be used to determine the rate of phenanthrene degradation and thus, the rate of metabolite accumulation.

The use of the radiolabeled phenanthrene allowed rapid measurements of the changes in the total supernatant and pellet concentrations as a function of time, but it did not give a direct measure of the rate of phenanthrene degradation. At any given time, the concentration of the ^{14}C label in the supernatant is:

$$C_{sup}^{^{14}C} = C_{sup}^{metab} + C_{sup}^{phen} \tag{4.2}$$

where sup represents the supernatant fraction, metab represents metabolites and phen represents phenanthrene. The rate of change then becomes:

$$\frac{dC_{sup}^{^{14}C}}{dt} = \frac{dC_{sup}^{metab}}{dt} + \frac{dC_{sup}^{phen}}{dt} \tag{4.3}$$

The total concentration of metabolites in the cell pellet was not significant, and the metabolites do not adsorb to the walls of the flask, therefore, the metabolites are related to the total rate of phenanthrene degradation as follows:

$$\frac{dC_{sup}^{metab}}{dt} \cong \frac{-dC_{sup}^{phen}}{dt} - \frac{dC_{ads}^{phen}}{dt} - \frac{dC_{pellet}^{phen}}{dt} = \frac{-dC_{total}^{phen}}{dt} \tag{4.4}$$

85

where ads represents the adsorption of phenanthrene onto the sides of the flask and pellet represents the pellet fraction. Substituting equation (4.4) into equation (4.3) gives:

$$\frac{dC_{sup}^{^{14}C}}{dt} = \frac{-dC_{total}^{phen}}{dt} + \frac{dC_{sup}^{phen}}{dt} = \frac{-dC_{ads}^{phen}}{dt} - \frac{dC_{pellet}^{phen}}{dt} \qquad (4.5)$$

Therefore, the initial rate of change in the supernatant concentration of total label gives a measure of the rate of phenanthrene degradation. At longer times, this relationship will fail for WEP due to the release of carbon dioxide, which was not included in the liquid-phase metabolites.

Similarly, the change in the pellet concentration of label gives a measure of the rate of change of phenanthrene in the pellet. Because phenanthrene partitions rapidly between the pellet, the supernatant and the walls of the flask, the rate of change of label in the pellet is an indirect indication of the overall rate of degradation of phenanthrene.

The rates of change were calculated using the linear sections of the curves in the cases where azide was added at t=0 and when no azide was added at all. Only the first three data points were used in the rate calculations where azide was added at t=9.5 min because the azide addition caused a slight change in the curve. Only the initial rates were of interest as non-linear kinetics were observed near the end of the assay. Figure 4.19 indicates which data points were used to calculate the rates in both fractions for all three cases by showing the regression lines from which the slopes were calculated.

The points that were used for the supernatant rate calculations were also used for the pellet rate calculations with one exception; when no azide was added, samples taken at 0.5, 4.5, 8.5 and 12.5 min were used to calculate the rate in the supernatant and samples taken at 4.5, 8.5, 12.5 and 16.5 min were used to calculate the rate in the pellet. This was due to the fact that the supernatant curves (Figures 4.15c, 4.16c, 4.17c and 4.18c) exhibited non-linear trends sooner in the case when no azide was added than in the other cases.

86
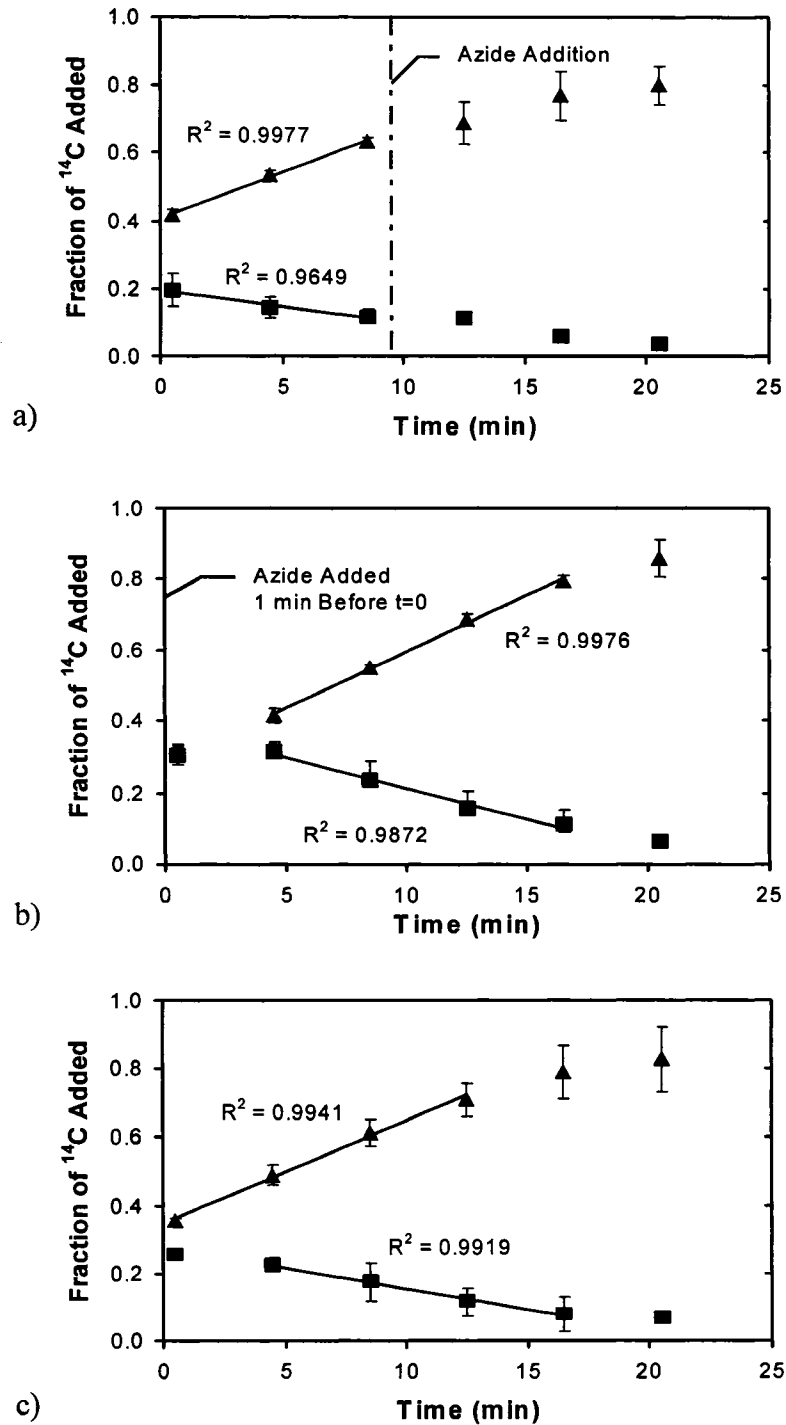
Figure 4.19 The rates were calculated from the slope of the regression lines for the supernatant (▲) and cell pellet (■) of WEP with a) azide added at t=9.5 min, b) azide added 1 min before the label was added, c) no azide addition. The data points are an average of three independent experiments and the error bars represent one standard deviation.

The non-linearity at longer incubation times was likely due to the diminishing concentration of phenanthrene in the supernatant. Therefore, in order to estimate the linear rate observed at the start of the assay, the last two samples were omitted from the rate calculation when no azide was added in the supernatant fraction.

Preliminary examination of the rates showed that the differences in the rates of degradation due to efflux were modest. In order to prove whether or not the difference was significant, detailed statistical analysis of the rate data was performed.

A multiple linear regression model including interaction terms was developed in order to test the second major hypothesis of this research project: the rate of degradation will increase if the EmhABC efflux system is blocked. Due to the fact that only certain pairs of data (efflux positive strain vs. efflux negative strain) needed to be compared to prove or disprove the hypothesis, the complete model was not required. Detailed information on the model is given in Appendix F.

The rates were compared using analysis of covariance (ANCOVA) techniques. The F statistic and the p-value were used to determine if the difference between two strains was statistically significant.

4.3.1 Rates of Phenanthrene Degradation in the Pellet Fraction

Table 4.4 shows the rates that were calculated in the cell pellet fractions as well as the statistics that were calculated when comparing the groups of data. The F_o value must be greater than the F_{value} and the p-value must be less than 0.05 in order for the difference between the two strains to be statistically significant.

88

In the case where azide was added at t=9.5 min, a total of 9 (n=9) points was used in the linear regression model. Therefore, the F_{value} is equal to 5.59. When azide was added at t=0 and when no azide was added, a total of 12 data points (n=12) was used and therefore the F_{value} decreases to 4.96.

Out of all the comparisons, only two groupings were statistically significantly different from each other. OREN degraded phenanthrene in the pellet fraction at a rate of 0.80 ± 0.11 nmol/mg protein/min whereas OREP degraded phenanthrene in the pellet fraction at a rate of 0.61 ± 0.10 nmol/mg protein/min in the case where azide was added at t=0. Thus, the efflux mechanism did in fact have an effect on the rate of phenanthrene metabolism although it was not large. The data points that were obtained from the radiolabeled transport assays as well as the regression lines are plotted in Figure 4.20 to illustrate that the slopes of the lines are indeed significantly different from one another.

Table 4.4 Comparison of the rates of phenanthrene degradation in the cell pellet fractions between the strains with and without efflux capabilities.

Comparison Between (azide):	Rate (nmol/mg protein/min)	Statistics		
		F_o[1]	p-value[2]	Significant?
WEP(t=9.5) WEN(t=9.5)	0.40±0.24 0.24±0.32	0.8300	0.3782	✗
WEP(t=0) WEN(t=0)	0.70±0.23 0.45±0.14	4.2318	0.0530	✗
WEP(none) WEN(none)	0.50±0.24 0.52±0.10	0.0632	0.8041	✗
OREP(t=9.5) OREN(t=9.5)	0.29±0.44 0.47±0.29	0.6400	0.4356	✗
OREP(t=0) OREN(t=0)	0.61±0.10 0.80±0.11	9.3293	0.0063	✓
OREP(none) OREN(none)	0.41±0.07 0.66±0.12	16.2307	0.0007	✓

[1] when $n=9$, $F_{value}=5.59$ and when $n=12$, $F_{value}=4.96$
F_o must be $>F_{value}$ for the result for the result to be statistically significant
[2] p-value must be <0.05 for the result to be statistically significant

90
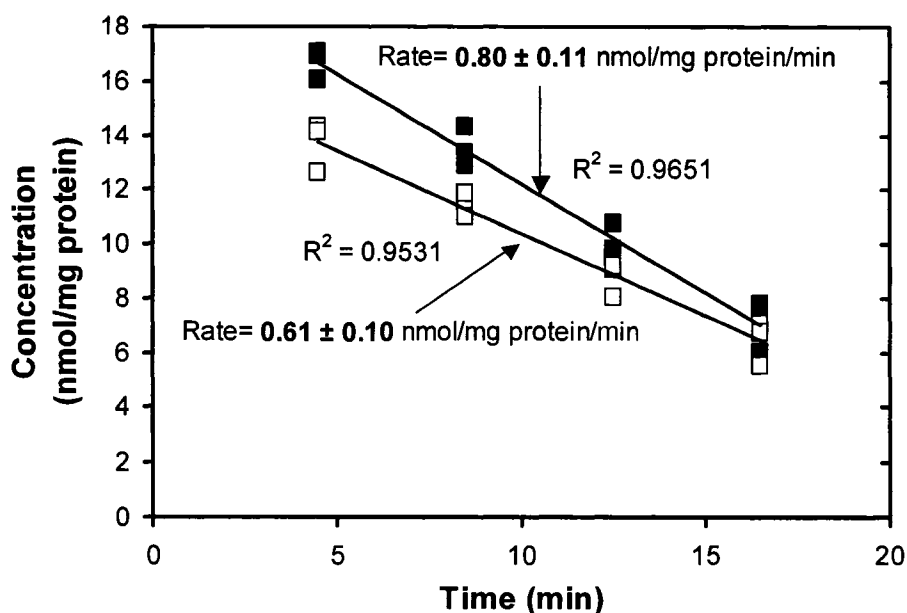
Figure 4.20 Plot of concentration versus time for the pellet fractions in OREN(■) and OREP(□) when azide was added at t=0. The regression lines used to determine the rates are illustrated.

Additionally, OREN degraded phenanthrene at a faster rate (0.66±0.12 nmol/mg protein/min) than OREP (0.41±0.07 nmol/mg protein/min) when no azide was added, further confirming the hypothesis that strains without efflux capabilities degrade phenanthrene in a shorter period of time. Figure 4.21 illustrates the significant difference in the slopes between the two strains.

The amount of phenanthrene initially present in the pellet fraction almost doubled when azide was added at t=0 (Figure 4.20) in comparison to when no azide was added (Figure 4.21). This observation was consistent with the fact that the rates of degradation were faster when azide was added at t=0 than when no azide was added to OREP and OREN cultures. Further analysis of the initial partitioning of phenanthrene will be discussed in Section 4.4.

91
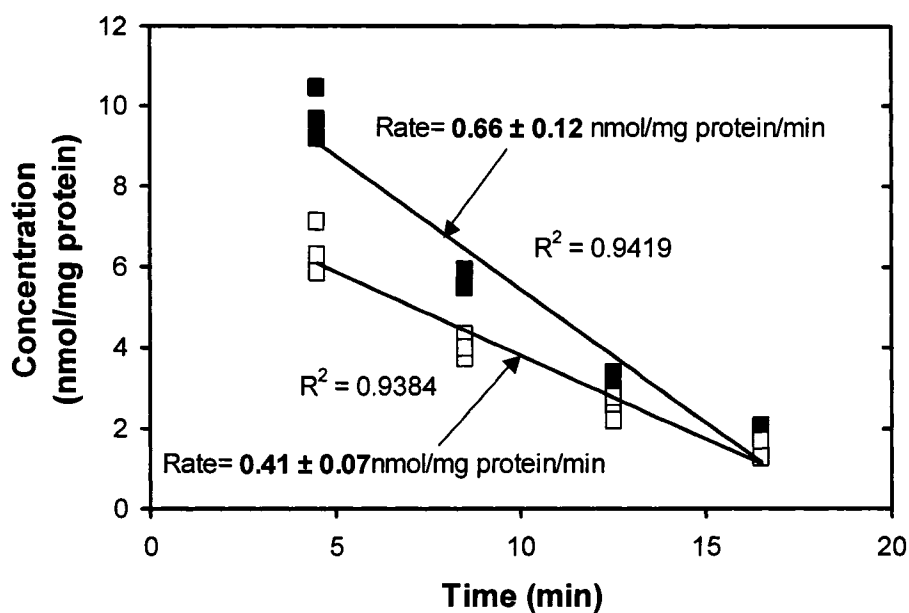
Figure 4.21 Plot of concentration versus time for the pellet fractions in OREN(■) and OREP(□) when no azide was added. The regression lines used to determine the rates are illustrated.

The lack of significant differences in the rates when azide was added at t=9.5 min was not surprising because the slopes were highly variable due to the fact that only three data points were used in the calculation and metabolism affects the steady state partitioning of phenanthrene (see Table 4.4). Taking more samples was not an option in this short period of time due to the time it takes to process each sample.

No significant differences in rate were noted between WEP and WEN, although the data of Table 4.4 indicate a p-value on the margin of significance for t=0. This observation was likely due the accumulation of inhibitory compounds or metabolites in WEN that was demonstrated in Section 4.1.2 and Section 4.1.3. Therefore, due to the numerous anomalies found in WEN, no further investigation into the rate differences between WEP and WEN were pursued.

92

4.3.2 Rates of Net Phenanthrene Metabolite Accumulation in the Supernatant Fraction

As indicated by equation (4.3), the increase in the supernatant concentration with time was the net result of metabolite accumulation and phenanthrene conversion. The net rates of phenanthrene metabolite accumulation that were calculated in the supernatant fractions are given in Table 4.5. The F_0 values and the p-values are also given in the table.

Of all the comparisons, only one group showed a statistically significant difference. OREN produced phenanthrene metabolites at a net rate of 1.54 ± 0.09 nmol/mg protein/min whereas OREP produced phenanthrene metabolites at a net rate of 1.14 ± 0.30 nmol/mg protein/min in the case where no azide was added (see Figure 4.22).

The rate data for OREP and OREN when azide was added at t=0 and when no azide was added also helped to confirm that phenanthrene metabolites in general were not substrates of the EmhABC efflux system. Figure 4.23 shows that the rates of metabolite accumulation are not affected by the addition of azide, as determined from the parallel slopes for the OREN cultures as well as the OREP cultures. Thus, the detailed rate calculations support the conclusion that azide effects on metabolism were limited.

93

Table 4.5 Comparison of the net rates of phenanthrene metabolite production in the cell supernatant fractions between the strains with and without efflux capabilities.

Comparison Between (azide):	Rate (nmol/mg protein/min)	Statistics		
		F_o[1]	p-value[2]	Significant?
OREP(t=9.5) OREN(t=9.5)	1.02±0.46 1.27±0.27	1.2745	0.2779	✗
OREP(t=0) OREN(t=0)	1.11±0.14 1.27±0.14	3.1203	0.0926	✗
OREP(none) OREN(none)	1.14±0.30 1.54±0.09	7.6979	0.0117	✓

[1] when n=9, F_{value}=5.59 and when n=12, F_{value}=4.96
F_o must be >F_{value} for the result for the result to be statistically significant
[2] p-value must be <0.05 for the result to be statistically significant
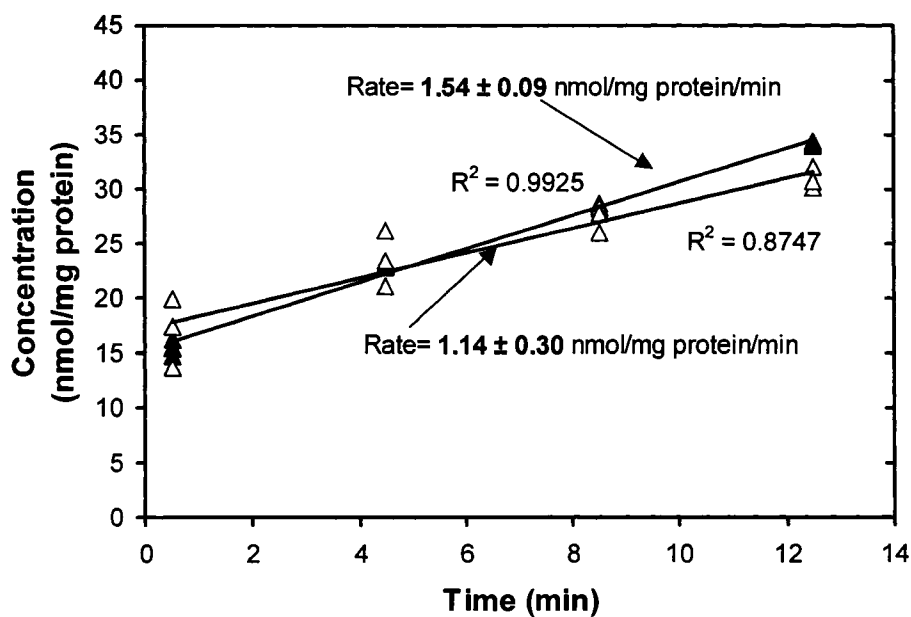
Figure 4.22 Plot of concentration versus time for the supernatant fractions in OREN(▲) and OREP(△) when no azide was added. The regression lines used to determine the rates are illustrated.
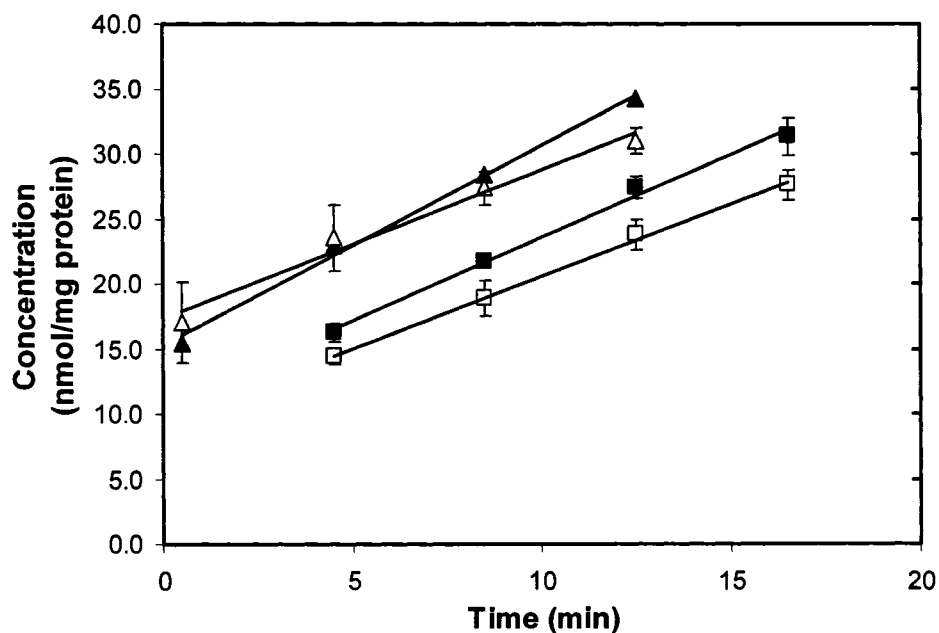
Figure 4.23 Plot of concentration versus time for the supernatant fractions in OREN(▲) and OREP(△) when no azide was added and in OREN(■) and OREP(□) when azide was added at t=0. The regression lines used to determine the rates are illustrated. The data points are an average of three independent experiments and the error bars represent one standard deviation.

4.4 Implications

4.4.1 Analysis of Initial Concentrations and Initial Rates

The results of Section 4.2 indicated that phenanthrene partitions into the cell pellet fraction almost immediately after it was added and the results of Section 4.3 showed that the amount of label in the supernatant fraction began to increase immediately as well. These observations provide evidence that metabolism occurred almost immediately after the substrate was added to the cell suspension. Since the enzymes involved in the metabolism of phenanthrene are intracellular, and the enzymes must gain access to the compound for metabolism to occur, the substrate must cross the cell membrane (Bressler and Gray 2003). Therefore the concentration of phenanthrene in the cytoplasm may play a role in the degradation kinetics.

The addition of azide at t=0 resulted in the highest initial partitioning of phenanthrene into the pellet fraction for all strains. The initial partitioning was determined from the samples taken at t=0.5 min despite that it is not an accurate method because the data were variable. The linear regression lines used to calculate the rates in Section 4.3 were extrapolated to t=0, and these intercepts were compared to the values for t=0.5 min. The intercepts predicted much higher concentrations than the t=0.5 data for the pellet fractions when azide was added at t=0 indicating that extrapolation was not useful in this case. The extrapolated values for the supernatant correlated very well with the data from t=0.5 min (see Table 4.6).

96

Table 4.6 Initial phenanthrene partitioning from the samples taken at t=0.5 min and the y-intercepts of the regression lines used to calculate rates.

Strain (azide)	Supernatant Concentration (nmol/mg protein)		Pellet Concentration (nmol/mg protein)	
	t=0.5	y-int	t=0.5	y-int
OREP[1]				
(t=0)	11.76±0.40	10.62	9.73±1.22	15.87
(none)	17.02±3.24	18.42	7.70±0.40	7.52
OREN[1]				
(t=0)	13.78±1.22	12.13	14.19±0.40	19.48
(none)	15.40±0.81	16.76	11.35±0.81	11.42

[1] Mean value of 3 replicates

In OREN, a 25% increase in the pellet concentration was observed when azide was added at t=0 (14.19±0.38) compared to when no azide was added at all (11.35±0.83) (see Table 4.6). Furthermore, the addition of azide at t=0 had a positive effect on the degradation rates. The highest rates of degradation were observed when azide was added at t=0. In OREN, an increase in the rate of degradation was observed when azide was added at t=0 (0.80±0.11 nmol phenanthrene/mg protein/min) compared to when no azide was added (0.66±0.12 nmol phenanthrene/mg protein/min) (see Table 4.4). Thus, the addition of azide resulted in a more efficient biocatalyst for the initial conversion of phenanthrene.

The initial partitioning of phenanthrene in strains with active efflux when azide was added at t=0 should theoretically be identical to the initial partitioning of the efflux-deficient mutant when no azide was added (either when azide was added at t=9.5 or not at all). In both cases, the efflux should be inhibited. No significant differences in the initial partitioning between OREP (t=0) and OREN (none); and OREP (t=0) and OREN (t=9.5) were discovered as was expected.

The transport assay measured the concentration of radiolabel in the supernatant, and the pellet concentration. The pellet concentration is an average concentration in the cells, including the lipid and aqueous phase concentrations. In order to utilize the measured values to determine the periplasmic concentration, the pellet concentration must be corrected to account for volume and partitioning. The periplasmic concentration is assumed to be the mean point between the cell wall and the inner membrane, with equal amounts of lipid in the inner and outer membrane to partition the phenanthrene.

After the addition of azide to NEP at t=9.5, the supernatant concentration must be equal to both the periplasmic concentration and the cytoplasmic concentration since active transport did not occur and phenanthrene was not being metabolized.

The amount of radiolabel in the pellet fraction, however, is not the concentration in the cells but rather the amount of label partitioned in the lipids. A correction factor, F, was derived from the data for NEP after addition of azide to estimate the periplasmic (i.e. mean) concentration from data for the supernatant and pellet concentrations.

$$F = \frac{C_{sup}\left(NEP - after\ azide\right)}{C_{pellet}\left(NEP - after\ azide\right)} \tag{4.6}$$

Since the three samples taken before azide addition in NEP were determined to be equal and the three samples taken after azide addition were determined to be equal from simple testing of the means, average concentrations were calculated before and after azide addition. Statistical testing showed that the means were equivalent between the three replicates. The averages and statistics are given in Table 4.7 below.

98

Table 4.7 Phenanthrene partitioning in NEP and the corresponding statistics.

Strain (azide)	Supernatant			Pellet		
	Fraction of ^{14}C Added	F	p-value	Fraction of ^{14}C Added	F	p-value
NEP (Before azide)	0.37±0.01	1.05	0.4078	0.20±0.03	4.22	0.0718
(After azide)	0.23±0.01	0.79	0.4952	0.33±0.02	0.60	0.5768

Thus, the following correction factor was used:

$$F = \frac{0.23}{0.33} = 0.70 \tag{4.7}$$

Therefore the pellet concentrations can be converted to periplasmic concentrations using the following equation:

$$C_{periplasm} = C_{pellet} \times F \tag{4.8}$$

where $C_{periplasm}$ is the concentration in the periplasm in nmol/mg protein and C_{pellet} is the pellet concentration in nmol/mg protein.

If a linear concentration gradient across the cell membrane is assumed, the cytoplasmic concentration of phenanthrene can be extrapolated using the measured supernatant concentration and the estimated periplasmic concentration. Figure 4.24 illustrates the concentration gradient between the supernatant concentration ($x=0$), the periplasmic concentration ($x=0.5$) and the cytoplasmic concentration ($x=1$) in NEP. The extrapolation suggests that the cytoplasmic concentration is negative, which indicates that one of the assumptions made in the calculation of the correction factor was incorrect. Therefore, more detailed modeling is required in order to estimate the intracellular concentrations and their dependence on active efflux and metabolism.
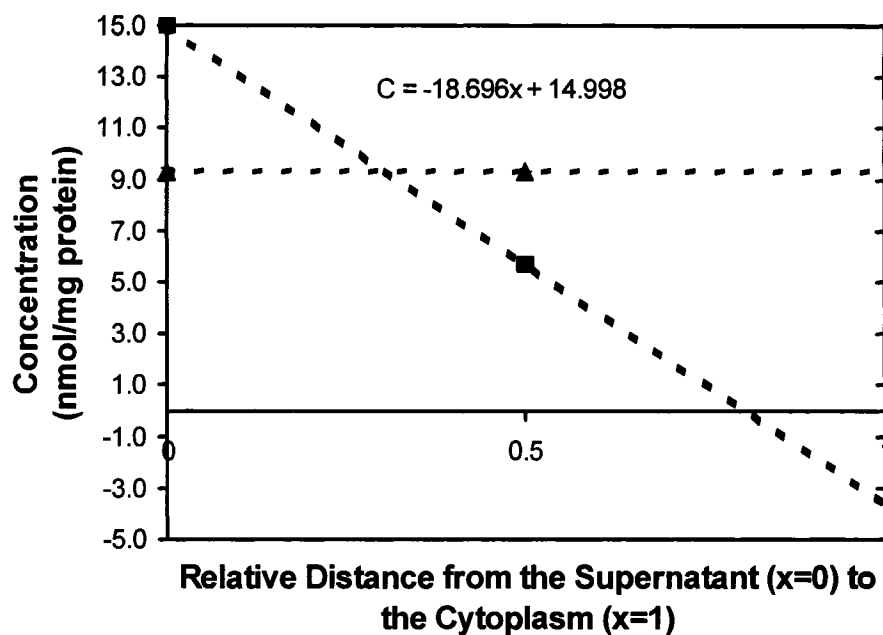
Figure 4.24 Schematic diagram of the phenanthrene concentration gradient in NEP (■) when no azide was added compared to NEP (▲) after azide was added.

Significant differences in the rate of phenanthrene degradation were determined between OREN and OREP in the pellet when azide was added at t=0 in the pellet and in both the pellet and supernatant fractions when no azide was added. The initial partitioning of phenanthrene in OREN pellets was greater than in the OREP pellets, and therefore the initial phenanthrene concentration may have an effect on the rate of degradation. According to Michaelis-Menten kinetics, the rate of degradation is related to the intracellular concentration of phenanthrene until the maximum velocity (V_{max}) is reached. At the point where V_{max} is reached, an increase in substrate concentration does not affect the rate of metabolism.

Despite the fact that the concentration gradient in NEP showed a negative intracellular phenanthrene concentration, the cytoplasmic concentrations in OREN and OREP when no azide was added were extrapolated from the measured supernatant concentrations and the estimated periplasmic concentrations. The concentration gradient for OREP an OREN when no azide was added is shown in Figure 4.25 below.

100
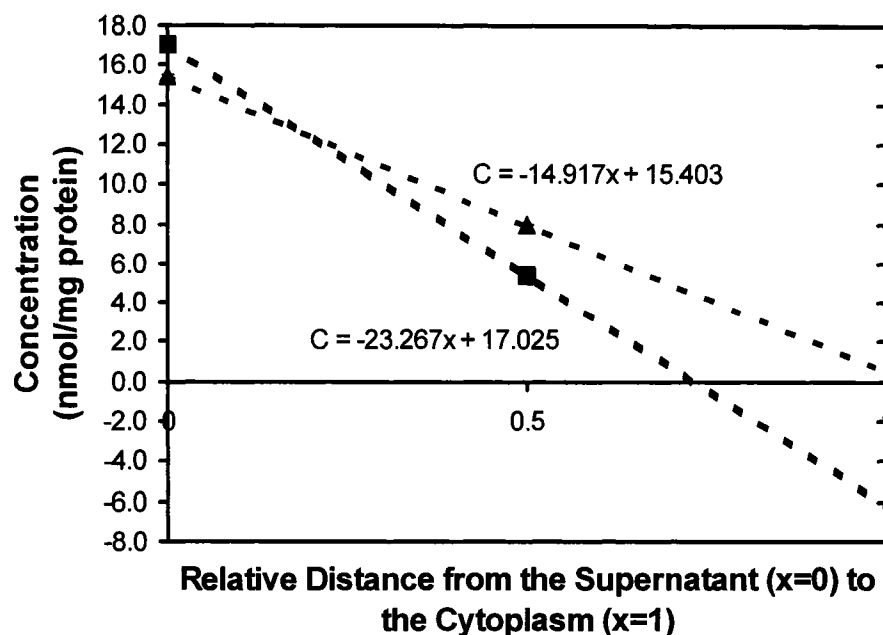
Figure 4.25 Schematic diagram of the phenanthrene concentration gradients in OREP (■) and OREN (▲) when no azide was added.

Figure 4.25 suggests that the cytoplasmic concentration of OREN is greater than the cytoplasmic concentration of OREP. The extrapolation shows a small, but positive, cytoplasmic concentration in OREN. The gradient also shows that the intracellular phenanthrene concentration must be low when efflux is active. Therefore, the K_m value for the initial enzyme for phenanthrene degradation must be low. If the cytoplasmic phenanthrene concentration is assumed to be less than 10% of the supernatant, or 1.5 nmol/mg protein, then the K_m value must also be less than 1.5 nmol/mg protein to account for the lack of response of the rate of degradation to phenanthrene concentration (see Figure 4.24).

Although the higher rate of degradation observed in OREN was statistically significant, it does not cause a large difference in the overall rate of degradation. This is likely due to the K_m value of the initial enzyme. If the substrate concentration is of the same order as K_m, then the rate of degradation will be somewhat dependent on the substrate concentration and the dependence will be nonlinear.

101

4.4.2 Follow-Up Research

Although the results of this study showed that phenanthrene metabolites in general were not substrates of the efflux system, the possibility that some metabolites were effluxed cannot be discounted. In order to classify specific metabolites as substrates of the pump, more sensitive techniques than the transport assay procedure must be used. Some upper pathway metabolites of phenanthrene may in fact be substrates of the pump since they are most similar to phenanthrene itself. Since only the radiolabel was traced as a function of time, the exact compounds that were present in the samples could not be determined. The autoradiography experiments provided some insight into the compounds that were present after specific incubation periods. More frequent sampling as a function of time and analysis by autoradiography might provide useful information.

When attempting to isolate metabolites, higher concentrations of phenanthrene are recommended to accumulate greater amounts of phenanthrene metabolites. The production of more metabolites would make the elucidation of the GC-MS spectra less complex. Additionally, the temperature program used in the GC-MS analysis could be altered to create greater separation of the peaks, which would also simplify the elucidation step.

The efflux-deficient mutants might in fact be useful in the production of enantiopure compounds that are desirable precursors in industry. Further investigation of phenanthrene metabolism might determine whether or not these compounds accumulate to appreciable amounts in LP6a strains.

Further study into the efflux mechanisms in LP6a would also be beneficial. If all efflux pumps could be effectively disrupted, differences in the rates between paired strains might be observed. Alternatively, the blockage of all the pumps could cause the accumulation of inhibitory compounds and therefore hinder the degradation process. Thus, insight into the structures of the compounds present in the cell matrix might lead to the determination of the possible inhibitory compounds and ultimately the reason why WEN was inhibited in the lower pathway.

In order to strengthen the statistical analysis, a greater number of samples are required. As it is next to impossible to take more than six samples in 20.5 min, staggering the sampling times in replicated experiments of the same cell culture would result in more data points, and therefore a more robust model.

Only phenanthrene was tested in this study but the partitioning and degradation rates of other PAHs are also of great interest. In addition to changing the substrate, the biocatalyst used could also be varied. The comparison of the results of this study to the active efflux of growth substrates in other bacterial strains could also provide insight into the function of the EmhABC efflux system.

5.0 CONCLUSIONS

Phenanthrene partitioning and degradation by *P. fluorescens* LP6a strains were studied using radiolabeled transport assays. The partitioning of ^{14}C labeled phenanthrene and metabolites between the cell pellet and supernatant fractions of aqueous cell suspensions showed that the degradation kinetics were affected by the presence of an active efflux system designated EmhABC which is responsible for pumping phenanthrene out of the cell matrix. This efflux mechanism is homologous to multidrug efflux pumps and solvent resistant pumps found in other bacterial strains (Hearn *et al.* 2003). This particular efflux system however, is unusual in that it pumps substrates such as phenanthrene that can be used by the microorganism as a source of carbon and energy.

The wild type microorganism, WEP possesses two main elements that affect phenanthrene degradation: a plasmid that encodes the degradative enzymes required to mineralize phenanthrene (pLP6a); and the chromosomally-encoded EmhABC efflux system. WEP produced 4-(1-hydroxynaphth-2-yl)-2-oxobutanoic acid (the open-ring compound), 1-hydroxy-2-napthoic acid and 1-naphthol within the 20.5-min transport assay. No unconverted phenanthrene was detectable in the cell suspension at the end of the assay. Additionally, $42\pm7\%$ of the radiolabel added as $[9-^{14}C]$phenanthrene was converted to $^{14}CO_2$ in WEP within 20.5 min. A mutant of WEP (i.e. WEN) was constructed by inserting the plasmid pLP6a into a cured strain of LP6a that was efflux-deficient. This mutant was expected to produce the same suite of metabolites as WEP; however, the strain was unable to mineralize phenanthrene and no lower pathway metabolites were detected by GC-MS analysis. The reason for this unexpected behaviour could be due to inhibition of the lower pathway enzymes or the accumulation of a certain compound to toxic levels within the cells. As a result of this oddity, comparison of the rates of degradation of phenanthrene in WEP and WEN was not useful.

104

In order to study the transport of phenanthrene metabolites by EmhABC, a transposon mutant of LP6a, unable to further degrade the open-ring compound (OREP), was studied as it was expected to accumulate this compound. An efflux-deficient mutant of this strain was constructed to compare the rates of degradation between strains with and without efflux activity. GC-MS analysis and TLC/autoradiography showed that the open-ring compound, 4-(1-hydroxynaphth-2-yl)-2-oxobutanoic acid, did in fact accumulate in both strains.

Transport assays were conducted with and without the addition of an active transport inhibitor (30 mM sodium azide) to ensure that all active transport processes were blocked. The change of the ^{14}C label as a function of time in the cell pellet and supernatant fractions was measured and the linear sections of these curves were used to calculate the rate of phenanthrene accumulation in the pellet and the rate of metabolite accumulation in the supernatant.

Because the metabolites are significantly more hydrophilic than phenanthrene, they tend to partition into the aqueous supernatant. In the case of the cured strains and killed-cell controls, just over 50% of the label was accounted for at all times. The remainder of the label was sorbed, although not strongly, to the glassware. At the end of the 20.5-min assay in OREN and OREP when no azide was added, the supernatant concentrations were equal to 86±4% and 98±1% of the initial label concentration respectively. Therefore this observation proved that polar metabolites were partitioning into the supernatant.

Azide was added 1 min before the start of the assay to determine if the extent of degradation was equivalent to the case in which no azide was added. Although the initial partitioning into the pellet was greater when azide was added at t=0, the rates for OREP (t=0) and OREP (none) remained very similar and the final supernatant concentrations accounted for 78±2% and 86±4% of the initial phenanthrene respectively. Therefore, there was no evidence that phenanthrene metabolites in general were substrates of the EmhABC efflux system. Nevertheless, the results to not disprove the fact that certain metabolites may be pumped out of the cell.

Statistically significant differences in the rate of degradation were detected in the pellet fractions of OREP and OREN, where OREN degrades phenanthrene at a higher rate when no azide was added at all (0.66 ± 0.12 vs. 0.41 ± 0.07 nmol/mg protein/min) and when azide was added at t=0 (0.80 ± 0.11 vs. 0.61 ± 0.10 nmol/mg protein/min). A statistically significant difference was also found between OREP and OREN in the supernatant concentration of the label when no azide was added, where OREN produced metabolites at a higher rate (1.54 ± 0.09 nmol/mg protein/min) than OREP (1.14 ± 0.30 nmol/mg protein/min). These observations confirmed that the rate of metabolite accumulation increases when the EmhABC efflux system is blocked in the case of OREN and OREP. However, the rate difference between strains with and without efflux capabilities was not as significant as was expected.

6.0 RECOMMENDATIONS

Throughout this research project, many interesting results were obtained. Firstly, the wild type efflux negative strain, WEN, was unable to mineralize phenanthrene when it possesses the plasmid that encodes the genetic information to produce the required enzymes. Further examination of the compounds that accumulate in the WEN pellet fraction would be useful in determining the reason why WEN did not behave as expected.

Secondly, this study showed that phenanthrene metabolites in general are not substrates of the EmhABC efflux system. Therefore there is a possibility that some metabolites are pumped by LP6a strains. More detailed experimentation, involving a method other than the transport assay used here, might be able to show whether or not any of the metabolites are pumped.

Thirdly, the statistical modeling showed that OREN degraded phenanthrene at a higher rate than OREP. Increased frequency in sampling times of the pellet and supernatant fractions would further validate the statistical analysis and therefore provide further insight into the effects of the EmhABC efflux system on phenanthrene degradation in *P. fluorescens* LP6a strains.

Finally, more sophisticated modeling of the cytoplasmic concentration might provide insight into the importance of initial partitioning of the substrate on the kinetics of degradation. Methods to increase the partitioning of polar compounds in the cell membranes without causing toxic effects would also be useful in enhancing the rate of biodegradation of xenobiotic compounds.

107

7.0 BIBILOGRAPHY

Adachi, K., T. Iwabuchi, H. Sano and S. Harayama. 1999. Structure of the ring cleavage product of 1-hydroxy-2-naphthoate, an intermediate of the phenanthrene-degradative pathway of *Nocardioides* sp strain KP7. Journal of Bacteriology **181**(3): 757-763.

Atlas, R. M. and J. Philp. 2005. Bioremediation: Applied Microbial Solutions for Real-World Environmental Cleanup. Washington, D.C., ASM Press.

Baboshin, M. A., B. P. Baskunov, Z. I. Finkelstein, E. L. Golovlev and L. A. Golovleva. 2005. The microbial transformation of phenanthrene and anthracene. Microbiology **74**(3): 303-309.

Bartha, R. and D. Pramer. 1965. Features of a flask and method for measuring the persistence and biological effects of pesticides in soil. Soil Science **100**: 68-70.

Bateman, J. N., B. Speer, L. Feduik and R. A. Hartline. 1986. Naphthalene association and uptake in *Pseudomonas putida*. Journal of Bacteriology **166**(1): 155-161.

Berezhkovskii, A. M., M. A. Pustovoit and S. M. Bezrukov. 2002. Channel-facilitated membrane transport: transit probability and interaction with the channel. Journal of Chemical Physics **116**(22): 9952-9956.

Boopathy, R. 2000. Factors limiting bioremediation technologies. Bioresource Technology **74**(1): 63-67.

Bosch, R., E. R. B. Moore, E. García-Valdés and D. H. Pieper. 1999. NahW, a novel, inducible salicylate hydroxylase involved in mineralization of naphthalene by *Pseudomonas stutzeri* AN10. Journal of Bacteriology **181**(8): 2315-2322.

Bressler, D. C. and P. M. Fedorak. 2001. Purification, stability, and mineralization of 3-hydroxy-2-formylbenzothiophene, a metabolite of dibenzothiophene. Applied and Environmental Microbiology **67**(2): 821-826.

Bressler, D. C. and M. R. Gray. 2003. Transport and reaction processes in bioremediation of organic contaminants. 1. A review of bacterial degradation and transport. International Journal of Chemical Reactor Engineering 1(R3).

Budzinski, H., T. Nadalig, N. Raymond, N. Matuzahroh and M. Gilewicz. 2000. Evidence of two metabolic pathways for degradation of 2-methylphenanthrene by *Sphingomonas sp.* strain (2MPII). Environmental Toxicology and Chemistry **19**(11): 2672-2677.

Bugg, T. 2000. Uptake and Efflux of PAHs across Bacterial Cell Membranes. M.Sc. Thesis. Department of Chemical and Materials Engineering. University of Alberta.

Bugg, T., J. M. Foght, M. A. Pickard and M. R. Gray. 2000. Uptake and active efflux of polycyclic aromatic hydrocarbons by *Pseudomonas fluorescens* LP6a. Applied and Environmental Microbiology **66**(12): 5387-5392.

Cerniglia, C. E. 1992. Biodegradation of polycyclic aromatic hydrocarbons. Biodegradation **3**: 351-368.

Chen, S.-H. and M. D. Aitken. 1999. Salicylate stimulates the degradation of high-molecular weight polycyclic aromatic hydrocarbons by *Pseudomonas saccharophila* P15. Environmental Science & Technology **33**(3): 435-439.

Cross, K. M., K. W. Biggar, K. Semple, J. Foght, S. E. Guigard and J. E. Armstrong. 2006. Intrinsic bioremediation of diesel-contaminated cold groundwater in bedrock. Journal of Environmental Engineering and Science **5**(1): 13-27.

Di Gennaro, P., P. Conforti, M. Lasagni, G. Bestetti, S. Bernasconi, F. Orsini and G. Sello. 2006. Dioxygenation of naphthalene by *Pseudomonas fluorescens* N3 dioxygenase: optimization of the process parameters. Biotechnology and Bioengineering **93**(3): 511-518.

Efroymson, R. A. and M. Alexander. 1991. Biodegradation by an *Arthrobacter* species of hydrocarbons partitioned into an organic solvent. Applied and Environmental Microbiology **57**(5): 1441-1447.

Fernandes, P., B. S. Ferreira and J. M. S. Cabral. 2003. Solvent tolerance in bacteria: role of efflux pumps and cross-resistance with antibiotics. International Journal of Antimicrobial Agents **22**: 211-216.

Foght, J. M. and D. W. S. Westlake. 1996. Transposon and spontaneous deletion mutants of plasmid-borne genes encoding polycyclic aromatic hydrocarbon degradation by a strain of *Pseudomonas fluorescens*. Biodegradation 7(4): 353-366.

Foght, J. M. 2004. Whole-cell bio-processing of aromatic compounds in crude oils and fuels. *In*: Petroleum Biotechnology: Developments and Perspectives. Surface Science and Catalysis. R. Vazquez-Duhalt and R. Quintero-Ramirez. Amsterdam, Netherlands, Elsevier B.V. **151**: 145-175.

García-Junco, M., E. De Olmeda and J. J. Ortega-Calvo. 2001. Bioavailability of solid and non-aqueous phase liquid (NAPL)-dissolved phenanthrene to the biosurfactant-producing bacterium *Pseudomonas aeruginosa* 19SJ. Environmental Microbiology 3(9): 561-569.

Gibson, D. T. and R. E. Parales. 2000. Aromatic hydrocarbon dioxygenases in environmental biotechnology. Current Opinion in Biotechnology **11**(3): 236-243.

Gray, M. R. and T. Bugg. 2001. Selective biocatalysis in bacteria controlled by active membrane transport. Industrial & Engineering Chemistry Research **40**(23): 5126-5131.

Hearn, E. M., J. J. Dennis, M. R. Gray and J. M. Foght. 2003. Identification and characterization of the *emh*ABC efflux system for polycyclic aromatic hydrocarbons in *Pseudomonas fluorescens* cLP6a. Journal of Bacteriology **185**(21): 6233-6240.

Hearn, E. M. 2005. Identification and Characterization of the EmhABC Efflux System for Polycyclic Aromatic Hydrocarbons in *Pseudomonas fluorescens* cLP6a. Ph.D. Thesis. Biological Sciences and Chemical and Materials Engineering. University of Alberta.

110

Hearn, E. M., M. R. Gray and J. M. Foght. 2006. Mutations in the central cavity and periplasmic domain affect efflux activity of the resistance-nodulation-division pump EmhB from *Pseudomonas fluorescens* cLP6a. Journal of Bacteriology **188**(1): 115-123.

Isken, S. and J. A. M. de Bont. 1996. Active efflux of toluene in a solvent-resistant bacterium. Journal of Bacteriology **178**(20): 6056-6058.

Johnson, R. A. and G. K. Bhattacharyya. 1996. Statistics: Principles and Methods. USA, John Wiley and Sons Inc.

Jördening, H.-J. and J. Winter. 2005. Environmental Biotechnology: Concepts and Applications. Weinheim, Wiley-VCH Verlag GmbH & Co. KGaA.

Kang, H., S. Y. Hwang, Y. M. Kim, E. Kim, Y.-S. Kim, S.-K. Kim, S. W. Kim, C. E. Cerniglia, K. L. Shuttleworth and G. J. Zylstra. 2003. Degradation of phenanthrene and naphthalene by a *Burkholderia* species strain. Canadian Journal of Microbiology **49**(2): 139-144.

Kieboom, J., J. J. Dennis, G. J. Zylstra and J. A. M. de Bont. 1998. Active efflux of organic solvents by *Pseudomonas putida* S12 is induced by solvents. Journal of Bacteriology **180**(24): 6769-6772.

Kieboom, J. and J. A. M. de Bont. 2001. Identification and molecular characterization of an efflux system involved in *Pseudomonas putida* S12 multidrug resistance. Microbiology **147**: 43-51.

Kieser, T. 1984. Factors affecting the isolation of DNA from *Streptomyces lividans* and *Escherichia coli*. Plasmid **12**: 19-36.

Kim, Y.-H., J. P. Freeman, J. D. Moody, K.-H. Engesser and C. E. Cerniglia. 2005. Effects of pH on the degradation of phenanthrene and pyrene by *Mycobacterium vanbaalenii* PYR-1. Applied Microbiology and Biotechnology **67**: 275-285.

Kiyohara, H., K. Nagao and K. Yana. 1982. Rapid screen for bacteria degrading water-insoluble, solid hydrocarbons on agar plates. Applied and Environmental Microbiology **43**: 454-457.

111

Knightes, C. D. and C. A. Peters. 2003. Aqueous phase biodegradation kinetics of 10 PAH compounds. Environmental Engineering Science **20**(3): 207-218.

Korytko, P. J., F. W. Quimby and J. G. Scott. 2000. Metabolism of phenanthrene by house fly CYP6D1 and dog liver cytochrome P450. Journal of Biochemical Molecular Toxicology **14**(1): 20-25.

Krivobok, S., S. Kuony, C. Meyer, M. Louwagie, J. C. Willison and Y. Jouanneau. 2003. Identification of pyrene-induced proteins in *Mycobacterium* sp. strain 6PY1: evidence for two ring-hydroxylating dioxygenases. Journal of Bacteriology **185**(13): 3828-3841.

Málač, J., K. Sigler and D. Gášková. 2005. Glucose-induced MDR pump resynthesis in respiring yeast cells depends on nutrient level. Biochemical and Biophysical Research Communications **337**: 138-141.

McClave, J. T. 1994. Statistics. Englewood Cliffs, NJ, U.S.A., MacMillian College Publishing Company, Inc.

Meylan, W. M., P. H. Howard and R. S. Boethling. 1996. Improved method for estimating water solubility from octanol/water partition coefficient. Environmental Toxicology and Chemistry **15**: 100-106.

Moody, J. D., J. P. Freeman, D. R. Doerge and C. E. Cerniglia. 2001. Degradation of phenanthrene and anthracene by cell suspensions of *Mycobacterium* sp. strain PYR-1. Applied and Environmental Microbiology **67**(4): 1476-1483.

Moody, J. D., J. P. Freeman, P. P. Fu and C. E. Cerniglia. 2004. Degradation of benzo[a]pyrene by *Mycobacterium vanbaalenii* PYR-1. Applied and Environmental Microbiology **70**(1): 340-345.

Moody, J. D., J. P. Freeman and C. E. Cerniglia. 2005. Degradation of benz[a]anthracene by *Mycobacterium vanbaalenii* strain PYR-1. Biodegradation **16**: 513-526.

Mosqueda, G. and J.-L. Ramos. 2000. A set of genes encoding a second toluene efflux system in *Pseudomonas putida* DOT-T1E is linked to the *tod* genes for toluene metabolism. Journal of Bacteriology **182**(4): 937-943.

Myrdal, P., G. H. Ward, R. M. Dannenfelser, D. Mishra and S. H. Yalkowsky. 1992. AQUAFAC 1: Aqueous functional group activity coefficients; application to hydrocarbons. Chemosphere **24**(8): 1047-1061.

Nair, B. M., K.-J. J. Cheung, A. Griffith and J. L. Burns. 2004. Salicylate induces an antibiotic efflux pump in *Burkholderia cepacia* complex genomovar III (*B. cenocepacia*). The Journal of Clinical Investigation **113**(3): 464-473.

Neumann, G., N. Kabelitz, A. Zehnsdorf, A. Miltner, H. Lippold, D. Meyer, A. Schmid and H. J. Heipieper. 2005. Prediction of the adaptability of *Pseudomonas putida* DOT-T1E to a second phase of a solvent for economically sound two-phase biotransformations. Applied and Environmental Microbiology **71**(11): 6602-6612.

Nikaido, H. 1996. Multidrug efflux pumps of gram-negative bacteria. Journal of Bacteriology **178**(20): 5853-5859.

NIST. 2005. National Institute of Standards and Technology Standard Reference Database 69. Retrieved September 2006. http://webbook.nist.gov/cgi/cbook.cgi?ID=C90153&Units=SI&Mask=200#Mass-Spec

Novoszad, M., M. H. Gerzabek, G. Haberhauer, M. Jakusch, H. Lischka, D. Tunega and H. Kirchmann. 2005. Sorption of naphthalene derivatives to soils from a long-term field experiment. Chemosphere **59**: 639-647.

Parales, R. E., S. M. Resnick, C. L. Yu, D. R. Boyd, N. D. Sharma and D. T. Gibson. 2000. Regioselectivity and enantioselectivity of naphthalene dioxygenase during arene *cis*-dihydroxylation: control by phenylalanine 352 in the α subunit. Journal of Bacteriology **182**(19): 5495-5504.

Park, W., C. O. Jeon, H. Cadillo, C. DeRito and E. L. Madsen. 2004. Survival of naphthalene-degrading *Pseudomonas putida* NCIB 9816-4 in naphthalene-amended soils: toxicity of naphthalene and its metabolites. Applied Microbiology and Biotechnology **64**: 429-435.

113

Pinyakong, O., H. Habe, N. Supaka, P. Pinpanichkarn, K. Juntongjin, T. Yoshida, K. Furihata, H. Nojiri, H. Yamane and T. Omori. 2000. Identification of novel metabolites in the degradation of phenanthrene by *Sphingomonas* sp. strain P2. FEMS Microbiology Letters **191**: 115-121.

Poole, K. 2005. Efflux-mediated antimicrobial resistance. Journal of Antimicrobial Chemotherapy **56**: 20-51.

Prabhu, Y. and P. S. Phale. 2003. Biodegradation of phenanthrene by *Pseudomonas* sp. strain PP2: novel metabolic pathway, role of biosurfactant and cell surface hydrophobicity in hydrocarbon assimilation. Applied Microbiology and Biotechnology **61**(4): 342-351.

Prescott, L. M., J. P. Harley and D. A. Klein. 2002. Microbiology. New York, McGraw Hill.

Resnick, S. M., K. Lee and D. T. Gibson. 1996. Diverse reactions catalyzed by naphthalene dioxygenase from *Pseudomonas* sp. strain NCIB 9816. Journal of Industrial Microbiology **17**: 438-457.

Samanta, S. K., A. K. Chakraborti and R. K. Jain. 1999. Degradation of phenanthrene by different bacteria: evidence for novel transformation sequences involving the formation of 1-naphthol. Applied Microbiology and Biotechnology **53**(1): 98-107.

Samanta, S. K., O. V. Singh and R. K. Jain. 2002. Polycyclic aromatic hydrocarbons: environmental pollution and bioremediation. TRENDS in Biotechnology **20**(6): 243-248.

Sanseverino, J., B. M. Applegate, J. M. H. King and G. S. Sayler. 1993. Plasmid-mediated mineralization of naphthalene, phenanthrene, and anthracene. Applied and Environmental Microbiology **59**(6): 1931-1937.

Sikkema, J., J. A. M. de Bont and B. Poolman. 1994. Interactions of cyclic hydrocarbons with biological membranes. Journal of Biological Chemistry **269**(11): 8022-8028.

Sikkema, J., J. A. M. de Bont and B. Poolman. 1995. Mechanisms of membrane toxicity of hydrocarbons. Microbiological Reviews **59**(2): 201-222.

Smith, P. K., R. I. Krohn, G. T. Hermanson, A. K. Mallia, F. H. Gartner, M. D. Provenzano, E. K. Fujimoto, N. M. Goeke, B. J. Olson and D. C. Klenk. 1985. Measurement of protein using bicinchoninic acid. Analytical Biochemistry **150**(1): 76-85.

Stryer, L. 1995. Biochemistry. New York, W. H. Freeman and Company.

Valko, K., C. M. Du, C. Bevan, D. P. Reynolds and M. H. Abraham. 2001. Rapid method for the estimation of octanol/water partition coefficient (log P_{oct}) from gradient RP-HPLC retention and a hydrogen bond acidity term ($\Sigma\alpha_2^H$). Current Medicinal Chemistry **8**: 1137-1146.

Van Hamme, J. D., A. Singh and O. P. Ward. 2003. Recent advances in petroleum microbiology. Microbiology and Molecular Biology Reviews **67**(4): 503-549.

Vila, J., Z. López, J. Sabaté, C. Minguillón, A. M. Solanas and M. Grifoll. 2001. Identification of a novel metabolite in the degradation of pyrene by *Mycobacterium* sp. strain AP1: actions of the isolate on two- and three-ring polycyclic aromatic hydrocarbons. Applied and Environmental Microbiology **67**(12): 5497-5505.

Wall, F. J. 1986. Statistical data analysis handbook / Francis J. Wall. U.S.A., McGraw - Hill Book Company.

Wammer, K. H. and C. A. Peters. 2005. Polycyclic aromatic hydrocarbon biodegradation rates: a structure-based study. Environmental Science & Technology **39**(8): 2571-2578.

Zink, G. and K. E. Lorber. 1995. Mass spectral identification of metabolites formed by microbial degradation of polycyclic aromatic hydrocarbons (PAH). Chemosphere **31**(9): 4077-4084.

APPENDIX A: MEDIA

Luria Bertani (LB) Medium (1 L)

Tryptone	10 g
Yeast	5 g
NaCl	10 g
Agar	15 g

Adjust to pH 7.5 with NaOH prior to adding the agar.

Autoclave and cool prior to adding antibiotics if necessary.

Bushnell Haas (1 L)

$MgSO_4$	0.2 g
$CaCl_2$	0.02 g
KH_2PO_4	1 g
K_2HPO_4	1 g
NH_4NO_3	1 g
$FeCl_3$	0.05 g
Noble Agar	15 g

Adjust to pH 7 prior to adding agar and autoclaving.

0.1 M Potassium Phosphate Buffer (1 L)

KH_2PO_4	6.65 g
K_2HPO_4	13.35 g

Adjust to pH 7 prior to use.

APPENDIX B: EQUATIONS

Mixture of ^{14}C and ^{12}C Phenanthrene:

The volume of radiolabeled phenanthrene added to the vial (V_1) was calculated as follows:

$$V_1 = \frac{Desired\ dpm}{\left(2.2 \times 10^6\ \frac{dpm}{\mu Ci}\right) \alpha\ C_1} \tag{B.1}$$

where α is the activity of radiolabeled phenanthrene ($\mu Ci/\mu mol$) and C_1 is the concentration of radiolabeled stock solution ($\mu mol/L$).

The volume of unlabeled phenanthrene that was added to the vial (V_2) was calculated as follows:

$$V_2 = \frac{C_i(V_t + V_l) - C_l V_l}{C_2 - C_i} \tag{B.2}$$

where C_i is the desired initial liquid phase concentration ($\mu mol/L$), V_t is the volume in flask and C_2 is the concentration of unlabeled stock solution ($\mu mol/L$).

Using the following data:

  Desired dpm= 100 000 dpm
  α= 19.5 $\mu Ci/\mu mol$
  C_1= 233.1 $\mu mol/L$
  C_i= 6.36 $\mu mol/L$
  V_t= 20 mL
  C_2= 6253.6 $\mu mol/L$

V_1 is equal to 10 μL and V_2 is equal to 20 μL. The two volumes were mixed and added to the Erlenmeyer flask at the start of the assay.

117

Liquid Scintillation Counts:

$$Fractional\ Amount = \frac{\dfrac{\left(Sample\ dpm - Background\ dpm\right)}{V}}{\dfrac{Stock\ dpm}{V_t}} \qquad (B.3)$$

where V is the volume of the sample and V_t is the total volume of liquid in the Erlenmeyer flask (20 mL).

Liquid Phase Phenanthrene Concentration (C_{phen}):

The fractional amounts were converted to concentrations using the following equation:

$$C_{phen} = \frac{Fractional\ Amount \times C_i}{C_p} \times \frac{L}{1000\ mL} \times \frac{1000\ nmol}{\mu mol} \times \frac{1000\ \mu g\ protein}{mg\ protein} \qquad (B.4)$$

where C_i is the initial concentration of phenanthrene in the liquid phase in μmol/L (6.36 μM) and C_p is the average protein concentration in μg protein/mL (156.9 μg protein/mL).

118

APPENDIX C: SALICYLIC ACID TRANSPORT ASSAY

In order to determine if the strains of *P. fluorescens* pump phenanthrene metabolites, the transport assay procedure was used to monitor the radiolabel added as [7-^{14}C]salicylic acid, a known phenanthrene metabolite. Salicylic acid was added at a concentration of 15 mM to increase the counts in the pellet fraction. In order to further increase the counts in the pellet sample, double the amount of cells (OD_{600}=2) were added in 0.1 M PB.

Due to the increased hydrophilicity of this compound, very low amounts of salicylic acid partitioned into the pellet phase. The increase in the number of cells did not greatly increase the pellet concentrations and it caused other complications. Therefore, this assay was not further pursued.

119
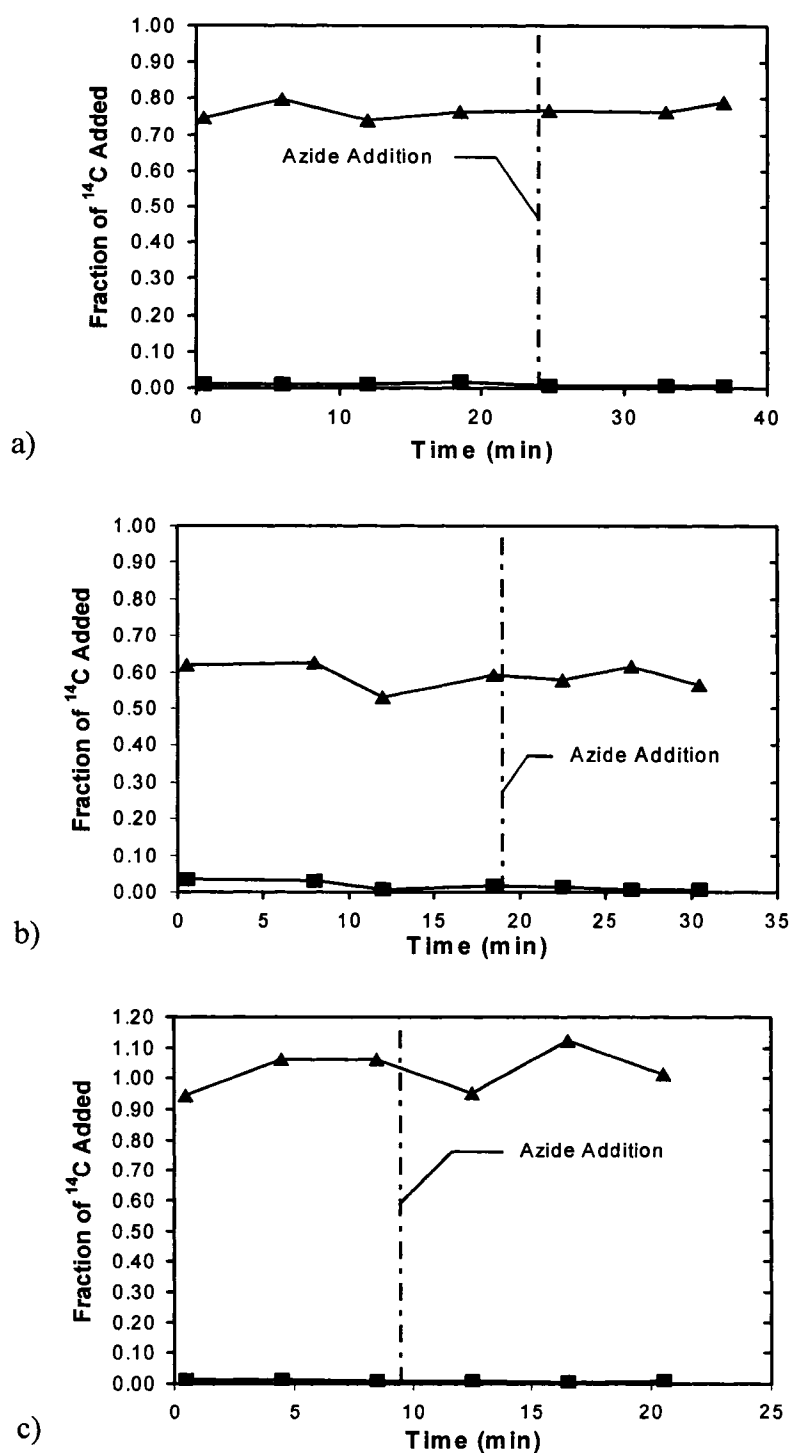
Figure C.1 Distribution of the radiolabel, added as [7-^{14}C]salicylic acid, between the supernatant (▲) and cell pellet (■) over time of a) NEP at an OD_{600} of 1, b) NEN at an OD_{600} of 1, c) NEP at an OD_{600} of 2.

120

APPENDIX D: INDUCTION EXPERIMENTS

Induction generally increases the production of metabolic enzymes and therefore the rate of degradation of the pollutant also increases. Wild type *P. fluorescens* LP6a was induced with sodium salicylate during the final 3 h of the 24-h growth phase of the liquid cultures. A 0.5 M stock solution of sodium salicylate in 95 % ethanol was prepared and 100 μL of this solution was added to the 100-mL liquid culture during the last 3 h of growth to obtain a final salicylate concentration of 0.5 mM. Transport assays were carried out as previously described with sodium azide addition at t=9.5 min.

As shown in Figure D.1, the cells appear to be inhibited or dead. Aliquots of the cultures were plated in order to determine if cells were still viable after the induction period. Additionally, small amounts of DBT crystals were also added to a sample of the liquid culture. The growth of colonies and the production of orange-coloured metabolites indicated that the cells were indeed viable and capable of metabolizing the substrate. The reason why the concentrations in the supernatant and pellet phases did not change with time was not understood.
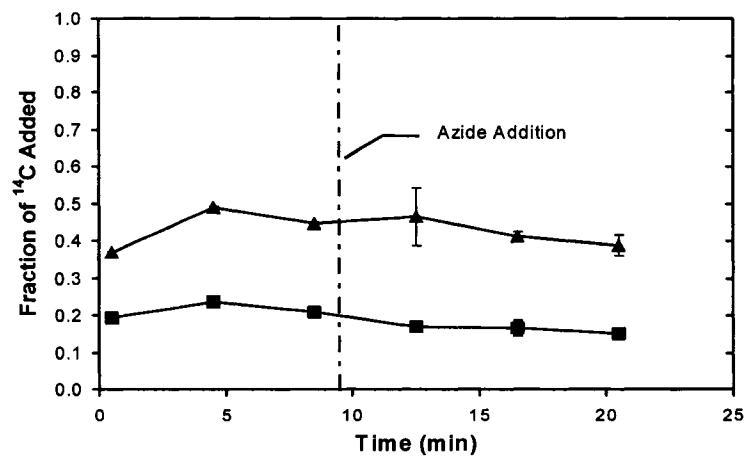
Figure D.1 Distribution of the radiolabel, added as [9-^{14}C]phenanthrene, between the supernatant (▲) and cell pellet (■) of induced cultures of WEP over time. The data points are an average of three independent experiments and the error bars represent one standard deviation.

121

APPENDIX E: EXTRACTION METHOD DEVELOPMENT

In order to develop a working extraction procedure to detect phenanthrene metabolites, a procedure was first developed for DBT metabolite extraction due to the fact that the solution turns bright orange indicating that metabolism was indeed occurring. The first extraction experiment was performed to determine if metabolites were present in the supernatant and/or the pellet fraction after a 24-h incubation period.

Cells were cultured using the procedure previously described in Section 3.3 with the culture volume increased to 200 mL. The cultures were induced with 200 μL of an ethanolic sodium salicylate solution to yield 0.5 mM final concentration during the last 3 h of the 24-h growth phase period. The cells were harvested by centrifugation, rinsed in 3 mM phosphate buffer, centrifuged again and then resuspended in 3 mM PB.

DBT was dissolved in either 2,2,4,4,6,8,8-heptamethylnonane (HMN) or dimethylformamide (DMF) in order to determine which system would yield the most consistent results. The benefit of using DMF is that it disperses tiny crystals throughout the cell suspension thus limiting bioavailability constraints. Adding DBT in HMN to the aqueous cell suspension would result in a 2-phase system and thus possibly cause bioavailability concerns. On the other hand, HMN is extremely useful for removing the unused substrate at the end of the reaction period. The DBT crystals were attempted to be removed by vacuum filtration through #3 Whatman filter paper. Most of the crystals were trapped on the filter paper but some did get through. Due to the high degree of dispersion with the DMF making it extremely difficult to separate out the unused substrate, the HMN system was chosen. A concentrated solution of DBT in HMN was prepared so that the addition of 1 mL of this solution to the culture flask would yield the desired final concentration of 0.5 mM.

122

Because the goal of this experiment was to extract metabolites from the solution, an excess of DBT was added to give a final concentration of 0.5 mM of DBT in a 200-mL culture flask. After shaking overnight at 200 rpm and 28°C, the cells were harvested by centrifugation for 10 min at 10 000 x g and at 4°C.

The supernatant was extracted at neutral pH with DCM to isolate putative dihydrodiols. The organic phase was filtered through sodium sulphate and collected in a round-bottomed flask. The extract was stored at 4°C in the dark due to the presence light-sensitive compounds until the concentration step. The extract was then concentrated by rotary evaporation and a stream of nitrogen to obtain an extract volume of 1-3 mL. A small amount of sodium sulphate was added to the flask in order to remove any remaining water. The extract was then filtered through glass wool to remove any minute solids. The extract was transferred to a glass GC vial with a Teflon liner and analyzed by GC-FID/GC-FPD. The samples were derivatized if necessary using BSTFA.

The aqueous phase was acidified to pH 2 with 2 mL of 4 N H_2SO_4 and was extracted thrice with 15 –25 mL of ethyl acetate to isolate weak organic acids. In the final extraction stage, the aqueous phase was acidified to pH <1 with 5 mL of concentrated HCl and extracted with DCM to isolate strong acids. Since the yellow-coloured metabolites did not partition into the organic phase, the aqueous phase was subsequently extracted with ethyl acetate.

The pellet was resuspended in 30 mL of 0.3 M NaOH in the plastic centrifuge bottles which were heated in a hot water bath at 60°C for 30 min. The pellet fraction was neutralized with concentrated hydrochloric acid and was then extracted using the same procedure as the supernatant with the exception that only 5 mL of solvent was added for each extraction step.

The extracts were run on the GC-FID/GC-FPD with a 30m x 0.25 m DB-5 column using the following temperature program: 90°C for 2 min, increase at 4°C/min to 250°C and then hold for 16 min.

123

In order to determine which peaks were from cell matter and which were not, extractions of NEP were performed without the addition of substrate. The extracts were run under the same conditions on the GC-FID/GC-FPD. A standard curve of DBT in ethyl acetate was prepared to roughly quantify the amount of compound as a function of peak area.

Two samples were run on the GC-MS using the following temperature program: 40°C for 1 min, 10°C per min until 130°C, hold 5 min at 180°C, 10°C per min until 250°C was reached.

In the subsequent extraction experiments, the cells were lysed using the following lysis solution containing 0.3M NaOH and 2% SDS.

The above extraction experiment was repeated using DBT but flasks were sacrificed at the following time intervals: 2, 4, 6, 9, 12, 15 and 24 h. Thus, seven 200 mL liquid cultures of WEP were pooled together in a large, sterile 1-L Erlenmeyer flask. Substrate-free controls were also taken at 2, 12 and 24 h. Uninoculated flasks with substrate were also taken at the same intervals. In this experiment, 100 mL of liquid culture was used as opposed to 200 mL in the previous experiment. A standard solution of *o*-terphenyl in ethanol was added to both the pellet and supernatant fractions. After numerous improvements to the extraction procedure reproducibility, the extraction procedure was used to isolate phenanthrene metabolites.

124

APPENDIX F: MULTIPLE LINEAR REGRESSION MODELING OF RATE DATA

A multiple linear regression model including interaction terms was developed in order to test the second major hypothesis of this research project: the rate of degradation will increase if the EmhABC efflux system is blocked. Dummy variables were created in order to differentiate each of the strains and the testing conditions (McClave 1994). The variable x2 was used to differentiate between strains with and without efflux activity. A value of 1 was assigned to x2 if the strain was capable of phenanthrene efflux whereas a value of 0 was assigned to x2 if the strain was efflux-deficient. Similarly in other variables, variable x3 differentiates between strains with (1) and without (0) azide addition, variable x4 differentiates between azide addition at t=0 (1) and at t=9.5 (0) and variable x5 differentiates between strains with (1) and without (0) the plasmid pLP6a. The dummy variables used in each case and strain are shown in Table F.1 below. The rates of change of label for NEP and NEN were also calculated to confirm that no metabolism was occurring.

Table F.1 Variables used in the multiple linear regression model.

Variable:	Quantitative	Dummy			
	x1 Time	x2 Pump?	x3 Azide?	x4 Azide at t=0?	x5 pLP6a?
WEP (t=9.5)	1	1	1	0	1
WEP (t=0)	1	1	1	1	1
WEP (none)	1	1	0	0	1
WEN (t=9.5)	1	0	1	0	1
WEN (t=0)	1	0	1	1	1
WEN (none)	1	0	0	0	1
OREP (t=9.5)	1	1	1	0	0
OREP (t=0)	1	1	1	1	0
OREP (none)	1	1	0	0	0
OREN (t=9.5)	1	0	1	0	0
OREN (t=0)	1	0	1	1	0
OREN (none)	1	0	0	0	0

The first step was to develop a multiple linear regression model as follows:

$$E(y) = \beta_0 + \beta_1 x_1 + \beta_2 x_2 + \beta_3 x_3 + \beta_4 x_4 + \beta_5 x_5 + \varepsilon \qquad (F.1)$$

where $E(y)$ is ^{14}C label concentration in the pellet in nmol phenanthrene/mg protein, β_i is a regression coefficient, ε is the random error, and x_i is a variable. The random error is assumed to be independent and to have a normal probability distribution with the mean equal to 0 and the variance equal to σ^2.

To determine if the characteristics of the bacterial strain and azide addition have an effect on phenanthrene concentration, interaction terms between the quantitative and qualitative variables were included. Thus, the following equation was used for statistical analysis:

$$E(y) = \beta_0 + \beta_1 x_1 + \beta_2 x_2 + \beta_3 x_3 + \beta_4 x_4 + \beta_5 x_5 + \beta_6 x_1 x_2 + \beta_7 x_1 x_3 + \beta_8 x_1 x_4 + \beta_9 x_1 x_5 + \varepsilon \qquad (F.2)$$

The equations for each of the 12 aforementioned transport assays were determined and are given in Table F.2 below. When a dummy variable has a value of 0, terms containing that variable will also become 0, resulting in causing the different equations.

126

Table F.2 Equations for each of the 12 transport assays.

Assay	Equation
WEP (t=9.5)	$E(y) = \beta_0 + \beta_1 x_1 + \beta_2 x_2 + \beta_3 x_3 + \beta_5 x_5 + \beta_6 x_1 x_2 + \beta_7 x_1 x_3 + \beta_9 x_1 x_5$ $= (\beta_0 + \beta_2 + \beta_3 + \beta_5) + (\beta_1 + \beta_6 + \beta_7 + \beta_9) x_1$
WEP (t=0)	$E(y) = \beta_0 + \beta_1 x_1 + \beta_2 x_2 + \beta_3 x_3 + \beta_4 x_4 + \beta_5 x_5 + \beta_6 x_1 x_2 + \beta_7 x_1 x_3 + \beta_8 x_1 x_4 + \beta_9 x_1 x_5$ $= (\beta_0 + \beta_2 + \beta_3 + \beta_4 + \beta_5) + (\beta_1 + \beta_6 + \beta_7 + \beta_8 + \beta_9) x_1$
WEP (none)	$E(y) = \beta_0 + \beta_1 x_1 + \beta_2 x_2 + \beta_5 x_5 + \beta_6 x_1 x_2 + \beta_9 x_1 x_5$ $= (\beta_0 + \beta_2 + \beta_5) + (\beta_1 + \beta_6 + \beta_9) x_1$
WEN (t=9.5)	$E(y) = \beta_0 + \beta_1 x_1 + \beta_3 x_3 + \beta_5 x_5 + \beta_7 x_1 x_3 + \beta_9 x_1 x_5$ $= (\beta_0 + \beta_3 + \beta_5) + (\beta_1 + \beta_7 + \beta_9) x_1$
WEN (t=0)	$E(y) = \beta_0 + \beta_1 x_1 + \beta_3 x_3 + \beta_4 x_4 + \beta_5 x_5 + \beta_7 x_1 x_3 + \beta_8 x_1 x_4 + \beta_9 x_1 x_5$ $= (\beta_0 + \beta_3 + \beta_4 + \beta_5) + (\beta_1 + \beta_7 + \beta_8 + \beta_9) x_1$
WEN (none)	$E(y) = \beta_0 + \beta_1 x_1 + \beta_5 x_5 + \beta_9 x_1 x_5$ $= (\beta_0 + \beta_5) + (\beta_1 + \beta_9) x_1$
OREP (t=9.5)	$E(y) = \beta_0 + \beta_1 x_1 + \beta_2 x_2 + \beta_3 x_3 + \beta_6 x_1 x_2 + \beta_7 x_1 x_3$ $= (\beta_0 + \beta_2 + \beta_3) + (\beta_1 + \beta_6 + \beta_7) x_1$
OREP (t=0)	$E(y) = \beta_0 + \beta_1 x_1 + \beta_2 x_2 + \beta_3 x_3 + \beta_4 x_4 + \beta_6 x_1 x_2 + \beta_7 x_1 x_3 + \beta_8 x_1 x_4$ $= (\beta_0 + \beta_2 + \beta_3 + \beta_4) + (\beta_1 + \beta_6 + \beta_7 + \beta_8) x_1$
OREP (none)	$E(y) = \beta_0 + \beta_1 x_1 + \beta_2 x_2 + \beta_6 x_1 x_2$ $= (\beta_0 + \beta_2) + (\beta_1 + \beta_6) x_1$
OREN (t=9.5)	$E(y) = \beta_0 + \beta_1 x_1 + \beta_3 x_3 + \beta_7 x_1 x_3$ $= (\beta_0 + \beta_3) + (\beta_1 + \beta_7) x_1$
OREN (t=0)	$E(y) = \beta_0 + \beta_1 x_1 + \beta_3 x_3 + \beta_4 x_4 + \beta_7 x_1 x_3 + \beta_8 x_1 x_4$ $= (\beta_0 + \beta_3 + \beta_4) + (\beta_1 + \beta_7 + \beta_8) x_1$
OREN (none)	$E(y) = \beta_0 + \beta_1 x_1$ $= (\beta_0) + (\beta_1) x_1$

After the model was finalized, the transport data was organized and imported into Matlab®. A Matlab® program was created to calculate the desired statistics used for the least squares regression analysis. These statistics were used to help determine whether or not the differences between strains were statistically significant.

In least squares regression analysis, the goal is to minimize the sum of squares of residuals (Johnson and Bhattacharyya 1996). The error associated with the prediction was computed by estimating σ^2, which is equal to the variance in ε. The ANOVA table (Table 3.2) is a common way to report important information obtained from fitting the data to the regression line.

Other statistics were used in order to complete the analysis and these statistics are listed below in Table F.3.

Table F.3 Statistics used to detect significant differences between strains.

Statistic	Formula
s	$s = \sqrt{SS\,\mathrm{Re}\,s \big/ n - p}$
F_{test}	$F = \dfrac{(SS\,\mathrm{Re}\,s_r - SS\,\mathrm{Re}\,s_c)/(k - g)}{s_c^2}$
t statistic	$t = \dfrac{\hat{\beta}_i}{s_{\hat{\beta}_i}}$ $t < -t_{\alpha/2}\ or\ t > t_{\alpha/2}$
R^2	$R^2 = 1 - \dfrac{\sum(y - \hat{y})^2}{\sum(y - \bar{y})^2} = 1 - \dfrac{SS\,\mathrm{Re}\,s}{SS_{yy}}$
$R^2_{adjusted}$	$R^2 adj = 1 - \dfrac{SS\,\mathrm{Re}\,s/(n - p)}{SS_T/(n - 1)}$

The pellet and supernatant rate data were separated to examine the rates separately. In order to determine if statistically significant differences in the rates amongst the strains with and without efflux activity exist, analysis of covariance (ANCOVA) techniques were utilized. ANCOVA allows for the comparison of slopes for data belonging to

128

different groups and thus was a most useful technique in this study since the slopes of the linear sections of the transport assay curves are equivalent to the degradation rate.

Numerous statistics were calculated to ensure that the analysis was robust. All rate differences were tested at the 5% significance level. The ß parameters were calculated and confidence intervals on each beta parameter were determined. If the confidence interval contained 0, the beta parameter was excluded from the model. F tests were also performed to determine if the model adequately described the data. The p-values were calculated to determine the probability of achieving the given results. From all of the generated data, four statistics were calculated and used to determine whether or not the data was being modeled effectively.

The statistic F_0 from the ANOVA table was used to determine whether or not the model was able to describe the given data. In the F test (McClave 1994), the following hypotheses are proposed:

H_o: $ß_1 = ß_2 = ... = ß_k = 0$

H_a: At least one $ß_i \neq 0$

If $F_o > F_\alpha$, the null hypothesis is rejected.

In addition to the F statistic, t statistics can be used determine the importance of a single regressor as well as to calculate the confidence intervals for each ß parameter. In this test, the following 2 hypotheses are proposed:

H_o: $ß_i = 0$

H_a: $ß_i \neq 0$

The t statistic was calculated and if $t < -t_{\alpha/2}$ or $t > t_{\alpha/2}$, the null hypothesis was rejected indicating that the ß parameter has some importance to the model.

129

Confidence intervals for the ß parameters were also used to determine if the regressors have any significance. If the interval contains 0, the parameter should be excluded from the model.

$$\hat{\beta}_i \pm t_{\alpha/2} s_{\hat{\beta}_i} \qquad (F.3)$$

$R^2_{adjusted}$ is another way to determine how much of the total variability is explained by the model. The usual R^2 statistic is not as reliable because the denominator does not vary as n increases and therefore the R^2 statistic will be higher when there is more data. Generally, a higher R^2 value is indicative of a better model.

A hypothesis test was performed with the null hypothesis that a single line characterizes the relationship between concentration and time against the alternate hypothesis that separate lines (one for each of the transport assays performed) are required to characterize the relationship.

H_o: $\beta_2 = \beta_3 = \beta_4 = \beta_5 = \beta_6 = \beta_7 = \beta_8 = \beta_9 = 0$
H_a: At least one of the regressors is not equal to 0.

To test this hypothesis, the data were fitted to the complete model as well as to a reduced model. The change in the sum of squares of the residuals was calculated and used to determine the value of F_{test} (Wall 1986). The degrees of freedom (dof) in the numerator equal the number of regressors that were removed for the reduced version. The denominator has the same number of degrees of freedom as associated with s^2 in the complete model. If the F_{test} is less than the $F_{0.05}$ value, the there is no evidence that the more complicated model is better.

The supernatant and pellet data sets both fit the full model (see equation F.2) relatively well, based on the F test and the $R^2_{adjusted}$ statistics. The F_o values that were obtained were all significantly higher than the F_{value} that was calculated at the 95% confidence level. $R^2_{adjusted}$ values of 0.90 and 0.82 were obtained for the supernatant and pellet data

130

respectively (see Table F.4). The model was accurate at describing the given data sets. However, after calculating the confidence intervals for the regressors (the ß parameters), only time, azide addition time and the interaction between time and azide presence were significant in the supernatant. For the pellet fraction, only azide presence, azide addition time and the interaction between time and the azide addition time were significant.

Due to the large variation in rates when azide was added at t=9.5 min, the data from these assays were excluded from the model. Therefore, a reduced model was used that did not involve azide addition time and its interaction term was used. The $R^2_{adjusted}$ values as well as the F values indicated that the fit of the model to the data was quite good but numerous regressors were still not important to the model. In the reduced model, time, azide addition and the presence of pLP6a were significant in the supernatant whereas only time and azide addition were important in the pellet. Since the reduced model was still unable to show differences due to the presence or absence of active efflux, comparisons for the two sets of paired mutant strains were performed to closely examine the effects of the EmhABC efflux system.

Table F.4 Statistics for the full and reduced multiple linear regression models for both the supernatant and pellet fractions.

Statistics	Supernatant		Pellet	
	Full	Reduced	Full	Reduced
SSR	3885.80	3144.30	1367.60	1278.40
MSR	431.75	449.19	151.95	182.62
SSRes	417.17	295.25	275.78	206.59
MSRes	3.42	3.36	2.26	2.35
Fo	1.85	1.83	1.50	1.53
Fvalue, .95	126.26	133.88	67.22	77.79
R^2	0.90	0.91	0.83	0.86
R^2_{adj}	0.90	0.91	0.82	0.85
t	1.96	2.12	1.96	2.12

The statistics that were calculated for each of these models are given in Tables F.5, F.6, F.7 and F.8 below.

131

Table F.5 Statistics for the supernatant full model.

Regressor	Statistics			
	β	t	CI, low	CI, high
β_0	15.01	23.90	13.77	16.25
β_1	1.39	18.35	1.24	1.54
β_2	**0.23**	**0.40**	**-0.93**	**1.40**
β_3	**-0.05**	**-0.07**	**-1.45**	**1.34**
β_4	-4.72	-5.49	-6.42	-3.02
β_5	**0.26**	**0.44**	**-0.90**	**1.42**
β_6	**-0.10**	**-1.52**	**-0.23**	**0.03**
β_7	-0.24	-2.13	-0.46	-0.02
β_8	**0.10**	**0.92**	**-0.12**	**0.32**
β_9	**-0.02**	**-0.25**	**-0.15**	**0.11**

Bold indicates that the regressor was not significant

Table F.6 Statistics for the supernatant reduced model.

Regressor	Statistics			
	β	t	CI, low	CI, high
β_0	16.06	22.76	14.66	17.46
β_1	1.32	16.47	1.16	1.48
β_2	**0.07**	**0.10**	**-1.41**	**1.56**
β_3	-4.77	-5.82	-6.40	-3.14
β_5	-1.68	-2.25	-3.17	-0.20
β_6	**-0.09**	**-1.19**	**-0.24**	**0.06**
β_7	**-0.13**	**-1.61**	**-0.30**	**0.03**
β_9	**0.12**	**1.61**	**-0.03**	**0.27**

Bold indicates that the regressor was not significant

Table F.7 Statistics for the pellet full model.

Regressor	Statistics			
	β	t	CI, low	CI, high
β_0	11.06	16.48	9.73	12.39
β_1	-0.55	-8.92	-0.67	-0.42
β_2	**-0.64**	**-1.20**	**-1.70**	**0.42**
β_3	-2.80	-4.01	-4.19	-1.42
β_4	9.00	12.87	7.61	10.38
β_5	**-0.82**	**-1.53**	**-1.88**	**0.24**
β_6	**0.01**	**0.26**	**-0.09**	**0.12**
β_7	**0.18**	**1.93**	**0.00**	**0.35**
β_8	-0.29	-3.20	-0.47	-0.11
β_9	**0.03**	**0.57**	**-0.07**	**0.13**

Bold indicates that the regressor was not significant

Table F.8 Statistics for the pellet reduced model.

Regressor	Statistics			
	β	t	CI, low	CI, high
β_0	11.72	14.68	10.13	13.30
β_1	-0.59	-8.48	-0.73	-0.45
β_2	**-1.24**	**-1.55**	**-2.83**	**0.35**
β_3	6.19	7.76	4.61	7.78
β_5	**-1.53**	**-1.92**	**-3.12**	**0.05**
β_6	**0.06**	**0.81**	**-0.08**	**0.20**
β_7	**-0.12**	**-1.65**	**-0.25**	**0.02**
β_9	**0.08**	**1.15**	**-0.06**	**0.22**

Bold indicates that the regressor was not significant